

# INAUGURAL-DISSERTATION

zur Erlangung der Doktorwürde der

GESAMTFAKULTÄT FÜR MATHEMATIK, INGENIEUR- UND  
NATURWISSENSCHAFTEN

der

RUPRECHT-KARLS-UNIVERSITÄT  
HEIDELBERG

vorgelegt von

**M. Sc. Johannes Kammerer**

aus Friedberg

Tag der mündlichen Prüfung

---



# Mathematical Modeling of the Nile Perch Fishery in Lake Victoria

Gutachter

Prof. Dr. Anna Marciniak-Czochra



# Abstract

The Lake Victoria ecosystem in East Africa is known to support the world's largest small-scale freshwater fishery. Economically, the most valuable fish in this ecosystem is the Nile perch, whose population plays a vital role for ecosystem stability. The question of the optimal regulatory paradigm for harvesting Nile perch is subject to considerable debate. Theoretical concepts such as 'balanced harvesting' with little size selectivity coexist with a practice of size-based instruments, targeting gear and catch sizes.

This thesis develops, analyzes and simulates a new bio-economic model of the Nile perch fishery that couples a bio-energetic fish population model to an economic model of the fishery, incorporating the size structure of the fish population and gear selectivity.

The existence of a unique, non-negative and regular solution of the model is proven. After validating the model against the empirical population size structure, we show that the current fishery is a steady state solution and that the effort is 2.0% above the optimal effort for fixed fleet selectivity. An alternative fleet selectivity that spares fish below 50 cm increases yield, income and stock biomass. The numerical optimization shows that the optimal fleet selectivity spares fish below at least 70 cm. Optimizing the fleet selectivity increases yield by 94.6% and income by 151.9%. The dynamic fishers response model shows that boat owners switch to using 6", 7" and 8" gillnets because of the high profitability.

The results indicate significant gains in yield and income from sparing small fish and allow three conclusions to be drawn: First, there is not necessarily a trade-off between harvest and stock biomass, but both can be increased through improved fishing. Second, sparing small fish is not a loss of catch, but exploits the growth potential of fish and increases reproduction and stock biomass. Third, our model suggests that fishing should be selective, focusing on larger fish. This result questions the dominant paradigm of balancing harvest across sizes in proportion to productivity, which implies targeting smaller fish more intensively. The novel size structured bio-economic fishery model therefore challenges the current understanding and suggests new directions for modeling the fishery of Lake Victoria.



# Zusammenfassung

Vom Ökosystem des Viktoriasees in Ostafrika ist bekannt, dass es die weltweit größte handwerkliche Süßwasserfischerei beherbergt. Der wirtschaftlich wertvollste Fisch in diesem Ökosystem ist der Nilbarsch, dessen Population eine entscheidende Rolle für die Stabilität des Ökosystems spielt. Die Frage nach dem optimalen Regulierungsparadigma für den Nilbarschfang ist Gegenstand erheblicher Debatten. Theoretische Konzepte wie "Ausgewogene Befischung" mit geringer Größenselektivität existieren neben einer Praxis größenbasierter Instrumente, die auf Fanggeräte und Fanggrößen abzielen.

In dieser Arbeit wird ein neues bioökonomisches Modell der Nilbarschfischerei entwickelt, analysiert und simuliert, das ein bioenergetisches Fischpopulationsmodell mit einem wirtschaftlichen Modell der Fischerei verbindet und dabei die Größenstruktur der Fischpopulation und der Fangselektivität berücksichtigt.

Die Existenz einer eindeutigen, nichtnegativen und regulären Lösung des Modells wird bewiesen. Nach der Validierung des Modells anhand der empirischen Populationsgrößenstruktur wird aufgezeigt, dass die derzeitige Fischerei eine Gleichgewichtslösung darstellt und dass der Fischereiaufwand 2,0% über dem optimalen Wert bei festgehaltener Flottenselektivität liegt. Eine alternative Flottenselektivität, die Fische unter 50 cm verschont, steigert Ertrag, Einkommen und Bestandsbiomasse. Die numerische Optimierung zeigt, dass die optimale Flottenselektivität Fische unterhalb von mindestens 70 cm Größe verschont. Die Optimierung der Flottenselektivität erhöht den Ertrag um 94,6% und das Einkommen um 151,9%. Das dynamische Reaktionsmodell der Fischer zeigt, dass die Bootseigner aufgrund der höheren Rentabilität auf 6"-, 7"- und 8"-Kiemennetze umsteigen.

Die Ergebnisse deuten auf erhebliche Ertrags- und Einkommenssteigerungen durch die Schonung kleiner Fische hin und erlauben die folgenden drei Schlussfolgerungen: Erstens besteht nicht unbedingt ein Zielkonflikt zwischen Fangmenge und Bestandsbiomasse, sondern beide können durch eine verbesserte Fischereiselektivität gesteigert werden. Zweitens bedeutet die Schonung kleiner Fische nicht einen Fangverlust, sondern sie nutzt das Wachstumspotential der Fische aus und erhöht die zudem die Reproduktion und damit die Bestandsbiomasse. Drittens legt unser Modell nahe, dass die Fischerei selektiv erfolgen und vorwiegend auf größere Fische abzielen sollte. Dieses Ergebnis stellt das vorherrschende Paradigma in Frage, nach dem Fische proportional zu ihrer biologischen Produktivität gefangen werden sollen, was eine intensivere Ausrichtung auf kleinere Fische impliziert. Das neuartige größenstrukturierte bioökonomische Fischereimodell stellt daher das derzeitige Verständnis in Frage und zeigt neue Wege für die Modellierung der Fischerei im Viktoriasee auf.



# Acknowledgments

First and foremost, I want to express my gratitude to my supervisor Prof. Dr. Anna Marciniak-Czochra for her continuous support, for the valuable and motivating discussions and for her expert advice. I am thankful for the support to participate and present the research in conferences and workshops, and for the opportunity to write the dissertation at the Institute for Mathematics at the University of Heidelberg.

I sincerely thank Prof. Timo Goeschl, PhD, my supervisor from the field of environmental economics, for the inspiring discussions and for the opportunity of a PhD as part of the exciting MultiTip project in an interdisciplinary field including research cooperation with scientists from multiple fields from economics to fisheries sciences. I am grateful for his support for the participation and presentation at conferences and workshops and for the valuable discussions and suggestions for the thesis.

Gratefully, I acknowledge the funding from the German Federal Ministry of Education and Research (BMBF) as part of the MultiTip project (grant number 01LC1822A).

I thank the Heidelberg Graduate School MathComp for the insights from lectures and courses in the PhD program.

Finally, I am grateful to my colleagues: To Santiago for the inspiring and helpful discussions, to Filip for discussions of the mathematical sections, to Tillmann and Sorell for discussions and suggestions, to the colleagues from the Research Centre for Environmental Economics and from the Applied Analysis and Modelling in Biosciences group and to the multiple research colleagues from various workshops and conferences, both from Europe and Africa, for discussions of this research.



# Contents

<b>Abstract</b>	<b>iii</b>
<b>Zusammenfassung</b>	<b>v</b>
<b>Acknowledgments</b>	<b>vii</b>
<b>1 Introduction</b>	<b>1</b>
1.1 Aims of the thesis . . . . .	1
1.2 Methods and results . . . . .	3
1.3 Outline of the thesis . . . . .	5
<b>2 Overview of the Nile perch fishery</b>	<b>9</b>
2.1 Fisheries at Lake Victoria . . . . .	9
2.2 Fishers' communities and stakeholders' perceptions . . . . .	12
2.3 Institutions, regulations and enforcement . . . . .	13
2.4 Previous modeling approaches . . . . .	14
<b>I Size structured model of the Nile perch fishery</b>	<b>17</b>
<b>3 Biological model</b>	<b>19</b>
3.1 Why use a size structured model? . . . . .	19
3.2 Biological processes . . . . .	20
3.2.1 Growth . . . . .	20
3.2.2 Reproduction . . . . .	23
3.2.3 Recruitment . . . . .	24
3.2.4 Mortality . . . . .	26
3.3 Size spectrum . . . . .	27
3.4 Parameters . . . . .	28

## Contents

<b>4</b>	<b>Economic model</b>	<b>31</b>
4.1	Open access fishery . . . . .	31
4.2	Size selectivity . . . . .	32
4.3	Bio-economic fishery model . . . . .	36
4.3.1	Harvest and effort . . . . .	36
4.3.2	Fishery production function . . . . .	37
4.3.3	Fishers' response . . . . .	40
4.4	Fisheries reference points . . . . .	40
4.5	Gear selectivity . . . . .	41
4.6	Fleet selectivity . . . . .	43
4.7	Parameters . . . . .	45
<b>5</b>	<b>Experimental survey data</b>	<b>49</b>
5.1	Fish population measurements . . . . .	49
5.2	Data processing . . . . .	50
<b>6</b>	<b>Mathematical analysis of the size structured population model</b>	<b>53</b>
6.1	Time dependent model . . . . .	53
6.2	Steady state model . . . . .	60
6.3	Perturbations of the fleet selectivity . . . . .	62
<b>II</b>	<b>Application to the regulation of the Nile perch fishery</b>	<b>67</b>
<b>7</b>	<b>Model validation and sensitivity analysis</b>	<b>69</b>
7.1	Numerical procedure . . . . .	69
7.2	Validation . . . . .	70
7.2.1	Growth curve . . . . .	70
7.2.2	Size spectrum . . . . .	71
7.3	Fishing mortality . . . . .	78
7.4	Sensitivity analysis . . . . .	80
7.5	Catch size distribution . . . . .	81
<b>8</b>	<b>Alternative fleet selectivity scenarios</b>	<b>85</b>
8.1	Slot size scenarios . . . . .	85
8.2	Gillnet scenarios . . . . .	90

<b>9</b>	<b>Optimal fleet selectivity</b>	<b>95</b>
9.1	Optimization problem . . . . .	96
9.2	Maximizing yield . . . . .	96
9.3	Maximizing income . . . . .	98
9.4	Discussion . . . . .	100
<b>10</b>	<b>Simulations of the coupled dynamic stock-fishery model</b>	<b>103</b>
10.1	Response of fishers in the dynamic model . . . . .	103
10.2	Application: Impact of panelling and opportunity costs . . . . .	108
10.2.1	Hypotheses . . . . .	108
10.2.2	Panelling . . . . .	110
10.2.3	Opportunity costs . . . . .	113
10.2.4	Comparison to an agent-based model . . . . .	117
10.2.5	Management implications . . . . .	119
<b>11</b>	<b>Integrating discussion and conclusions</b>	<b>123</b>
11.1	Social-ecological systems modeling . . . . .	123
11.2	Discussion of the results . . . . .	124
11.3	Limitations and future research . . . . .	128
11.4	Conclusions . . . . .	129
<b>12</b>	<b>Summary</b>	<b>131</b>
	<b>Bibliography</b>	<b>133</b>
	<b>List of Figures</b>	<b>152</b>
	<b>List of Tables</b>	<b>153</b>
	<b>List of Publications</b>	<b>155</b>
	<b>Appendices</b>	<b>159</b>
<b>A</b>	<b>Mathematical methods</b>	<b>159</b>
A.1	Ordinary differential equations . . . . .	159
A.2	Solution to the age structured population model . . . . .	161
A.3	Convergence of the growth function . . . . .	162
A.4	Ordinary least squares . . . . .	165

A.5 Optimization methods . . . . .	166
A.6 Density conversion . . . . .	168
<b>B Ecological parameters</b>	<b>173</b>
B.1 Growth parameter . . . . .	173
B.2 Physiological mortality . . . . .	174

# 1 Introduction

## 1.1 Aims of the thesis

The aim of this thesis is to build, analyze and simulate a model of the Nile perch fishery to assess the consequences of size-related fishing regulations.

The importance of the fishery at Lake Victoria for food security and income implies that the high exploitation level poses a serious threat to the livelihood of three to four million people in the region. The Lake Victoria ecosystem is a system that has historically seen a tipping point in the 1980s, when the complex, original food web with 500 native species collapsed, simultaneously with an explosion of the Nile perch population [193]. Therefore, Nile perch as top level predator plays a particularly important role and has the potential to drastically transform the ecosystem of the whole lake.

It is a common theme among scholars and policymakers dealing with Lake Victoria to suggest that Nile perch is substantially overfished and that the population will soon collapse if the fishing is not drastically reduced [124, 143]. While many ecosystem models of the lake have been developed, little focus has been laid so far on size structured bio-economic models.

As the Nile perch exploitation has many characteristics of an open access fishery, the fishery managers and policymakers have to design simple tools to regulate the fishery and avoid the degradation of the resource which could in this case lead to both ecologically and socially devastating results. It is key to develop tools that allow an evaluation of management options before they are implemented to predict the consequences of each scenario and to rank them with respect to appropriate metrics like the annual harvest or aggregate income of the the fishery. To do so, the size structured stock-fishery model is used to address the following four questions regarding the Nile perch fishery of Lake Victoria.

## 1 Introduction

### 1. Sustainability of the current exploitation

Can the current exploitation of the Nile perch fishery be sustained over time? Which level of fishing intensity would produce the maximum sustainable yield (keeping the size selectivity of the fleet fixed)?

### 2. Alternative size and gear based exploitation patterns

Which modifications of the current fishing pattern would improve steady state yield and income? When does a perturbation of the pattern increase the yield? What size based and gear based exploitation patterns are superior to the current situation?

### 3. Optimal fishing selectivity

If a sole-owner managed the fishery and wanted to maximize steady state yield or income, respectively: What size selectivity should his fleet have? How does this compare to the current exploitation and to the regulation of minimum legal fish size and minimum mesh size? What gain in yield and income is possible from optimizing the fleet selectivity?

### 4. Fishers' response

How do fishers respond to the fish stock in a dynamic coupled stock-fishery model? Which state would the fishery naturally tend to, from fishers' proper profit interest? Can this explain the observed behavior of fishers around the lake?

The four questions are addressed in the following order and connection. After the development of the size structured model and its mathematical analysis, we first assess whether the current exploitation scheme is sustainable and whether the level of exploitation is optimal (Question 1). Then we assess alternative exploitation schemes, similar to the proposals currently discussed among Lake Victoria managers - corresponding to the question "what if?"<sup>1</sup> (Question 2). Afterwards we take the perspective of a sole-owner who seeks to maximize yield or income of the fishery. Which is the optimal fleet selectivity pattern he should aim for, that produces the largest yield or income in steady state - this corresponds to the question "what's best?" (Question 3). Finally, we simulate the dynamic model including the fishers' response to the stock and analyze the behavior in the model compared to reality

---

<sup>1</sup>As suggested in [172], bio-economic models can be categorized as simulations addressing "what if?" questions, and optimizations addressing "what's best?".

(Question 4), together with an application to an ongoing theme in Lake Victoria's fishery management around panelling. This approach provides a systematic assessment of the current exploitation scheme and the possible improvements.

## 1.2 Methods and results

The Social-Ecological Systems (SES) approach allows to systematically identify the model components and their interactions (Fig. 1.1) [163, 91, 177, 128, 32]. The resource system is the Lake Victoria ecosystem as a whole, in which the resource units (individual Nile perch) are produced. The users (fishers) interact with the fish population to generate outcomes (harvest), while being regulated by the governance system. The model itself focuses on the fish population and the fishers, while the regulator comes in when alternative size and gear restrictions are analyzed. Variations of the ecosystem are studied in the sensitivity analysis with respect to variations of the parameters of somatic growth and natural mortality. With the sensitivity analysis we quantified the impact of uncertainty in the parameter values on the relevant outcome variables.

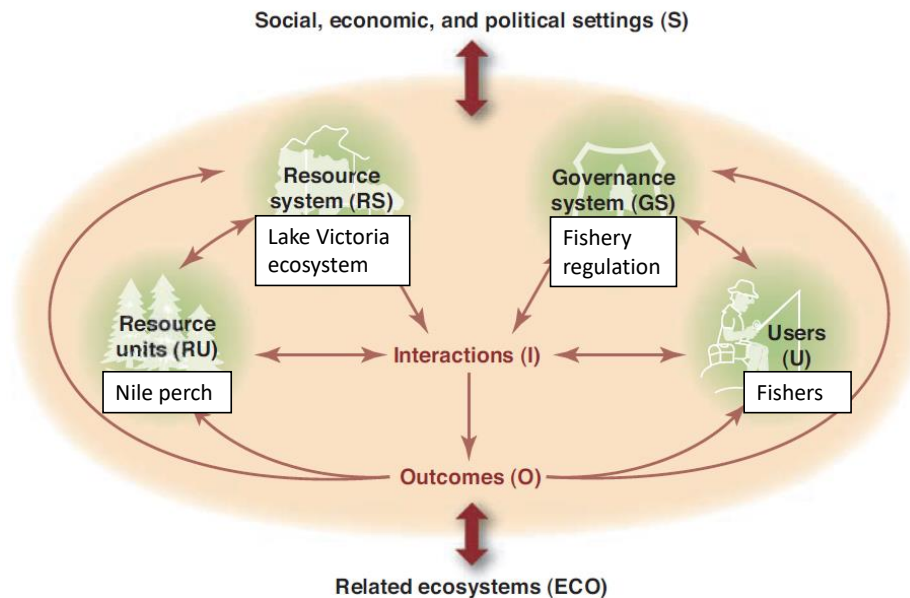


Figure 1.1: The components and their connections in the Social-Ecological Systems approach with the respective specifications for the Nile perch fishery model in the white boxes. Adapted from [163].

## 1 Introduction

The mathematical model incorporates the relevant components of the SES. Mathematical models, in particular population models, are highly capable tools to describe, analyze and predict biological phenomena across all fields from fisheries to epidemiology and cell biology [62, 126, 140, 39, 40, 41]. Dynamics of heterogeneous populations can be appropriately described by structured population models (SPM) that include a transport equation in the form of a first order hyperbolic partial differential equation (PDE) with a nonlocal boundary condition. In SPMs, the heterogeneous population is structured by a functionally relevant feature, such as age, size or another trait dimension of the population [104, 197, 95, 84, 54, 83, 85, 96]. Building on previous work on size structured population models [96], we prove the existence of unique, non-negative solutions of the stock model both for the time dependent case with exogenous fishing mortality and for the steady state case. If the initial condition fulfills a compatibility condition, the solutions are regular.

We derive a general condition by which it can be assessed whether perturbations of the fishing pattern increase or decrease the steady state yield. In the model validation, it is found that the model prediction agrees with the size structure from the bottom trawl and the catch assessment survey, but disagrees from the hydroacoustic survey data. In the analysis we find that the effort (if one keeps the fleet selectivity fixed) is 2.0% above the value that produces the maximum sustainable yield (MSY), thus the stock is fished at a mostly appropriate level, provided that only effort (and not size selectivity) is variable. With a sensitivity analysis we found that the MSY fishing mortality and the recruitment are most sensitive to the parameter of physiological mortality, which parametrizes the density of predators in the ecosystem. Therefore, future biological studies need to determine this parameter as precisely as possible.

In a comparison with eight hypothetical fleet selectivities we find that patterns which shift the focus to targeting larger fish lead higher steady state yield and to a more healthy fish stock with more fecund females. Completely sparing fish below 50 cm would, *ceteris paribus*, increase steady state yield by 17.7% and spawning stock biomass by 31.9%.

This finding is corroborated by a numerical optimization procedure to maximize steady yield or income, respectively. The optimal fishing pattern targets exclusively fish above 70 cm or 90 cm, respectively, dependent on the assumptions about senescent mortality. Thus the optimal minimum catch size is at least 20 cm above the lower bound of the slot size (50 cm) and also larger than the range that is targeted with the smallest legal gillnet mesh size (5", targeting fish in the range

47.69 ± 7.90 cm). Therefore, from the model's perspective, the minimum size regulation is too low when compared to the optimal minimum catch size.

In the final chapter, the previous model is coupled to a gear based model of fishers' response to the fish stock level, mediated through the profits. We find that within the first year, all unprofitable gears are abandoned, leaving a state where only gillnets with 6", 7" and 8" mesh size are used because of their profitability. Even though longlines catch also large fish, they cannot compete with gillnets because they have additional bait costs. An application of the dynamic model shows that there are two regimes of the fishery (high and low value) and that changes in the gear efficiency and in the opportunity costs can induce a transition from one regime to the other.

Our findings with the size structured model challenge the common theme of over-fishing and suggest a rather sustainable exploitation pattern. However, sustainable does not necessarily mean that the population is harvested optimally. Quite the contrary, we find that substantial increases in harvest are possible from shifting the exploitation toward larger fish. This also contests the conception that improvements of the fish stock level necessarily require reductions in harvest. With the size structured model we can give new indication that an appropriate size structure of the catch can simultaneously increase the abundance of fish (especially the large spawners) while not impairing (and even increasing) harvest. This challenges a common theme among Lake Victoria managers and scientists [147], opens new directions for modeling the Lake Victoria fisheries and calls for more research to develop and investigate alternative proposals for fishery regulations.

## 1.3 Outline of the thesis

Here we explain the outline of the thesis (Fig. 1.2). **Chapter 2** explains the context and the characteristics of the Nile perch fishery at Lake Victoria. The following **first part of the thesis (Chapters 3-6)** develops, explains and analyses the size structured model of the Nile perch fishery. **Chapter 3** explains the biological component of the model, which includes the functional form of all processes within the life history of individual fish, starting from the egg through hatching, recruitment growth and maturation to the adults that are fecund and reproduce. **Chapter 4** builds the economic component of the model, including the size selectivity of gillnets and longlines. It also explains how fishers' adaptation is represented in the model and introduces relevant concepts from fisheries sciences like the fisheries reference

## 1 Introduction

points. **Chapter 5** provides an overview of the experimental fish population survey techniques and the processing of the survey data. **Chapter 6** analyzes the mathematical properties of the bio-economic model. The existence of unique, non-negative solutions is proven for the time dependent case with exogenous constant fishing mortality and for the steady state case.

The **second part (Chapters 7-10)** contains the application of the model to recent questions in the regulation of the Nile perch fishery. In **Chapter 7**, the numerical procedure is explained together with a validation of the model against the experimental surveys. The sensitivity of the results to the uncertain key parameters is assessed. **Chapter 8** studies the effect of the size selectivity on steady state yield and income. The sustainability of the current exploitation pattern is evaluated and in a first study, the current fleet selectivity is compared to three hypothetical slot size related scenarios. Additionally, five gear related scenarios are simulated and ranked with respect to steady state yield and income. **Chapter 9** is an optimization study where steady state yield or income, respectively, is maximized. This functions as a benchmark to assess other scenarios. **Chapter 10** simulates how fishers would adapt the effort given the profits they make from fishing. We simulate the development without exogenous regulations and compare the final state with the current fishery. In an application we analyze how panelling or changes in opportunity costs would impact the state of the fishery and compare the results to an agent-based model. **Chapter 11** involves an integrating discussion and directions for future research. **Chapter 12** summarizes the thesis.

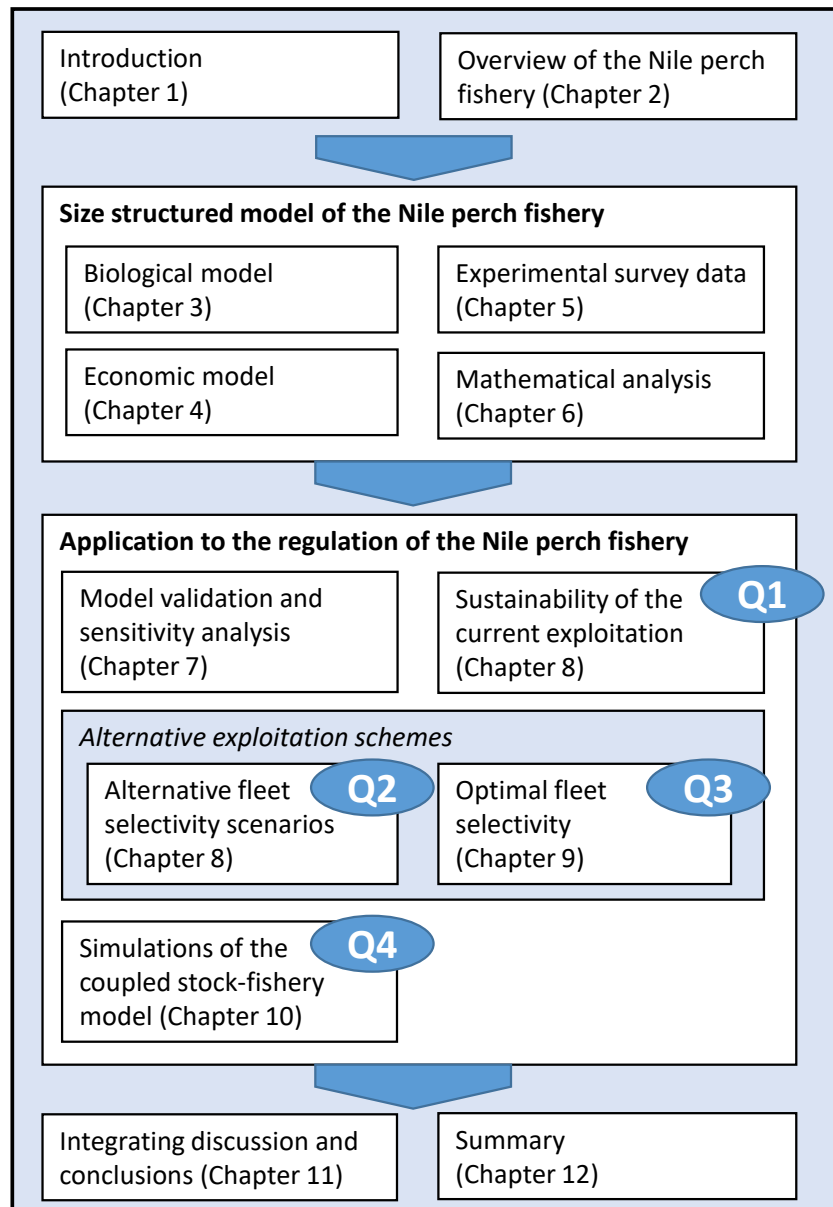


Figure 1.2: Outline of the thesis together with the four main questions Q1-Q4.



## 2 Overview of the Nile perch fishery

### 2.1 Fisheries at Lake Victoria

Lake Victoria (LV) is the world's second largest freshwater lake with 68,000 km<sup>2</sup> surface area, shared by the three riparian countries Tanzania (51%), Uganda (43%) and Kenya (6%) (Fig. 2.1). Situated at an altitude of 1,134m above sea level, it is a shallow lake with 40m mean depth, 68m maximum depth and 3,450km shoreline [99, 193, 102, 124]. Until the 1970s, the fish fauna was dominated by more than 500 extremely diverse, endemic haplochromine cichlid (*Haplochromini*) species [193]. In the 1950s, Nile perch (*Lates niloticus*) was introduced to replace the bony haplochromines which were of low value to the fisheries [160, 159, 154]. It took around 25 years for Nile perch to reach a high population level - until the 1980s, when rapid eutrophication, a Nile perch boom and a haplochromine collapse coincided [150]. Within few years, from 1982-1985 in Uganda and from 1983-1987 in Tanzania, Nile perch replaced most of the indigenous species in the lake and became of major relevance to the fisheries [60]. While the destruction of the food web is generally seen as an ecological catastrophe, the annual fish production increased from about 100,000 t in 1980 to almost one million tonnes today [193, 133, 127].

The reasons and the dynamics of the dramatic changes in the ecosystem are highly debated, with explanations ranging from the top-down hypothesis (Nile perch killing haplochromines through predation pressure) via the simple hypothesis of slow logistic growth to the bottom-up hypothesis, where an externally (climate or eutrophication) induced perturbation temporarily increased the haplochromine mortality, enabling Nile perch eggs and fry to escape the predation by haplochromines in large numbers [60, 199, 127]. Eventually, in the 2000s, the dagaa population (*Rastrineobola argentea*, *Silver cyprinid*) increased strongly and haplochromines reappeared, but are still far below the original levels.

The lake supports the largest small-scale fresh water fishery in the world [106]. The high nutritional and commercial value of Nile perch lead to a growth of the fishing industry in the 1990s, with the lake now being the most important source of

## 2 Overview of the Nile perch fishery



Figure 2.1: Map of the Lake Victoria region. From [141].

protein to the riparian population [158]. In the 1980s and 1990s, processing facilities were established around the lake, and Nile perch is today exported to Europe, Asia, and North America [65]. For Nile perch, the two main commercially relevant gears are gillnets (GN) and longlines (LL) with hooks (Fig. 2.2).

There are about 200,000 fishers involved in the fisheries, with three to four million livelihoods connected to the fisheries [150]. The Nile perch fishery is the most valuable one, contributing around 52% to the value of the fisheries, estimated at 550 million USD for the catch at beach level [164]. The export value (260 million USD) comes mainly from Nile perch. In terms of catch weight, dagaa plays also an important role. The fisheries provide a total catch of 900,000 tonnes per year, of which around 200,000 t are from Nile perch and 500,000 t from dagaa [121].

Given the complex nature of the Lake Victoria fisheries, various attempts have been made to understand the socio-economic feedbacks [58], the limnological drivers [193] and the impact of the fisheries [148, 156]. Surveys among fishers and stakeholders have shown that the main factors driving the development of the Nile perch stock are considered to be the fishing effort, illegal fishing gears and methods as well as limnological parameters like the eutrophication of the lake [106, 108, 119, 133, 135].

2.1 Fisheries at Lake Victoria

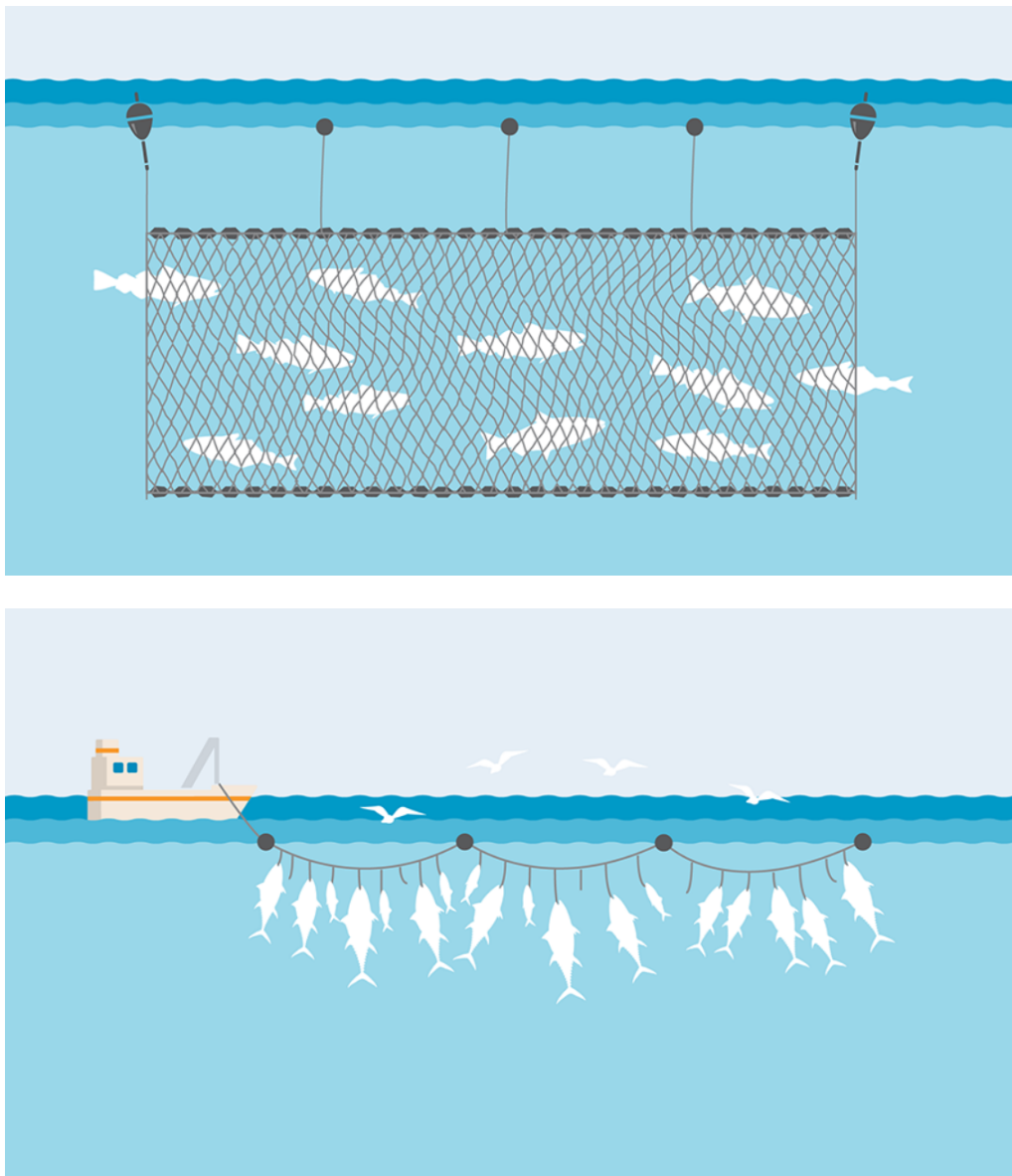


Figure 2.2: The two main gears in the Nile perch fishery are gillnets (top) and long-lines with hooks (bottom). From [36, 37].

## **2.2 Fishers' communities and stakeholders' perceptions**

Lake Victoria is a center point of the social, economic and demographic dynamics in the region. Regional migration and demographic patterns add to the growth of the local population. In the Nile perch fishery, the boats go on the lake in the morning and during the daytime, with the crew consisting of typically two to three persons per boat. The fishers in a small-scale fishing community on the eastern shores of Lake Victoria in Kenya reported that the catch value is shared between the crew (60%) and the boat owner (40%) [98]. Commuting is rare, and most fishers spend their daily lives in the community of the landing site where they fish [98]. Due to the economic pressures, many fishers work additionally in agriculture [42].

Multiple surveys have studied how stakeholders, including members of the fishing community, governmental institutions, NGOs and fish processors, perceive the development of the Nile perch fish stock and the main impact factors [19, 20, 22, 106, 21]. Many stakeholders perceive a decline in the Nile perch stock and agree strongly about the drivers of the decline: fishing in breeding grounds, overfishing and the use of destructive fishing gear and methods. They assume that a lack of awareness of sustainable fishing practices and monitoring, as well as corruption exacerbate the situation [21]. The fact that fishers tend to acknowledge the role of fishing activities, in particular gear choice and (non-)compliance with regulations, as main driver of the fish stock, could be a leverage point for effective regulations [21].

In practice, however, illegal fishing practices are still wide spread. Tanzanian artisanal fishers stated that the decisions to violate the regulations are influenced by the probability of detection and punishment, but also depend on whether the regulations and the management institutions are perceived as legitimate and on personal characteristics and social factors [65]. A lab-in-the-field experiment with Tanzanian fishers found that risk taking of fishers increases the rate of risky decisions of the peers, while risk avoiding behavior is not imitated [42]. Concerning the behavior of fishers, one has to consider that the reaction to adverse events tends to depend on the perceived cause of the event: If the event is attributed to an anthropogenic cause (as opposed to a natural cause), participants in an experimental study were found to respond by reducing the exploitation, even at a cost to themselves [46].

## 2.3 Institutions, regulations and enforcement

The formal institutions around Lake Victoria have low effectiveness in combating violations of the fishing regulations due to weakened state capacity and limited resources for monitoring and enforcement [48]. In the 1990s, the World Bank initiated and funded coordination and management efforts resulting in the re-establishment of the Lake Victoria Fisheries Organization (LVFO) in 1997, under the remit of the East African Community (EAC), with the mandate to promote the sustainable management and development of fisheries and aquaculture [152]. With the following establishment of local, community-based Beach Management Units (BMUs) in the late 1990s, the regulators aimed to enhance the participation of the fishers' communities in the surveillance and enforcement of the fishing rules [65, 157]. Today, there are BMUs at most landing sites of the lake which provide information and enforce the regulations. In Kenya, fishers must be registered at the local BMU to land and sell the catch. The BMUs are obliged to report illegal fishing practices, but often omit to do so. Furthermore, they are subject to practices of corrupt fisheries officers, and they are occasionally involved in conflicts with village governments [152]. While the BMUs successfully reduced the use of poison and dynamite fishing and lead to an increase in the efficiency of the fisheries through knowledge exchange, their overall effectiveness is contested [65, 157].

The regulation of the Nile perch fishery is in the form of restrictions of the inputs (legal fishing gears) and outputs (minimum catch size and the slot size for industrial processing) [65, 80]. There are no quotas or restrictions on the number of boats [78]. Fishers have to pay a small annual fee (approximately 20 US dollars, equivalent to the gross revenue from one to two days of fishing), but apart from that, there is no entry restriction [65]. For gill nets, the minimum legal mesh size is 5" in Kenya, 6" in Tanzania and 7" in Uganda, respectively, and for longline hooks, the sizes 4-9 are legal<sup>1</sup> [122]. The minimum catch size is 50 cm and the slot size range is 50-85 cm [157, 124].

The rules are enforced through visits at landing sites and patrols on the lake. Fishing officers carry out patrols on the lake and inspect landing sites with random sampling of vessels. If a violation is detected, the illegal gear is destroyed, the catch is confiscated, and the fishers may be fined [65]. This direct enforcement is intended to deter illegal gear use as fishers would incorporate the monetary damage from

---

<sup>1</sup>To each longline hook size, a number is assigned, with the main sizes ranging from numbers 4 to 14 [122, 80]. Smaller numbers indicate larger hooks.

## 2 Overview of the Nile perch fishery

the risk of detection and punishment into their decision about (non-)compliance. In practice, however, the result is infrequent, but harsh enforcement that leads to the destruction of fishers' livelihoods and to serious conflicts between fishers and officers. Therefore, the approach is criticized for creating limited deterrence at a high societal cost [109, 157, 29, 156]. Subsidizing legal gears instead of the detect-and-punish approach might be an alternative [47].

Despite the regulation of fishing gears, there is still vast non-compliance around Lake Victoria, which has various reasons, primarily the wish for better catches and higher income [29].

### 2.4 Previous modeling approaches

With regard to the population structure, the models of the Nile perch fishery at Lake Victoria can be classified into single compartment models [60, 195], stage models that distinguish between juvenile and adult Nile perch [57, 146] and models with an age structure [105, 153] or size structure [59, 199]. With respect to the number of species, one can distinguish between single species models [105, 59, 60], predator-prey models [195, 199] and ecosystem models like Ecopath with Ecosim (Ewe) [57, 146, 144] or Atlantis [153, 155].

Several studies in the recent years have built and analyzed ecosystem models of Lake Victoria [144]. The two leading ecosystem model frameworks are EwE [30] and Atlantis [73], which comply with the idea of ecosystem-based fisheries management (EBFM) [118, 142]. A study from 2017 assessed the usage of the two leading ecosystem models EwE and Atlantis in the Great African Lakes and found that half of the 14 EwE models were built for Lake Victoria, but (until then) no Atlantis model had been developed [142]. Of the EwE models, only four included an extension of the steady state Ecopath model with the Ecosim component to derive predictions of different management options. None of the models included the spatial component Ecospace and only one of the Lake Victoria models studied a period after the year 2000 [57], and this one was criticized for ecologically unrealistic outputs due to inappropriate parameter estimates [107, 56].

In the meantime, the first Atlantis ecosystem model for Lake Victoria has been developed [153]. It is the first end-to-end whole ecosystem model for the lake, being spatially resolved into 12 areas, including 38 functional groups and four fishing fleets, and the simulation running from 1985 to 2015. The dynamics are captured by differential equations which are solved by a simple forward difference scheme

## 2.4 Previous modeling approaches

[73]. It includes the biological processes of consumption, production, migration, predation, recruitment and mortality, among others. The parameters are initially tuned simultaneously in such a way that no functional group goes extinct, and, in a second step, to reproduce the biomass and catch observations across time. After the validation, the model was used to simulate various fishing scenarios and found that reducing the harvest of the main prey species (haplochromines) would result in the best ecosystem performance, providing the highest yield at minimal socio-economic cost [155].

However, for many of the parameters in the EwE and Atlantis models, there are no measurements available. These parameters have to be estimated and, with various heuristic checks, one seeks to reduce the risk of inaccurate parameter values. The complex nature of the whole-ecosystem models like EwE and Atlantis implies the difficulty to calculate how the uncertainty of the model parameters translates to the uncertainty of the output results. Using multiple ecosystem models for the same scenarios and comparing the results can, to some degree, reduce the potential defects of each single model. A comparison between EwE and Atlantis models under several fishing scenarios showed that the direction of change (increase/decrease) in the abundance of major harvested groups was in agreement, but the magnitude of the change revealed substantial differences [145]. Therefore, using structurally different models and comparing the results is key to giving robust policy advice.

Studies that explicitly model the dynamics of the economic component are rather seldom. A study from 2009 combined a Nile perch growth model (however, without size or age structure) together with a harvest and cost function to find the optimal path of fishing effort over time and to estimate the optimal effort, harvest and rents [9]. They find that a 40% reduction in effort (number of vessels) would increase the harvest by 10% and the economic rents by 227%. An Atlantis study [155] simulates six alternative scenarios of fishing effort with size selective gears, but without explicit adaptation of individual gears.



## **Part I**

# **Size structured model of the Nile perch fishery**



## 3 Biological model

### 3.1 Why use a size structured model?

When one designs a model for a fish population, one has to find the most appropriate way to represent the population, while requiring the model to be mathematically tractable, numerically solvable and still able to capture the characteristic variables that determine how the population will evolve over time. Size structured models, which belong to the more general class of physiologically structured models, offer a mechanistic description of the processes of feeding, growth, predation, mortality, reproduction, spawning and hatching and, quantitatively, the rates at which the processes take place. The size of the fish determines which other organisms it can eat, by which predators it is attacked, how many eggs a female lays, and to which fishing gears the fish is susceptible. The model assumes that size (wet weight) is the determinant trait variable, this means that fish of the same size behave in the same way. Thus we have the following assumptions of the biological model:

#### Assumptions of the biological model

1. The development of the population can be derived from the growth and death rates of individual fish.
2. Each fish has a bio-energetic budget that is supplied from its food and spent on standard metabolism, activity, assimilation, growth and reproduction.
3. The rates of growth, predation mortality and reproduction can be derived from the rates of predator-prey interactions and from the bio-energetic budget of the fish.
4. The rates scale with the size in the form of a power-law relationship.

### 3 Biological model

Weight, rather than age, proved to be the most convenient variable for the formulation of the model for the following reasons. First, the revenue from selling fish is connected to the weight, not the age of the fish. While there are tables of the per-kg price of fish of each weight class, no one pays for a fish dependent on its age. Second, while in most surveys the weight or length of the fish is measured, age is (if at all) much more complicated to measure and surely not possible remotely (like the weight in the hydroacoustic surveys). Third, length and weight can be easily converted into one another with a robust and common conversion formula, whereas the conversion between size and age requires already a model of the growth (e.g. the van Bertalanffy growth equation). Additionally, size/weight structured models are frequently used for fish populations [15, 117, 43, 44, 93, 116, 112, 115, 170, 169, 113, 27, 114], including Nile perch [59, 199] <sup>1</sup>.

## 3.2 Biological processes

### 3.2.1 Growth

Larger fish can search a larger volume for food and thus have a higher (maximum) ingestion rate. Observations show that the maximum ingestion rate scales as a power-law function of weight with the exponent being around 3/4 (Fig. 3.1), which also holds for the maximum consumption [2].

A fish receives energy from consumption, which is then invested into standard metabolism, activity, reproduction and growth. What is left after standard metabolism, assimilation losses and activity is called the "available energy". We assume that this energy also follows a power-law function in the form

$$C(w) = A_C w^n \tag{3.1}$$

with fish weight  $w$ , the metabolic exponent  $n$  and some coefficient  $A_C$ . The power-law form and its exponent can be understood through the following considerations. The food has to be assimilated through the surfaces of the digestive tract. The surface of a cube or a ball would scale quadratic with its length, therefore like

---

<sup>1</sup>To augment the robustness of the conclusions, we have also built and simulated an age structured model in the form of a discrete matrix population model, including an optimization of the fishing pattern to maximize the net present value of yield over a time period of 30 years, which demonstrated the superiority of sparing small fish, in qualitative agreement with the results from this thesis (not shown here).

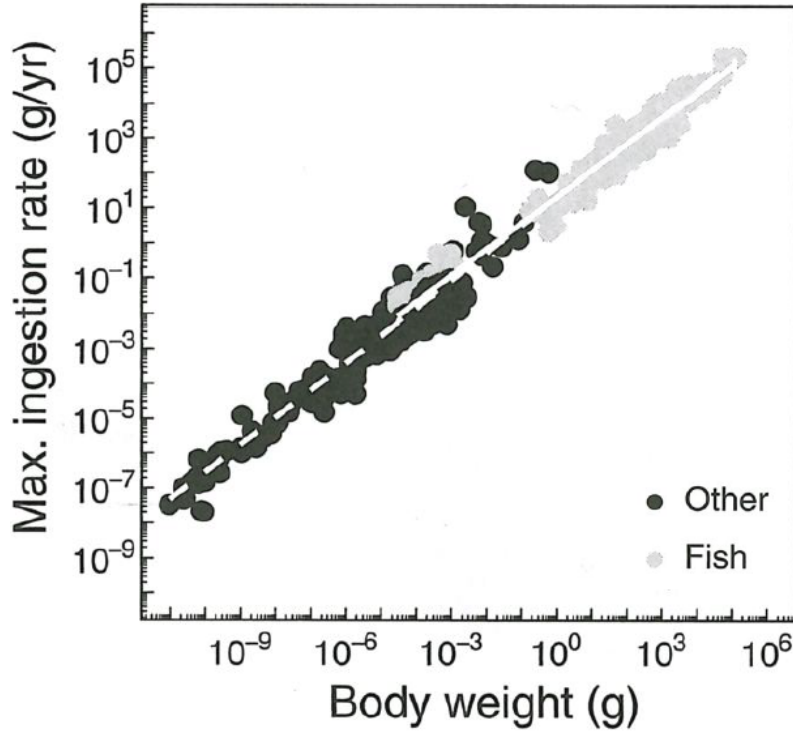


Figure 3.1: The maximum ingestion rate as a function of the body weight for a wide range of fish species (gray points) and other marine organisms (black points). The dashed line is the power-law relationship (fit) of all points, the solid white line has exponent  $3/4$ . Adapted from [2].

$\propto w^{2/3}$  with the weight  $w$  of the object. However, the surface of the digestive tract is strongly folded which increases the exponent. Data show that the exponent  $n = 3/4$  conforms best with data, making it the "canonical value" of the metabolic exponent [8]. Dependent on the availability of food in the ecosystem, only some fraction, called the feeding level, of the maximum consumption is actually achieved. The consumed energy is invested also into standard metabolism, assimilation losses and activity, such that the available energy is a fraction of the consumption rate. For the moment it is only relevant that the scaling  $\propto w^n$  is also valid for the available energy.

For juveniles that do not reproduce yet, we assume that the available energy is invested into somatic growth. Therefore, the juvenile growth rate is

$$g_J(w) = Aw^n \quad (3.2)$$

### 3 Biological model

with the metabolic exponent  $n$  from (3.1) and the growth parameter  $A$  that depends on the availability of food in the ecosystem and on the investments into activity and metabolism.

Mature fish tend to invest a certain fraction of the body weight into reproduction. Let  $\psi_m(w)$  denote the probability that an individual with weight  $w$  is mature, then the energy available for growth is, on average:

$$g_{bp}(w) = Aw^n - \psi_m(w)kw, \quad (3.3)$$

where the parameter  $k$  is a coefficient of the reproduction investment. This model distinguishes between the two phases in the fish life before and after maturation with the transition determined by the maturation function  $\psi_m(w)$ . Therefore this model is a "biphasic growth model" [2]. As derived in [2], the fraction invested into reproduction  $k = AW_\infty^{n-1}$  is related to the growth parameter and the asymptotic weight  $W_\infty$ , therefore the biphasic growth rate can be re-formulated:

$$g_{bp}(w) = Aw^n \left( 1 - \psi_m(w) \left( \frac{w}{W_\infty} \right)^{1-n} \right). \quad (3.4)$$

Later the results from the biphasic model will be compared to the van Bertalanffy (vB) growth curve [188]

$$\begin{cases} \frac{dL(t)}{dt} = K(L_\infty - L(t)) \\ L(t_0) = 0, \end{cases} \quad (3.5)$$

where  $L$  is the length of the fish,  $L_\infty$  the asymptotic length,  $t_0$  the time of zero length and  $K$  the curvature parameter. This differential equation has the solution

$$L(t) = L_\infty \left( 1 - e^{-K(t-t_0)} \right). \quad (3.6)$$

The length-at-age curve describes a deterministic, density independent life history, where  $K$  measures the curvature of the length-at-age function and  $L_\infty$  the asymptotic length at which the growth rate vanishes. As fish start their life with a finite size, one has to introduce the hypothetical (negative) time  $t_0$ , where the fish would have zero length. The van Bertalanffy growth formula is used frequently, also for Nile perch [196]. Later it is shown that the growth curve which emerges from the growth rate (3.4) is not identical to the vB growth curve, but reproduces its shape.

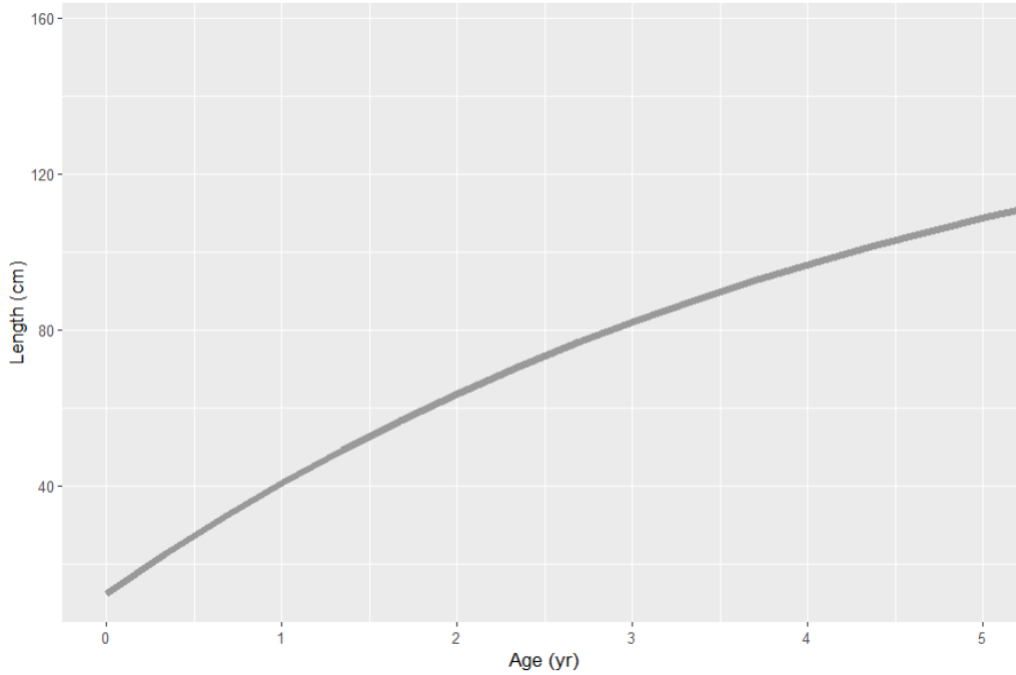


Figure 3.2: The van Bertalanffy growth curve connects the length of a fish to its age. Here the curve for Nile perch with the parameters from Table 3.1.

### 3.2.2 Reproduction

During the lifetime, fish become mature, but not all fish mature at the same size. Therefore one measures the likelihood that a fish with weight  $w$  is mature. An example of the maturation curve is provided in Fig. 3.3. We adopt the common assumption that there are always enough males to fertilize the eggs such that the reproduction is only limited through the eggs that are laid by the females. The maturation curve is modeled through the likelihood  $\psi_m(w)$  that a female is mature:

$$\psi_m(w) = \frac{1}{1 + \left(\frac{w}{w_m}\right)^{-\kappa}} \quad (3.7)$$

where  $w_m$  is the weight at which the likelihood is 50% and the exponent  $\kappa = 5$  determines the steepness of the maturation curve.

As mentioned before, the investment into reproduction is proportional to the weight, so the average investment is  $\psi_m(w)kw$ . The investment is transformed into egg weight with the reproductive efficiency  $\epsilon_{egg}$ , such that the relative reproductive output (egg weight divided by spawner weight) of a female with size  $w$  is

$$R_{egg} = \epsilon_{egg}k = \epsilon_{egg}AW_{\infty}^{n-1}. \quad (3.8)$$

### 3 Biological model

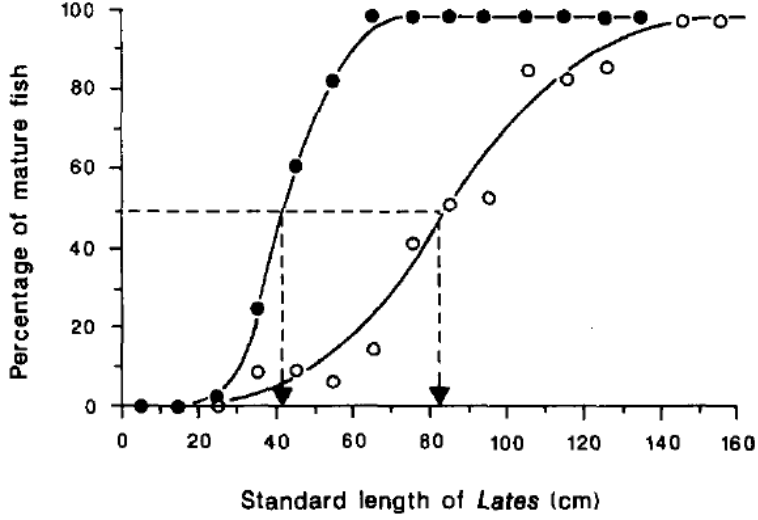


Figure 3.3: The percentage of mature males (filled circles) and females (empty circles) of Nile perch in Lake Kyoga from measurements between 1978 and 1982. Arrows indicate the length at 50% maturity. From [160].

The spawning stock biomass of the population is the expected value of the biomass of the mature fish in the stock:

$$SSB(t) = \int_{w_0}^{W_\infty} w\psi_m(w)u(w, t)dw, \quad (3.9)$$

where  $u(w, t)$  is the number density of individuals with weight  $w$  at time  $t$ . Then the total reproductive output (weight of eggs) is

$$B_{egg} = R_{egg}SSB, \quad (3.10)$$

which contains

$$N_{egg} = \frac{1}{w_0}R_{egg}SSB \quad (3.11)$$

individuals eggs, where where  $w_0$  is the average egg weight. The fact that only females lay eggs, while the  $SSB$  is calculated from both males and females, is compensated for in the numerical value of  $\epsilon_{egg}$ .

#### 3.2.3 Recruitment

In fish population models, it is often assumed that most processes of growth and mortality are density independent [26]. This means that the rates do not depend on

the number of individuals in the population<sup>2</sup>. If the population is larger or smaller, the rates stay still the same. This presupposes that the individuals act independently of each other and do not compete for resources, shelter or prey in a way that would influence the growth rate or the mortality rate [190]. Density dependence, on the contrary, means that the growth rate or the mortality rate is influenced by the number of fish in the population (the population size). To simplify the modeling of fish populations, it is common to assume that the density dependent processes are concentrated in one phase of the life (typically the early stage) and only in that stage somatic growth and natural mortality are influenced by the population size. This assumption seems to be valid in large habitats (like large lakes and marine systems), while in small lakes, density dependent regulation can also occur late in life [6].

The first phase in life, where the mortality is strongly influenced by the density of individuals, is called the recruitment phase. The fish that survive are called "recruits" or "recruited fish". During the recruitment phase, it is assumed that the fish compete strongly and that the mortality increases with a higher density of individuals. This means that a smaller *proportion* of fish survives if more eggs are laid (and fertilized). Conversely, if the number of fertilized eggs is reduced (e.g. by a reduced number of spawning adults), the density dependent mortality is also lower due to a reduction in competition, consequently the number of surviving recruits is reduced less strongly. In this way, the density dependent mortality "compensates" for the reduction in the spawning stock, therefore the density dependence is referred to as "compensatory" [26].

There are various shapes that are used for the recruitment function (a list can be found in [92]). One of the most common is the Beverton-Holt recruitment function which has two parameters: the "shape parameter"  $\alpha$  of the slope of the recruitment function in the origin that describes the coefficient of proportionality between eggs and recruits for low densities, and secondly, the "scale parameter"  $\beta$  that determines that maximal recruitment [45]. If the number of fertilized eggs tends to infinity, the number of recruits goes to the ratio  $\alpha/\beta$ . The functional form of the Beverton-Holt recruitment is  $R = \frac{\alpha SSB}{1 + \beta SSB}$ , where  $SSB$  denotes the spawning stock biomass.

Assuming that a fraction  $\epsilon_R$  would survive in the density independent case, the "shape parameter" is  $\alpha = \epsilon_R R_{egg}/w_0$ . Defining the maximum recruitment propor-

---

<sup>2</sup>In general, the numbers per volume are relevant (therefore the term density dependence), but for a lake with a well-mixed population, numbers and density are equivalent.

### 3 Biological model

tion  $\alpha/\beta$  as  $R_{max}$ , the Beverton-Holt recruitment function can be re-written as

$$R_{BH}(SSB) = \frac{R_{max} \epsilon_R \frac{R_{egg}}{w_0} SSB}{R_{max} + \epsilon_R \frac{R_{egg}}{w_0} SSB}. \quad (3.12)$$

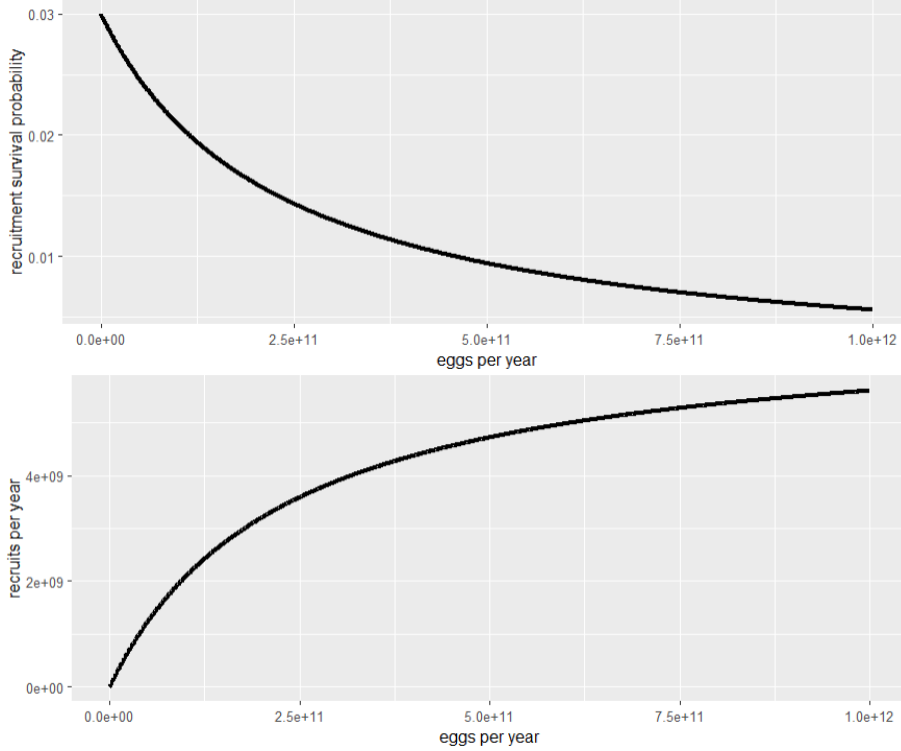


Figure 3.4: Recruitment survival probability decreases with the number of eggs due to competition (compensatory density dependence, top). The process is modeled in the form of a Beverton-Holt recruitment function, where the (absolute) recruitment (number of recruits) converges toward the maximum recruitment (bottom). Curves from the model with parameters from Table 3.1.

#### 3.2.4 Mortality

Individual fish experience various forms of mortality. They can die from being eaten by other fish (predation mortality), from being harvested (fishing mortality) or from other natural causes, e.g. dying of age (senescent mortality). Fishing mortality is the technical term used in the biological modeling, which simply represents the consequences of harvesting from the perspective of the fish population. The fish killed from fishing (if not discarded) constitute the harvest (also called catch or yield) which is the prime variable in bio-economic modeling.

As most fish die from predation or fishing and only very few ones from mere age or other deceases, the main model does not include other causes of mortality besides fishing and predation. To test the robustness of the results, however, also a model with a senescent mortality is simulated.

From considerations of the community size spectrum [7], it can be shown that the predation mortality scales like  $\mu_p(w) \propto w^{n-1}$ . With the introduction of a new parameter, the physiological mortality  $a$ , the predation mortality reads [2]:

$$\mu_p(w) = aAw^{n-1}. \quad (3.13)$$

For the cases with a senescent mortality, two different shapes are used: First, increasing linearly with weight ,

$$\mu_s = \frac{2w}{W_\infty}, \quad (3.14)$$

and second, a hyperbolic shape,

$$\mu_s(w) = \frac{\alpha_s}{a_\dagger - \text{age}(w)}, \quad (3.15)$$

where  $\alpha_s \in \{1, 3\}$  parametrizes the strength of the mortality,  $a_\dagger = 16yr$  is the maximum age [181] and  $\text{age}(w)$  the age at weight  $w$ , respectively. As little is known about the senescent mortality of Nile perch, we set the parameters to produce roughly realistic values. The hyperbolic senescent mortality has the purpose that the integral of the mortality up to any age below the maximum age is finite, but it diverges at the maximum age, which will be used in Chapter 6 for the mathematical proofs.

## 3.3 Size spectrum

The size structure of a population is a function of length or weight that describes how many fish of each size there are in the population. It can be represented in numbers or as biomass contribution. The number spectrum indicates how many fish of the population have a specific size. As the size dimension is continuous, the respective quantity is the number density  $u(w)$ , such that the number of fish with weight between  $w_1$  and  $w_2$  is  $\int_{w_1}^{w_2} u(w)dw$ . If multiplied with weight, the number spectrum turns into the biomass spectrum. We give the definition of two basic concepts (for a glossary with detailed explanations, see [183]).

### 3 Biological model

#### Size structure

**Definition 3.1.** The size structure of a population is a function of size (length, weight) and it describes how frequent the fish of each size appear in the population. It can be represented in numbers or as biomass contribution. In a continuous setting, it is technically a density: numbers (or biomass) divided by the width of the size bin.

#### Size spectrum

**Definition 3.2.** The size spectrum is the diagram that displays the size structure of a population: the number density as a function of size (weight). When it shows the biomass density, it is called a biomass spectrum.

Later it will be useful to consider the quantity called cohort biomass. In the equilibrium, the distribution of cohorts over size is identical to the development of one cohort over time [50]. If the survival probability from birth to size  $w$  is given by  $P(w)$ , then the biomass of one cohort at weight  $w$  is [2]

$$B_{coh}(w) = P(w)w. \quad (3.16)$$

## 3.4 Parameters

The parameters are informed from biological studies, official landings statistics and catch assessment surveys [102]. Limnological data, length frequency assessments, grow parameters estimations and catch assessment surveys have been conducted over the years around LV [105, 149]. Here we explain the biological parameters used in the simulations (Table 3.1). The length-weight conversion of Nile perch in LV,

$$w = cL^b, \quad (3.17)$$

was established in [103] with the parameters  $c = 0.0042$ ,  $b = 3.26$ . The van Bertalanffy growth constant comes from [196], the age-at-zero-length from [69]. The asymptotic weight and the weight at maturation come from [199]. The growth coefficient is calculated from the life history parameters according to (B.7). The adult mortality  $M$  is calculated using the formula from [165] with  $K$  and  $L_\infty$ . The physiological mortality is hard to measure directly, but there are two ways to estimate it: First, from the life history parameters, second from theoretical feeding consid-

erations (see Appendix B.2). As the estimates from the two ways disagree (0.244 and 0.522, respectively), but the first estimate is more closely related to measurable parameters of Nile perch, we use  $a = 0.3$  as standard throughout the thesis, and additionally we test how the results would change with  $a \in \{0.2, 0.3, 0.4, 0.5\}$ . Furthermore, we calculate the sensitivity of results with respect to  $a$  (section 7.4).

Table 3.1: The species-specific standard parameters used in the model simulations, if not stated otherwise.

parameter	value	explanation	source
$c$	0.0042	length-weight-coefficient	[103]
$b$	3.26	length-weight-exponent	[103]
$K$	0.22	van Bertalanffy growth constant	[196]
$t_0$	-0.37	van Bertalanffy age-at-zero-length	[69]
$W_\infty$	60,000 g	asymptotic weight	[199]
$L_\infty$	156.6 cm	asymptotic length	from $W_\infty$
$w_{mat}$	4400 g	weight at maturation	[199]
$\eta_m$	0.0733	relative maturation size	$w_{mat}/W_\infty$
$A$	13.02	growth coefficient	(B.7)
$M$	0.39/yr	adult mortality	[165]
$a$	0.3	physiological morality	model standard (see text)

Table 3.2: The species-independent parameters used in the model simulations from [4].

parameter	value	explanation
$n$	0.75	metabolic exponent
$\epsilon_{egg}$	0.22	reproductive efficiency
$w_0$	0.001 g	egg weight
$\epsilon_R$	0.03	recruitment efficiency



## 4 Economic model

### 4.1 Open access fishery

A fish stock without access restrictions is a common pool resource with a rival, but non-excludable good: Each fish can only be caught by a single fisher (rival), but it is not possible to prevent fishers from catching fish (non-excludable) [34]. These properties are captured in the concept of an open access fishery that is defined by three characteristics.

#### Open access fishery

**Definition 4.1.** A fishery is called open access if it fulfills the following properties [166].

1. The fishery is exploited by a large number of independent fishing ‘firms’.
2. There are no impediments to entry into or exit from the fishery.
3. There are no property rights over the resource *in situ*, i.e. the fish in the water.

The first two conditions are contained in the standard perfect competition model, while the third property is characteristic of the open access situation and is connected to the fact that the fish are spatially mobile within the lake.

In the Nile perch fishery, there are approximately 40,000 vessels targeting Nile perch [122], acting independently without the existence of monopolistic firms, therefore the first condition is fulfilled for LV. There is no restriction on the total number of boats and apart from a license fee there is no entry impediment. The annual license fee is not a serious impediment as it is around 20 US dollars, corresponding to the gross revenue from one to two days of fishing [65]. In addition, at LV, there is no scheme in place that would assign property rights to individual boat owners, therefore LV can be effectively considered an open access fishery.

#### 4 *Economic model*

The consequence is that the exploitation of the resource forms an externality, where the individual fishers do not incorporate the stock externality of their activities - the reduction in the resource level - into their economic decisions [110]. This situation would lead to the dissipation of all rents, as has been famously derived by Gordon [81] and Scott [178] and popularized as the "tragedy of the commons" by Hardin [90]. The individually rational agents act collectively in a way that can eventually bring about the destruction of the resource, in this case the collapse of the fish stock.

A common solution to mitigate the stock externality is the allocation of individual transferable quotas (ITQ). The owner of the ITQ has the right to harvest a specified quantity of the stock, and the right is divisible and transferable across the resource users [34]. At LV, there is no quota scheme implemented, and it is not among the realistic options in the range of policies that are currently broadly discussed among the LV managers. Due to the weak institutional power, no entity could currently implement and enforce an ITQ scheme. Rather the realistic and widely discussed policy options focus on restrictions of the fishing gears and techniques, together with protected areas or closed seasons. The analysis of restrictions on the legal gears requires an understanding of the size selectivity of the gears which is developed in the following sections.

## 4.2 **Size selectivity**

Two notions of overfishing can be distinguished. "Recruitment overfishing" describes a situation where the fish are harvested before maturation such that the fraction reaching the reproductive age is not sufficient to replenish the stock. The other notion, "growth overfishing" means that the fish are harvested when the growth potential is not efficiently utilized, i.e. before they reach the economically optimal size for harvest [50, 135]. Models without a size or age structure like the standard Schaefer production model capture only recruitment overfishing. In order to incorporate both types of overfishing, the model of this thesis is size structured both on the biological and the economic side.

In addition, this relates closely to the current and proposed regulations of the Nile perch fishery that focus on size restrictions of the gears and the landed fish. The size structured model is therefore suited to assess the fishery regulations of the Nile perch fishery.

In this section, concepts around the selectivity are introduced [192, 131, 191]. We begin with the exploitation pattern.

#### Exploitation pattern

**Definition 4.2.** The exploitation pattern is the "distribution of fishing mortality over the length or age composition" of the fish population [67].

Fishing mortality is here the technical term describing the effect of harvesting on the fish population. The fishing mortality is a function of the size of the fish. The size selectivity of a gear is described by the retention probability, here in the sense of the contact selection curve<sup>1</sup>.

#### Retention probability

**Definition 4.3.** The retention probability is proportional to the probability that a fish of size  $w$  is entangled in the net once it has touched the net. It determines the size selectivity of a gear. Often, the retention probability is normalized such that the maximum equals one.

The cumulative result of the retention curves in a fishery, weighted by the frequency and effectiveness of each gear, is the "exploitation pattern", also, typically if normalized, it is called "fleet selectivity".

#### Gear selectivity, fleet selectivity, yield and income

**Definition 4.4.** The gear selectivity  $\psi_F^j(w)$  is the retention probability of a specific gear  $j$  (e.g. a gillnet with a particular mesh size or a longline with a particular hook size). The fleet selectivity  $\psi_F(w)$  is the sum of the fishing selectivities of all gears uses in the fishery, weighted by the frequency  $E_j$  and catchability  $q_j$  of each gear.

$$\psi_F(w) = \sum_j E_j q_j \psi_F^j(w) \quad (4.1)$$

<sup>1</sup>Because of the lack of detailed data, we assume that the availability (which part of the fish population is available to a gear) and the avoidance (whether fish avoid a gear when they are close to it) is independent of the fishing gear. Consequentially, there is no need to differentiate between the "contact-selection-curve" (relative probability that a fish is captured once it has touched the gear), the "available-selection-curve" (relative probability that a fish is captured if it is available) and the "population-selection-curve" (relative probability that a fish from the population is captured) [131].

#### 4 Economic model

The aggregate harvest of the vessels using gear  $j$  from a fish population  $u(w)$  is

$$Y^j = \int_{w_0}^{W_\infty} u(w)\psi_F^j(w)dw. \quad (4.2)$$

If  $\psi_F(w)$  is the normalized fleet selectivity and  $F$  the level of fishing intensity, then the fleet induces the fishing mortality

$$\mu_F(w) = F\psi_F(w) \quad (4.3)$$

on the population  $u(w)$ . This leads to aggregate harvest

$$Y = \int_{w_0}^{W_\infty} u(w)\mu_F(w)dw \quad (4.4)$$

and fishery income

$$I = \int_{w_0}^{W_\infty} p(w)wu(w)\mu_F(w)dw, \quad (4.5)$$

where  $p(w)$  is the per-kg price of a fish with weight  $w$ .

There are two important categories of gears with respect to the shape of the selectivity function. With gillnets, the fish get entangled in the net with their gills. These nets only catch in a specific size range: Smaller fish can pass through the mesh holes and can escape, while larger fish are too big to get entangled with the gills. Therefore, gillnets belong to the gears with a unimodal selectivity curve (Fig. 4.1). Dependent on the type, construction, employment and operation of the gears, the peak can be broader or more narrow, which has to be determined empirically. The selectivity curve  $\psi_{GN}$  of gillnets is modeled with a normal (Gaussian) function,

$$\psi_{GN}(L) = \exp\left(-\frac{(L - \mu)^2}{2\sigma^2}\right), \quad (4.6)$$

where  $\mu$  is the mean and  $\sigma$  the standard deviation (4.6) [131]. The standard deviation and the variance  $\sigma^2$  determine the width of the curve, while  $\mu$  marks the point of the largest selectivity, i.e. the peak of the selectivity function, where  $L$  is the total length of fish.

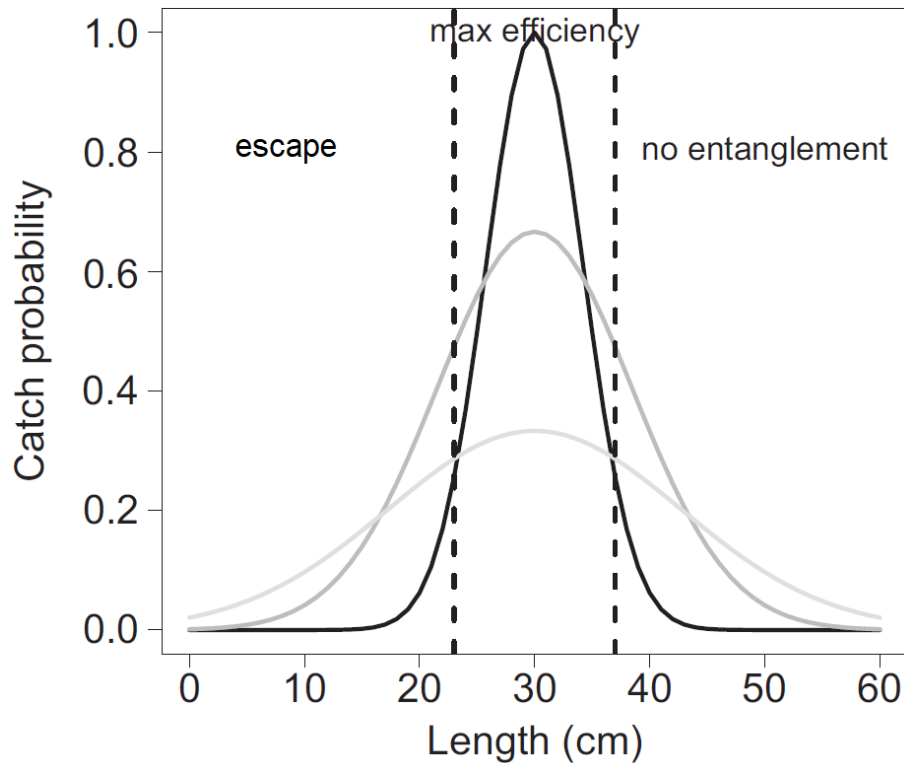


Figure 4.1: Gillnets have a selectivity curve that is unimodal with one peak that marks the point of highest catch probability. Smaller fish can escape (left), while larger fish do not get entangled in the net (right). The curve can be more narrow (black) or broader (gray) depending on the gear specifications and the fishing methods. Adapted from [67].

In the second category, the selectivity function has a sigmoidal shape (Fig. 4.2). Small fish escape through the mesh, while all larger fish are caught. Typically, trawl fishing is modeled with a sigmoidal retention curve, even though also here some of the larger fish could escape due to having a higher swimming speed than the speed of the trawl boat [108].

For longline hooks, it is not a priori clear to which category they are most similar, and, what is more, the selectivity depends in large parts on the bait type [80]. Therefore, for longlines, we derive the fishing selectivity only from empirical data and do not prescribe a specific shape of the function.

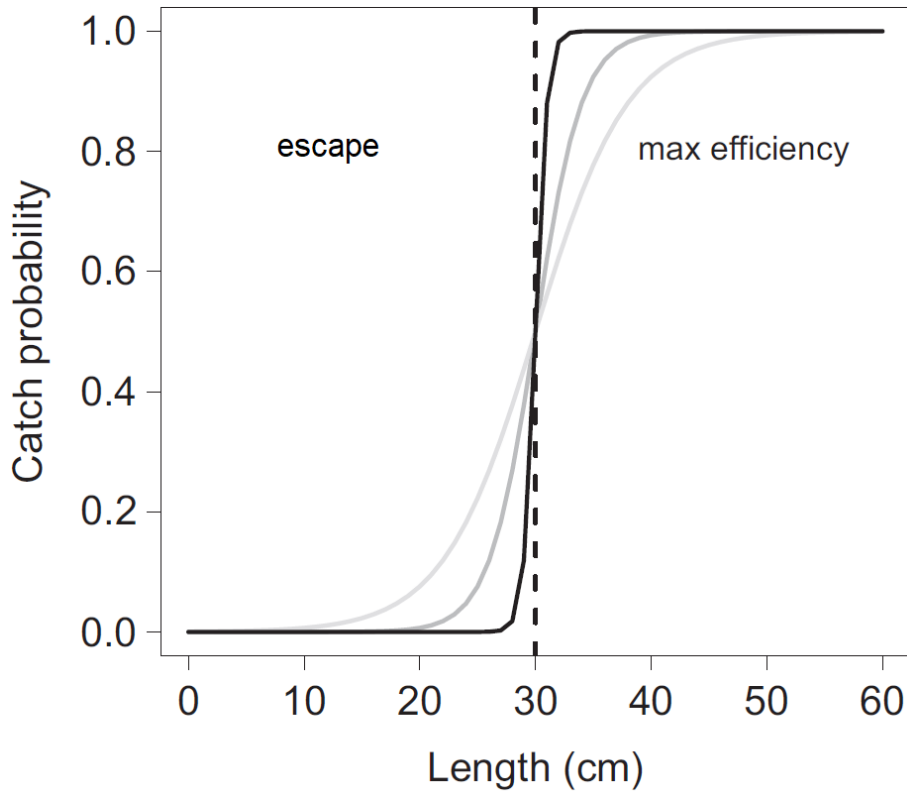


Figure 4.2: The selectivity (catch probability) of trawl-like gears has a sigmoidal shape. The transition between the non-selective range (left) and selective range (right) can be more or less steep (black to gray). Adapted from [67].

### 4.3 Bio-economic fishery model

In this section we explain the fishery model. First we briefly introduce the classic thinking about the relationship between harvest and effort, followed by the translation to the size structured case with a gear-differentiated fishery.

#### 4.3.1 Harvest and effort

The fishery production model determines the harvest in each period, and it depends on two factors: First, on the resources devoted to fishing by the boat owners, which is called fishing effort  $E$ , measured as number of boat trips (vessel-days) during the respective period. Second, the harvest depends on the biomass  $S$  of fish in the lake that is susceptible to the gear. Then harvest  $Y$  (also called yield or catch) is [166]

$$Y = Y(E, S). \quad (4.7)$$

Often it is assumed that the catch is proportional to both effort and stock level,

$$Y = qES, \tag{4.8}$$

where  $q$  is the "catchability coefficient". In that case,  $F = qE$  is the "fishing mortality", with units of 1/time. This linear<sup>2</sup> form is also called the catch-per-unit-effort (CPUE) production function because the value  $Y/E = qS$  is proportional to the stock level  $S$  with a fixed coefficient of proportionality  $q$ . The assumptions behind the CPUE production function are (1) the uniform distribution of the fish population in the water, (2) non-saturation of fishing gears and (3) non-congestion of fishing vessels [31].

Schaefer develops the rate of change of fishing effort,  $dE/dt$ , by assuming "that the incentive for new investment is proportional to the return to be expected" [176], in other words a linear relationship between the rate of change and the profit  $\Pi = pY - cE$  (revenue), which is the difference between the income  $I = pY$  (catch weight times average per-kg price  $p$ ) and the fishing cost  $C = cE$ , where  $c$  is the cost per unit of effort [81, 176]. If one assumes that the harvest function is linear in stock and effort, and that the costs are linear in effort, the model reads [182, 166]

$$\frac{dE}{dt} \propto E(pqS - c). \tag{4.9}$$

### 4.3.2 Fishery production function

Now we need to develop a fishery production function with size selective gears. To capture the fact that the fishery is composed of vessels using different gears, we disaggregate the fishery into sub-fleets. A sub-fleet consists of all vessels using a particular gear. Therefore, if there are  $J$  gears (gillnets with different mesh sizes and a generalized longline gear), there will be  $J$  sub-fleets in the model. We assume that the hooks do not differ in their selectivity as most hook sizes produce a similar catch distribution (Fig. 4.3). As we have no data available on the baits, the effect of bait type is not included here. Furthermore, we assume for simplicity that all vessels in a sub-fleet are identical in the catchability coefficient.

---

<sup>2</sup>Next to the linear form,  $Y = qES$ , one often encounters other forms of the harvest function like  $Y = S(1 - e^{-qE})$  [33, 184], or a Cobb-Douglas function  $Y = S^\alpha E^{1-\alpha}$  [187, 186] or a function with a schooling parameter  $d$ ,  $Y = qES^d$  [9].

#### 4 Economic model

Each gear type  $j$  is characterized by the size selectivity  $\psi_F^j(w)$  and the catchability coefficient  $c_j$ , which summarizes the characteristics of the gear as well as the skills of fishers. The governing variable is the number of vessels  $E_j$  (effort) of each gear  $j$ .

In addition, we assume that the fish stock is well-mixed, this means that a spatial dimension is not included, neither is the heterogeneity of fishers in terms of location or skills. We also assume that each vessel uses only one gear.

Going beyond the basic bio-economic models without age or size structure, Beverton and Holt [16] developed a fundamental framework for the study of age structured fish populations. In recent years, the framework has been systematically extended and analyzed with a focus on age structures fish populations [52, 53, 45, 50, 51, 185]. For example, in the case of [185], the harvest  $Y_t$  in period  $t$  is

$$Y_t = B_t^\chi E_t, \quad t = 0, 1, \dots \quad (4.10)$$

with an exponent  $0 < \chi \leq 1$  taking the role of a schooling parameter, where  $E_t$  is effort, and  $B_t$  the "efficient biomass", which is the fish biomass weighted by the age-specific catchability factor. A similar approach was taken in [53], where the harvest  $Y_{a,t}$  of fish in age group  $a$  at time  $t$  from the sub-fleet using gear  $j$  is

$$Y_{a,t} = B_{a,t} F_a(E_t^j, E_t^{-j}, m), \quad (4.11)$$

where  $B_{a,t}$  is the biomass of fish in age group  $a$  at time  $t$  and  $F_a(E_t^j, E_t^{-j}, m)$  is the fishing mortality in that age group, dependent on the effort  $E_t^j$  of the sub-fleet  $j$  from a gear with selectivity  $m$  and on the effort of other gears,  $E_t^{-j}$ . The aggregate harvest from all age classes is then

$$Y_t = \sum_a Y_{a,t} = \sum_a B_{a,t} F_a(E_t^j, E_t^{-j}, m). \quad (4.12)$$

In order to find the corresponding formula for our model, we have to consider that the model has not, like the one in [53], discrete age classes, but a continuous weight structure with number density  $u(w, t)$  such that the number of fish with weight between  $w_1$  and  $w_2$  at time  $t$  is  $\int_{w_1}^{w_2} u(w, t) dw$ . As a consequence of the continuous size structure, we have to use an integral over the weight domain instead of the sum over the age classes.

Therefore, the annual yield  $Y_j$  of sub-fleet  $j \in J$  is the catch of all vessels in the fleet (Definition 4.4) with the integral over the population biomass and the fishing

### 4.3 Bio-economic fishery model

mortality  $E_j q_j \psi_F^j(w)$ ,

$$Y_j = \int_{w_0}^{W_\infty} E_j q_j \psi_F^j(w) w u(w) dw, \quad (4.13)$$

where  $u(w)$  is the number density of fish with weight  $w$ . The yield is measured in *kg/yr*.

The aggregate fishing mortality is then

$$\mu_F(w) = \sum_j E_j \psi_F^j(w) \quad (4.14)$$

and the aggregate yield of the fishery is

$$Y = \sum_{j=1}^J Y_j = \int_{w_0}^{W_\infty} u(w, t) w \mu_F(w, E) dw. \quad (4.15)$$

The annual income  $I_j$  of sub-fleet  $j$  is the monetary value of the annual yield, in the unit *US dollars per year*,

$$I_j = \int_{w_0}^{W_\infty} E_j q_j \psi_F^j(w) w p(w) u(w) dw, \quad (4.16)$$

where  $p(w)$  is the per-kg price of a fish with weight  $w$ . The aggregate income  $I$  of the fishery is

$$I = \sum_{j=1}^J I_j = \int_{w_0}^{W_\infty} p(w) u(w, t) w \mu_F(w) dw. \quad (4.17)$$

The variable (operation) costs of sub-fleet  $j$  are assumed to be linear in effort,

$$C_j(E_j) = c_j E_j, \quad (4.18)$$

where  $c_j$  are the costs per unit of effort using gear  $j$ . The aggregate costs of the fishery are

$$C = \sum_{j=1}^J C_j. \quad (4.19)$$

## 4 Economic model

The aggregate profit of the sub-fleet  $j$  is the difference between annual income and annual costs [166],

$$\Pi_j = I_j - C_j. \quad (4.20)$$

and the profit of the fishery is  $\Pi = I - C$ .

### 4.3.3 Fishers' response

In Chapter 10, the scenario will be studied where boat owners respond to the level of profit through entry and exit decisions. We follow the assumption in [182, 166] that the effort will increase as long as the economic profits are positive, and that the rate of entry into or exit from the fishery is proportional to the profit with the coefficient  $k$ , where we use  $k = 10^{-3}$  in the unit *vessels per US dollar*.

The assumption that the boat owners of each sub-fleet adapt the number of vessels  $E_j$  on the lake to the (aggregate) profit  $\Pi_j$  with the rate  $k$  can be formulated as an ordinary differential equation,

$$\begin{cases} \frac{dE_j(t)}{dt} = k\Pi_j(E_j(t), t) \\ E_j(0) = E_j^0, \end{cases} \quad (4.21)$$

where  $E_j^0$  is the initial effort in sub-fleet  $j$ . In the simulation,  $E_j(t)$  is, after each time step, rounded to integer values (numbers of vessels).

## 4.4 Fisheries reference points

In fisheries management, reference points play a crucial role as guide for sustainable harvesting. There are two types: target reference points that act as management goals, and limit reference points that can be understood as thresholds beyond which the stock is depleted in such a way that the fishery is at risk. Each type can have one of two forms: (1) level of biomass or spawning stock biomass (SSB) and (2) level of the exploitation, i.e. the fishing mortality [2]. In general, both types are involved in the analysis of the state of a given stock. If, for example, the target biomass level is reached, but the fishing mortality exceeds the limit reference point and is expected to do so for a substantial time, then the biomass will become impaired with time and will finally fall below the biomass limit reference point. Probably the most famous reference point is the maximum sustainable yield (MSY). Here

the fish stock is regarded as a production facility where one seeks to maximize the steady state output (yield). As Andersen [2] pointed out, 'sustainable' in 'maximum sustainable yield' actually rather means 'sustained', i.e. in steady state, and does not necessarily refer to other, broader concepts of sustainability.

#### Maximum sustainable yield (MSY)

**Definition 4.5.** Maximum sustainable yield is the "maximum average annual catch that can be removed from a stock over an indefinite period without having any negative effect on resource potential production under prevailing environmental conditions." [124] The fishing mortality that leads to MSY is referred to as  $F_{MSY}$ .

Fishing has in two aspects negative impacts on the stock. First, it depletes the current stock, and second, it reduces the stock's reproduction and thus the future stock. The recruitment connects the first effect to the second. In many cases, however, only the first effect is considered. This is equivalent to an analysis of the 'yield per recruit',  $Y/R$ , i.e. the yield normalized by recruitment. If the recruitment of a stock is not impaired by fishing, it is a legitimate approximation to the actual steady state yield, but it is not applicable if the recruitment is notably affected by fishing.

The idea of maximum sustainable yield also translates to size structured models of the fishery, but here the situation becomes more complicated: not only the amount of biomass extracted from the stock matters - but also *which* fish are harvested, i.e. the size distribution of the harvest. Therefore, an optimal situation implies that both the level of fishing effort and the target size of fish are chosen optimally [49]. As the fishery consists of a range of gears, it is possible to optimize the effort (number of vessels) of each sub-fleet.

## 4.5 Gear selectivity

The size selectivity was derived in the following way (see [80] for more details). The data sources are the catch assessment surveys (CAS) from 2005-2015 and the frame surveys (FS) 2010 and 2020. In the CAS, for each boat the weight of the catch and the number of fish in the catch are reported. After filtering the data for vessels that only use one type of gear and one size, the dataset contains 16,549 observations for gillnets and 11,225 for longline hooks. For each vessel, the average weight and

#### 4 Economic model

length of the fish are calculated. Then, for each gear type and size, the distribution of the average length is calculated.

Assuming that the fishing operation represents a Poisson process [132] and further assuming that the average length scales proportional to the mesh size, the parameters can be fitted to the distribution, for each gear type and size [80]. For hooks, the data show that the average length does not scale with the hook size (Fig. 4.3, compare also to [139, Figs. 5 and 6]). From the size distribution of the catch and the gear selectivity of gillnets, the supposed size distribution of the fish in the lake is calculated. Then the selectivity of hooks can be derived directly from the catch distribution without requiring an assumption on the shape of the hook selectivity curve. The catch distribution of longline hooks is shown in Fig. 4.3.

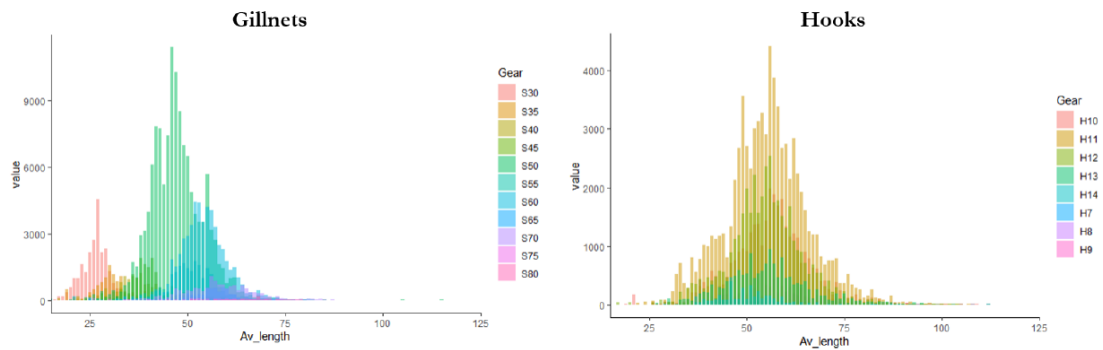


Figure 4.3: The (frequency) distribution of the average length (cm) of the catch per boat, for gillnets 3” to 8” (left) and for hooks of size 7-14 (right). From [80].

The results, the selectivity curves, are depicted in Fig. 4.4 and given in Table 4.1. The peak of the selectivity curve of 3” gillnets is at 28.6 cm and for larger mesh sizes it increases in proportion<sup>3</sup>.

It is important to note that the smallest legal mesh size, 5”, has the peak of the selectivity curve at 47.7 cm, i.e. outside of the slot size range 50-85 cm. This means that even strict adherence to the gear regulation would produce a significant share of the catch being below 50 cm. In fact, 56.6% of the area under the selectivity curve

<sup>3</sup>It is important to mention that the selectivity curve is not necessarily identical to the size distribution of the catch, in fact they disagree in general. They are related by the size distribution of the fish population in the lake. For a uniform distribution (equal numbers of all sizes in the lake), selectivity curve and catch distribution are identical. For a population that has a decreasing population density (more small than large fish), the peak of the catch is distribution is, in general, to the left of the peak of the selectivity curve (cf. also [175]).

are below 50 cm for 5" gillnets (Table 4.2). For gillnets with 7", only 5.3% of the area are below 50 cm.

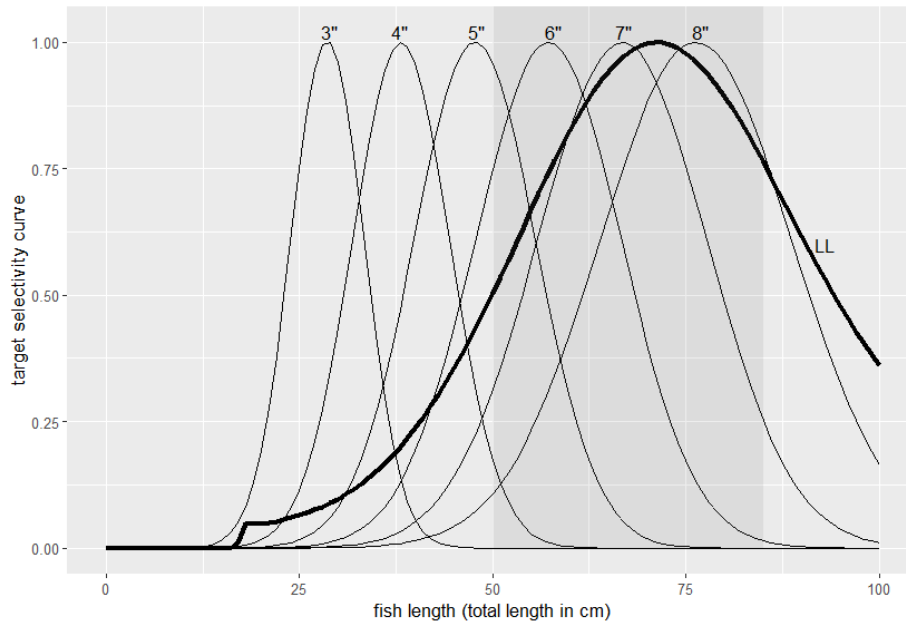


Figure 4.4: The fishing selectivity curves of gillnets 3"-8" (thin) and longline hooks (bold). The kink at the left of the longline curve comes from sparse data (very few small fish in the catch of longlines).

## 4.6 Fleet selectivity

From the selectivity curves of individual gears, one can construct the fleet selectivity using the frequency of each gear in the fishery. Using the frame surveys and the relative fishing power of gillnets versus longlines [80], the fleet selectivity is constructed for 2010 and 2020. Fig. 4.5 depicts the aggregated fishing selectivity for longlines and gillnets as well as the fleet selectivity, together with the respective prediction of the catch distribution. Note that other gears like beach seines or small seines are not included here. The selectivity of 2020 is referred to as the "current fleet selectivity" in the following text.

From 2010 to 2020, the fraction in the catch from gillnets which is below 50 cm has decreased (Fig. 4.5, middle row). This is the result from a shift to a more prominent use of larger gillnets. Whether this comes from the strict enforcement in Uganda [137, 138, 156], the increased demand for large Nile perch through the fish maw (swim bladder) trade [12, 14, 161], or from other causes is still to be discussed.

#### 4 Economic model

Table 4.1: Selectivity parameters of gillnets derived from CAS data from 2020 [80]. Values are the mean  $\mu$  and standard deviation  $\sigma$  of a normal distribution. The values of the mesh sizes 4"-7" were determined from the data, the other values (3", 3.5", 7.5", 8") from a linear extrapolation both of  $\mu$  and  $\sigma$ .

Gillnet mesh size	$\mu$ (cm)	$\sigma$ (cm)
3 "	28.6	4.7
3.5"	33.4	5.5
4 "	38.2	6.3
4.5"	42.9	7.1
5 "	47.7	7.9
5.5"	52.5	8.7
6 "	57.2	9.5
6.5"	62.0	10.3
7 "	66.8	11.1
7.5"	71.5	11.9
8 "	76.3	12.6

There was also a change in the size composition of the longline hooks, but this has not lead to a major change in the selectivity or the catch distribution because of the limited effect of the hook size on the selectivity [80].

Table 4.2: The fraction of the area under the selectivity curve that is below 50 cm, for gillnets 3"-8" and longline hooks.

Gear	Fraction below 50 cm (%)
GN 3"	100.0
GN 4"	95.7
GN 5"	56.6
GN 6"	19.3
GN 7"	5.3
GN 8"	1.4
LL	10.2

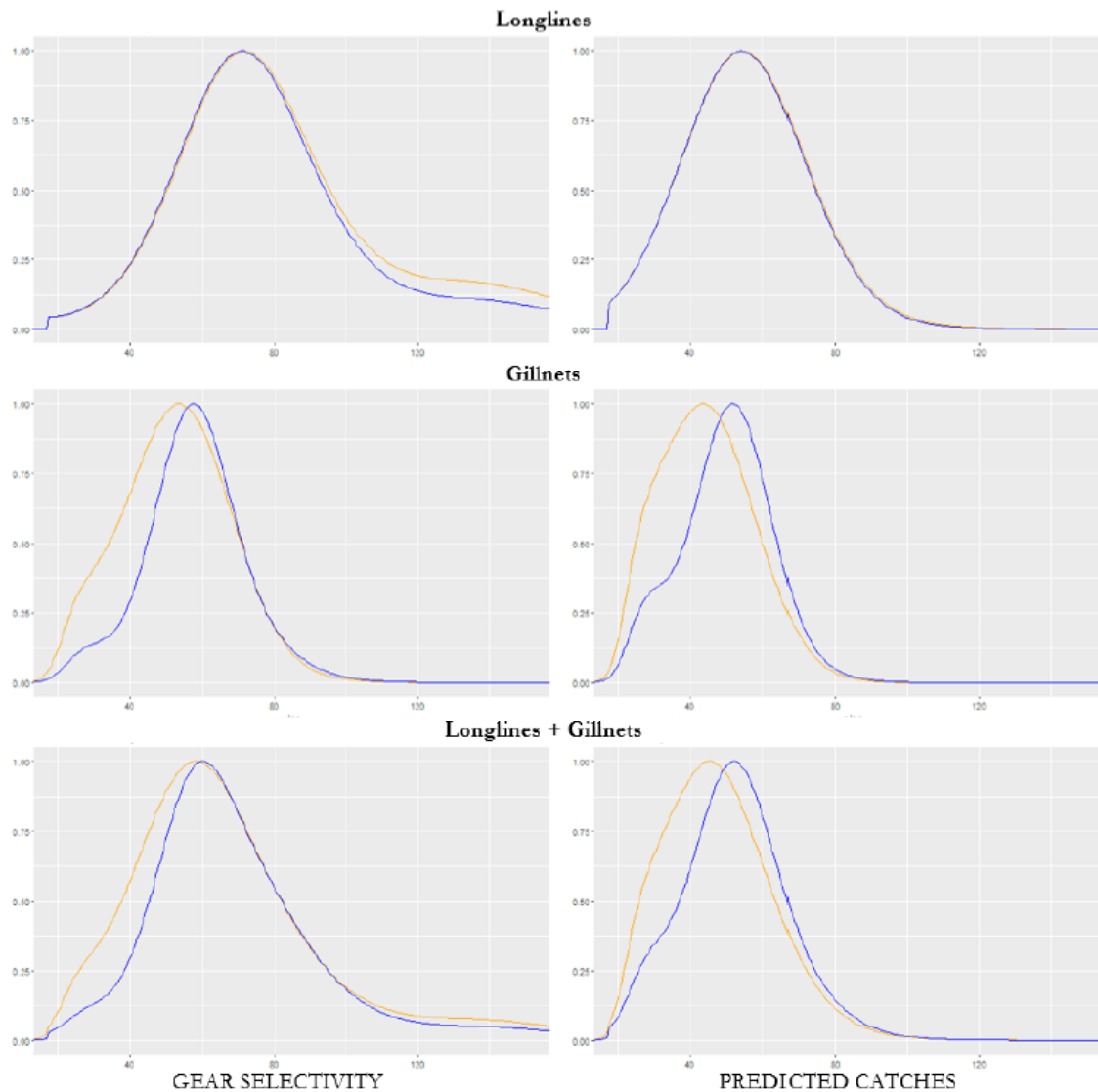


Figure 4.5: The aggregated selectivity of longlines (top left), gillnets (middle left) and the fleet selectivity (bottom left) of the Nile perch fishery in the years 2010 (yellow) and 2020 (blue). The right column shows the predicted catch distribution. The bottom left figure shows that the empirical fleet selectivity peaks at around 60.2 cm (2659.2 g). From [80].

## 4.7 Parameters

The fishery in the model is assembled from a (generalized) longline hook and from six gillnets with mesh sizes ranging from 3" to 8" in steps of 1". The frequency of each gear comes from the frame survey 2016 [122]. The gears with half-integer mesh sizes were assigned to the next lower integer gear (i.e. 3.5" to 3" etc.). Gears below 3" and above 8" are added to the numbers of 3" or 8" gears, respectively. There

#### 4 Economic model

are 39,551 vessels in total that target Nile perch [122]. We take the ratio between gillnet and longline vessels from [80] which makes 23,566 gillnet boats and 15,985 longline boats.

Table 4.3: Numbers of vessels in the standard model derived from [122, Table 2].

gear	numbers
GN3	3,182
GN4	1,562
GN5	4,307
GN6	10,627
GN7	2,295
GN8	1,594
LL	15,985
Total	39,552

Larger gillnets ( $\geq 5.5''$ ) typically use motorized vessels, while the paddle boats dominate for small mesh sizes [137]. As there are only integer-valued mesh sizes in the model, we assume that the boats with gillnets  $\geq 5''$  are operated with motors, the ones  $< 5''$  with paddles. We assume that all vessels with longline hooks are motorized.

The catchability factors  $q_j$  of the gears were chosen such that, for each gear, the simulated catch-per-unit-effort (CPUE) agrees with the empirical CPUE [121]. We assume that motorized gillnets vessels have twice the CPUE of vessels with paddles [137].

The crew wage is 17.36 USD per day (or 6335.76 USD/yr), the remaining part is the revenue of the boat owner [125, 162]. The fuel costs (for the boats with motor) are 14.2 USD per day, the bait costs (only for boats with longline hooks) are 37.5 USD per day<sup>4</sup>. We assume the opportunity costs at 2000 USD/yr, which is around twice the minimum wage for unskilled labor in Kenya [162]. The price per kg of Nile perch (beach value) depends on the size of the fish (Table 4.4). The data come from a survey among Tanzanian fishers collected in March 2021<sup>5</sup>.

For the standard estimate of biomass stock and yield we use the most recent year for which both values are available, which is 2015. The biomass is  $B = 683.18$  kt (1 kt=10<sup>6</sup> kg) [120], and, because of the large fluctuation, for the yield, we use the average of 2014 and 2015, which is  $Y = 208$  kt [121]. Using the model simulation of

<sup>4</sup>A survey among a limited number of Ugandan fishers found that bait costs are in the range 17-58 USD (S. Gómez, pers. comm., Oct. 2022). We use the median of that range.

<sup>5</sup>S. Gómez, pers. comm., 05.10.2022

Table 4.4: Fish price of Nile perch in US dollar per kg.

fish weight (kg)	price per kg (US-Dollar)
<1.0	0.83
1.0 to 2.5	2.086
2.5 to 5.0	2.504
5.0 to 10.0	2.921
10.0 to 15.0	3.338
>15.0	3.548

the current fleet selectivity, maximum recruitment  $R_{max}$  and "pristine" biomass  $B_0$  (biomass in steady state without fishing) are calculated (Table 4.5).

Table 4.5: Standard values of biomass, catch and recruitment in the model.

parameter	value	explanation
B	683.18 kt	stock biomass
Y	208 kt	annual yield
$R_{max}$	$6.904 \cdot 10^9$ /yr	maximum recruitment
$B_0$	3788.4 kt	pristine stock biomass



# 5 Experimental survey data

## 5.1 Fish population measurements

### Bottom trawl surveys

The fisheries research institutes (NaFIRRI, TAFIRI and KMFRI) and the Lake Victoria Fisheries Organization (LVFO) regularly conduct bottom trawl (BT) surveys, where measurements at up to 80 stations are taken. The stations are distributed over various depth ranges with a focus on the shallow locations [102, 130]. At each station, a 30 minutes sample is measured using the bottom trawl technique (Fig. 5.1). The operation procedures prescribe a mesh size of 25 mm, and in more recent studies a finer cod end (4 mm) was added [120]. The catch rates (in kg/h) are interpreted as an indicator of the true population density at the sampling location. The speed of the boat during the sampling is typically between 2.5 and 3.5 knots<sup>1</sup>. The trawls are fully selective for fish from about 10 cm to 40 cm [108]. It is subject to a current discussion whether the trawl technique has a lower selectivity for fish larger than 40 cm because they might be capable of escaping the trawl as their swimming speed is comparable to (or higher than) the trawl speed. Indeed, the number of large specimen in the trawl surveys is very low [130]. For more information, the reader is referred to [108].

### Catch assessment surveys

The Catch assessment surveys (CAS), regularly conducted by the LVFO, provide information about the catch, the catch distribution, the effort, and the catch per unit of effort (CPUE). From 2005 to 2015, fifteen CAS were carried out in Kenya, Tanzania and Uganda at 143 landing sites - which are approximately 10% of the landing sites at the lake [121]. The CAS surveys provide monitoring of the fisheries to the partner states within the East African Community (EAC).

---

<sup>1</sup>R. Kayanda, pers. comm., Sep. 2020

### **Frame surveys**

The harmonized fisheries data collection conducted by EAC through the LVFO also includes also bi-annual Frame surveys (FS). The results indicate the effects of the fisheries management and provide baseline data for fisheries planning and development, including the number of landing sites, of fishers, and of gear and craft combinations by target species [122]. Craft/gear combinations are randomly sampled at each location by the field enumerator in harmonized data forms. For each species and each craft-gear combination, the CPUE (kg per boat per day) is estimated.

### **Hydroacoustic surveys**

A widely used, non-destructive method to estimate stock densities in marine and freshwater systems are hydroacoustic (HA) surveys [66]. The method uses underwater sound to detect and measure the size and the distribution of fish (Fig. 5.1). Its advantage is that the surveys can easily cover large spatial scales with a high area covered per time, a fast data acquisition and high cost effectiveness while being non-destructive [120]. The difficulty of the method lies in its limited capacity to measure fish close to the surface and the bottom and in differentiating the species. Therefore, it is often combined with bottom net hauls to gather species-specific information. At Lake Victoria, the acoustic surveys are part of routine stock assessments to survey large areas of the lake at high spatial resolution. The surveys sample four groups: Nile perch, dagaa, haplochromines and *Caridina nilotica* (a freshwater prawn). Nile perch, a strong acoustic target, is detected as individual fish ('single targets', i.e. not in schools) by echo counting, which measures individual fish  $\geq 10$  cm total length (TL) [123, 120]. The acoustic survey tracks ('transects') are done with the research vessel at a constant speed around 9 knots in deep ( $>40$  m depth), coastal (20-40 m) and inshore ( $<20$  m) strata. Raw data are processed with the software Echoview [61]. The weight of single targets is estimated by the target strength (TS) to weight/length relationship developed in [103].

## **5.2 Data processing**

Most empirical spectrum measurements are designed as length measurements, e.g. bottom trawl and hydroacoustic surveys. For example, the result from the hydroacoustic surveys is a list of single targets with the respective length. The spectrum in

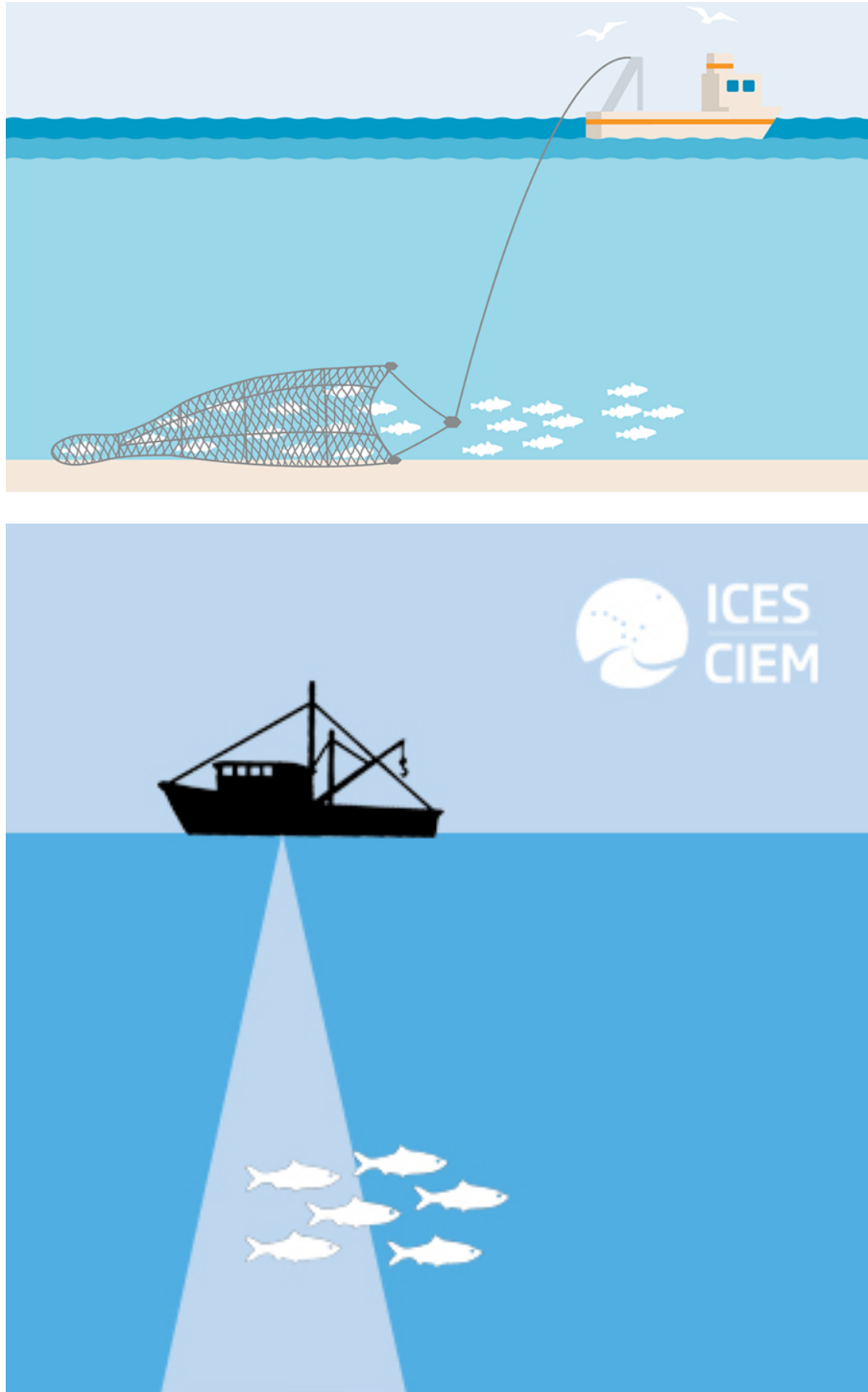


Figure 5.1: The bottom trawl technique (top) and the hydroacoustic method (bottom) are used to conduct fish population surveys. From [35, 97].

## 5 *Experimental survey data*

the length domain is, however, not identical to the spectrum in the weight domain, as they are related by the non-linear relationship (3.17) which must be considered in the analysis and interpretation of length-frequency data [64, 63].

In the Appendix A.6.2, it is demonstrated how the density can be converted from length to weight. Our algorithm to process the length frequency measurements has two steps.

1. The single target data files are read and converted to a histogram with 1 cm bins (centered), defining how many single targets had a length in that bin.
2. The centered length values are converted to the corresponding weight (3.17) and the number density from the length domain to the weight domain (A.53).

The algorithm was validated against the established method LBNbiom [64].

# 6 Mathematical analysis of the size structured population model

## 6.1 Time dependent model

In Chapters 3 and 4, we have described and explained the mathematical, size (weight) structured model of the Nile perch fishery (Fig. 6.1) that includes the biological processes of growth, reproduction, recruitment and mortality, and which is connected to the fishery through the fishing mortality  $\mu_F$  (4.3). Mathematically,

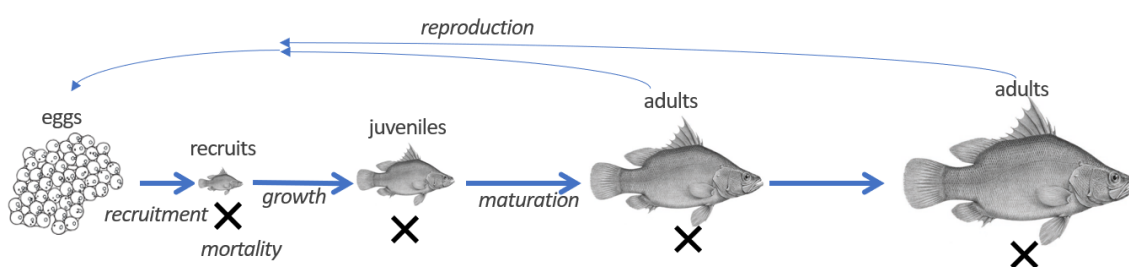


Figure 6.1: The model describes the life history of individual fish in a population that grow, mature, reproduce and die.

the model has the form of a first order hyperbolic partial differential equation equation with a non-local, non-linear boundary condition. We can write the model in the following form of the McKendrick-von Foerster equation [129, 71]:

## Time dependent model

$$\left\{ \begin{array}{ll} (i) & \frac{\partial}{\partial t}u(w, t) + \frac{\partial}{\partial w}(g(w)u(w, t)) = -\mu(w)u(w, t) \quad \text{on } [w_0, W_\infty) \times [0, T], \\ (ii) & u(w, 0) = u_0(w) \quad \text{on } [w_0, W_\infty), \\ (iii) & u(w_0, t) = \frac{1}{g(w_0)} \frac{\epsilon_0 SSB(t)}{1 + \epsilon_1 SSB(t)} \quad \text{on } [0, T], \\ (iv) & SSB(t) = \int_{w_0}^{W_\infty} \beta(w)u(w, t)dw. \end{array} \right. \quad (6.1)$$

Here, the population density of weight  $w$  at time  $t$  is denoted  $u(w, t)$ , such that the number of fish at time  $t$  with weight in  $[w_1, w_2]$  is

$$\int_{w_1}^{w_2} u(w, t) dw. \quad (6.2)$$

The first equation (6.1)(i) describes the 'transport' of fish along the weight dimension. The life of a fish starts at the minimum weight  $w_0$  and the fish grows toward the (finite) maximal weight  $W_\infty$ <sup>1</sup>. The domain  $[w_0, W_\infty)$  ends at the point where the growth function vanishes, such that  $g(W_\infty) = 0$ . We restrict ourselves to the finite time range  $[0, T]$  as we will always consider limited time horizons of the fishery managers. We set the maximum age  $a_\dagger$  in line with the biological estimate as 16 years [181]. Individual fish grow with growth rate  $g(w)$  from (3.4) dependent on the weight  $w$  at age  $a$ :

$$\frac{dw(a)}{da} = g(w(a)). \quad (6.3)$$

In the appendix A.3 (Lemma A.15), we prove that the maximal weight  $W_\infty$  is asymptotically approached, but not reached in finite time. The total mortality,

---

<sup>1</sup>Biologists tend to label the parameter  $W_\infty$  that appears in (3.4) the "asymptotic weight". This comes from the derivation of formula (3.4), where, for the juvenile growth function, the parameter is indeed the asymptotic weight where the growth rates vanishes. In the biphasic model, this is however not exactly right because in the formula, the function of maturation probability approaches one but never takes exactly the value one for finite size. Therefore, the parameter  $W_\infty$  in (3.4) is not any more exactly the "asymptotic" weight, where  $g(w) = 0$ . It is true that the difference is so small that for all biological or numerical purposes one makes no big mistake when interpreting the parameter from (3.4) as asymptotic weight. Yet to be precise in the mathematical analysis and at the same time to avoid needless confusion, we distinguish in this chapter between the true asymptotic weight  $W_\infty$ , where  $g(W_\infty) = 0$ , and the parameter in (3.4), and therefore denote the parameter from (3.4) as  $W_\dagger$ , and keep the label "asymptotic weight" in the other chapters for the parameter appearing in (3.4).

## 6.1 Time dependent model

both biological and from fishing,  $\mu(w)$ , is also dependent on the weight  $w$ . The population density at  $t = 0$  is given by the initial population density  $u_0$  (6.1)(ii). The Dirichlet boundary condition (6.1)(iii) determines the recruitment  $u(w_0, t)$  of newborn fish into the population at time  $t$ . The recruitment is a function of the spawning stock biomass  $SSB(t)$ , which is the aggregate biomass of the mature fish in the population (6.1)(iv), where the function  $\beta(w)$  denotes the expected fecundity<sup>2</sup> of a fish with weight  $w$ . The parameters  $\epsilon_0$  and  $\epsilon_1 = \frac{\epsilon_0}{R_{max}}$  in (6.1) capture the reproductive efficiency, where the biological quantity  $R_{max}$  is the maximum recruitment (see Section 3.2.3). The relationship between the spawning stock biomass and the recruitment has the shape of a Holling type II functional response, which is a concave function that starts linear in the origin and then converges toward the finite cap  $\frac{\epsilon_0}{\epsilon_1} = R_{max}$  for  $SSB \rightarrow \infty$  (Fig. 3.4).

In this section, we will proceed in the following way: First, we show that, for the weight of an individual fish, the solution  $w(a)$  to (6.3) exists uniquely in  $[0, \infty)$  (Lemma 6.1). Then we show that we can apply the theorems from [96], summarized in Proposition A.12, to proof that there exists a unique and regular solution to (6.1). To do so, we first have to show that (6.1) can be transformed to an equivalent system based on age instead of weight. Then, from the solution to the age-based system guaranteed by Proposition A.12, we can deduce the existence of a unique solution to (6.1) with analogous properties.

**Lemma 6.1.** *The growth curve  $w(a)$  of the individual fish is the solution to the ordinary differential equation (ODE)*

$$\begin{cases} \frac{dw(a)}{da} = g(w(a)) = Aw(a)^n \left( 1 - \frac{1}{1 + \left(\frac{w(a)}{w_m}\right)^{-\kappa}} \left(\frac{w(a)}{W_{\dagger}}\right)^{1-n} \right) & \text{in } [0, \infty), \\ w(0) = w_0. \end{cases} \quad (6.4)$$

Given the parameters<sup>3</sup>  $A, n, \kappa, w_m \in (0, \infty)$ ,  $0 < w_0 < W_{\dagger} < \infty$ , the ODE has a unique, continuously differentiable solution  $w(a)$  in  $[0, \infty)$ .

*Proof.* The absolute value of the derivative of  $g(w)$  has an upper bound in  $[0, \infty)$ . The weight  $W_{\infty}$  is defined as the solution of  $g(w) = 0$ , thus  $g(w) > 0$  for  $w \in [w_0, W_{\infty})$ . Hence  $w(a)$  is a monotonous function, moreover it is bounded by  $W_{\infty}$  due to the fact that  $g(W_{\infty}) = 0$ . Furthermore, as  $g(w)$  consists of products and sums of continuously differentiable functions, it follows that  $g(w)$  is continuously

<sup>2</sup>The fact that only females produce eggs is accounted for in the parameter  $\epsilon_0$ .

<sup>3</sup>For  $W_{\dagger}$ , see the footnote on the previous page.

## 6 Mathematical analysis of the size structured population model

differentiable for  $w \in [w_0, W_\infty)$ . Additionally, the derivative is bounded:

$$\begin{aligned}
 |g'(w)| &= |nAw^{n-1} \left( 1 - \frac{1}{1 + \left(\frac{w}{w_m}\right)^{-u}} \left(\frac{w}{W_\dagger}\right)^{1-n} \right) \\
 &\quad + Aw^n \frac{-\frac{u}{w} \left(\frac{w}{w_m}\right)^{-u}}{\left(1 + \left(\frac{w}{w_m}\right)^{-u}\right)^2} \left(\frac{w}{W_\dagger}\right)^{1-n} \\
 &\quad + Aw^n \frac{1}{1 + \left(\frac{w}{w_m}\right)^{-u}} \frac{1-n}{w} \left(\frac{w}{W_\dagger}\right)^{1-n} \quad | \tag{6.5} \\
 &\leq |nAW_\infty^{n-1}| \\
 &\quad + | - uAw^{n-1} \left(\frac{w_m}{w_0}\right)^u | \\
 &\quad + |(1-n)Aw^{n-1}| \\
 &\leq L < \infty.
 \end{aligned}$$

with some  $L < \infty$ . Therefore  $g(w)$  is also Lipschitz continuous in  $[w_0, W_\infty]$ . Due to the Picard-Lindelöf theorem, there exists a local (in  $a$ ) unique solution to (6.4). This solution may be extended to  $[0, \infty)$  by a continuation argument. The expression on the right-hand side of the first equation in (6.4) is continuous, thus the solution to (6.4) is continuously differentiable.  $\square$

**Remark 6.2.** Note that the fact that  $g(w) \in C^\infty([w_0, W_\infty])$  implies

$$w(a) \in C^\infty((0, \infty)). \tag{6.6}$$

**Remark 6.3.** As  $W_\infty$  is not reached in finite time (Lemma A.15) and therefore

$$w'(a) = g(w(a)) \neq 0 \tag{6.7}$$

in  $[0, \infty)$ , it follows that  $w(a)$  is invertible to a function  $w^{-1} : [w_0, W_\infty) \rightarrow [0, \infty)$  with

$$w^{-1}(w(a)) = a \quad \forall a \in [0, \infty). \tag{6.8}$$

In the next step, we show now that there is a unique mapping between the representation of the population in the weight and in the age domain, respectively.

**Lemma 6.4.** *The representation of the population in the age domain is related to the weight domain by*

$$p(a, t) = u(w(a), t) \frac{dw(a)}{da} = u(w(a), t)g(w(a)). \quad (6.9)$$

*The regularity of  $p(a, t)$  translates to  $u(w, t)$ .*

*Proof.* The growth rate  $g(w)$  from (6.4) is continuously differentiable with  $w'(a) = g(w(a)) \neq 0$  in  $[0, \infty)$ . Then, as is shown in the appendix A.6.1, the representations of the population in the age domain,  $p(a, t)$ , and in the weight domain,  $u(w, t)$ , are related by (6.9). Because  $g(w)$  is continuously differentiable with  $w'(a) = g(w(a)) \neq 0$  in  $[0, \infty)$ , the regularity of one representation translates to the other.  $\square$

Now we show that (6.1) can be transformed to a system of equations of the corresponding age density  $p(a, t)$ , that fulfills the requirements of Proposition A.12. Then, a unique solution exists to the system (A.1) and, correspondingly, this yields the existence of a unique solution  $u(w, t)$  to (6.1) with the same regularity. We make two assumptions.

#### Assumptions

- We assume that the initial population density belongs to  $L^\infty$  and non-negative,

$$u_0 \in L^\infty((w_0, W_\infty)), u_0 \geq 0. \quad (6.10)$$

- We assume that predation mortality  $\mu_{pred}$  and fishing mortality  $\mu_F$  are continuously differentiable and bounded,

$$\mu_{pred}, \mu_F \in C^1((w_0, W_\infty)), \quad 0 \leq \mu_{pred}, \mu_F \leq \mu_+ < \infty \text{ in } (w_0, W_\infty). \quad (6.11)$$

Existence of a unique non-negative solution to the time dependent model

**Theorem 6.5.** *Under the assumptions (6.10) and (6.11), there exists a unique, non-negative solution to (6.1). If in addition, the compatibility condition between the initial age density and the fertility function,*

$$u(w_0, 0) = \frac{1}{g(w_0)} \frac{\epsilon_0 SSB(0)}{1 + \epsilon_1 SSB(0)}, \quad (6.12)$$

*is fulfilled, then the solution is regular.*

*Proof.* First, we transform (6.1) to the age domain through the transformation from  $u(w, t)$  to  $p(a, t)$  from Lemma 6.4. This yields the equivalent system for  $p(a, t)$ :

$$\left\{ \begin{array}{ll} (i) & \frac{\partial}{\partial t} p(a, t) + \frac{\partial}{\partial a} p(a, t) = -\mu(w(a))p(a, t) \quad \text{on } [0, a_{\dagger}] \times [0, T], \\ (ii) & p(a, 0) = p_0(a) \quad \text{on } [0, a_{\dagger}], \\ (iii) & p(0, t) = \frac{\epsilon_0 SSB(t)}{1 + \epsilon_1 SSB(t)} \quad \text{on } [0, T], \\ (iv) & SSB(t) = \int_0^{a_{\dagger}} \beta(w(a))p(a, t) da. \end{array} \right. \quad (6.13)$$

Here  $p(a, t) : [0, a_{\dagger}] \times \mathbb{R}_+ \rightarrow \mathbb{R}_+$  is the population density dependent on age  $a$  and time  $t$  with maximum age  $a_{\dagger} < \infty$ . We will now show that this system corresponds to (A.1). Obviously, (6.13)(i) and (A.1)(i) are equivalent, as well as (6.13)(ii) and (A.1)(ii), respectively. To see that (6.13)(iii) is the equivalent to (A.1)(iii), we define

$$\Phi(SSB) = \frac{R_{max}}{R_{max} + \epsilon_0 SSB}, \quad (6.14)$$

$$R_0 = \frac{\epsilon_0}{\tilde{\epsilon}}, \quad (6.15)$$

$$\tilde{\beta}_0(a) = \tilde{\epsilon} \beta(w(a)), \quad (6.16)$$

where we have introduced the dimensionless parameter  $\tilde{\epsilon}$  to assure the normalization in (A.4)(ii). With these definitions, the conditions (A.2) are fulfilled. Finally, it can directly be seen that (6.13)(iv) corresponds to (A.1)(iv) if we set  $\tilde{\gamma}(a) = \beta(w(a))$  and identify  $S$  with  $SSB$ .

We will now show that each of the five conditions of (A.4) are fulfilled for our model, such that we can apply Proposition A.12 to solve (6.13).

## 6.1 Time dependent model

(i)  $\tilde{\beta}_0 \in C_b((0, a_\dagger))$ ,  $0 \leq \tilde{\beta}_0(a) \leq \tilde{\beta}_+$  a.e. in  $[0, a_\dagger]$ :

As  $0 < \beta(w(a)) = w(a)\psi_m(w(a)) = \frac{w(a)}{1+(\frac{w(a)}{w_m})^{-\kappa}} < \infty$  in  $[0, a_\dagger]$  with  $w(a)$  being continuously differentiable (Lemma 6.1), the condition is fulfilled.

(ii)  $\int_0^{a_\dagger} \tilde{\beta}_0(a)\Pi_0(a)da = 1$ :

$\Pi_0(a) = e^{-\int_0^a \tilde{\mu}(\sigma)d\sigma}$  is the baseline survival probability. Note that we can set the normalization parameter  $\tilde{\epsilon} > 0$  arbitrarily. If we define

$$I = \int_{w_0}^{W_\infty} w\psi_m(w) \frac{1}{g(w)} e^{-\int_{w_0}^w \frac{\mu(\bar{w})}{g(\bar{w})} d\bar{w}} dw \quad (6.17)$$

and set

$$\tilde{\epsilon} = \frac{1}{I}, \quad (6.18)$$

then the condition is fulfilled as it holds:

$$\int_0^{a_\dagger} \tilde{\beta}_0(a)\Pi_0(a)da = \tilde{\epsilon} \int_{w_0}^{W_\infty} w\psi_m(w) \frac{1}{g(w)} e^{-\int_{w_0}^w \frac{\mu(\bar{w})}{g(\bar{w})} d\bar{w}} dw = \tilde{\epsilon}I = 1, \quad (6.19)$$

where the integrals were transformed using the relation  $\frac{dw}{da} = g(w)$ .

(iii)  $p_0 \in L^\infty(0, a_\dagger)$ ,  $p_0(a) \geq 0$  a.e. in  $[0, a_\dagger]$ :

This condition is fulfilled by assumption (6.10).

(iv)  $\tilde{\mu} \in L^1_{loc}([0, a_\dagger])$ ;  $\tilde{\mu}(a) \geq 0$  a.e. in  $[0, a_\dagger]$ ;  $\int_0^{a_\dagger} \tilde{\mu}(a)da = +\infty$ :

We show that the condition is fulfilled for the case with the senescent mortality

$$\mu(w(a)) = \mu_{pred}(w(a)) + \mu_F(w(a)) + \mu_s(w(a)) \quad (6.20)$$

with

$$\mu_s(w(a)) = \frac{\alpha_s}{a_\dagger - a} \quad (6.21)$$

with some  $\alpha_s > 0$ . This ensures that no fish lives longer than to the age  $a_\dagger$  (indeed that all fish die before  $a_\dagger$ ), because  $\int_0^{a_\dagger} \tilde{\mu}(a)da = +\infty$ , while still maintaining that on each compact subset of  $[0, a_\dagger)$ , the integral over the mor-

## 6 Mathematical analysis of the size structured population model

tality is finite, such that  $\tilde{\mu} \in L^1_{loc}([0, a_+))$ . Thus (6.20) with (6.21) assures that condition (iv) is fulfilled<sup>4</sup>.

(v)  $\tilde{\gamma} \in C_b((0, a_+))$ ,  $0 \leq \tilde{\gamma}(a) \leq \tilde{\gamma}_+$  a.e. in  $[0, a_+]$ :

As  $\tilde{\gamma} = \beta(w(a))$  and  $0 < \tilde{\epsilon} < \infty$ , conditions (i) implies also condition (v).

As all the conditions in (A.2) and (A.4) are fulfilled, Proposition A.12 guarantees that there exists a unique, non-negative solution to (6.13). From Lemma 6.4, together with Remarks 6.2 and 6.3, it follows that a unique, non-negative solution  $u(w, t)$  to the original system (6.1) exists. If the *compatibility condition* (6.12) is fulfilled, then the solution is regular (cf. Remark A.13).  $\square$

## 6.2 Steady state model

Next we will consider the steady state of the system (6.1), which reads as follows:

### Steady state model

The steady state model is

$$\begin{cases} i) & \frac{d}{dw}(u(w)g(w)) = -\mu(w)u(w) \quad \text{on } [w_0, W_\infty) \\ ii) & u(w_0) = \frac{1}{g(w_0)} \frac{\epsilon_0 SSB}{1 + \epsilon_1 SSB}, \\ iii) & SSB = \int_{w_0}^{W_\infty} \beta(w)u(w)dw \end{cases} \quad (6.22)$$

with the steady state density  $u(w)$ , and the variables and parameters from (6.1).

Note that the spawning stock biomass  $SSB$  is no more time dependent. Then we can make the following statement:

<sup>4</sup>In the simulations we will not always use the senescent mortality. As we can set  $\alpha_s$  arbitrarily, we can always guarantee that the effect of the additional mortality is sufficiently small and late in life such that it has no noticeable impact on the simulations in the time range  $[0, T]$  of (6.1).

## Solution to the steady state model

**Theorem 6.6.** *The steady state model (6.22) has a unique non-trivial solution, if and only if  $\epsilon_0 I > 1$ . In this case, the solution is given by*

$$\begin{cases} u(w) = R_{max} \left(1 - \frac{1}{\epsilon_0 I}\right) \frac{1}{g(w)} e^{-\int_{w_0}^w \frac{\mu(\bar{w})}{g(\bar{w})} d\bar{w}} & \text{on } [w_0, W_\infty) \\ I = \int_{w_0}^{W_\infty} w \psi_m(w) \frac{1}{g(w)} e^{-\int_{w_0}^w \frac{\mu(\bar{w})}{g(\bar{w})} d\bar{w}} dw \end{cases} \quad (6.23)$$

*Otherwise if  $\epsilon_0 I \leq 1$ , there is only the trivial solution  $u(w) \equiv 0$ .*

*Proof.* Under the assumptions of Theorem 6.5 one can apply Proposition A.14, which guarantees that the system (A.1) has a unique non-trivial steady state solution, if and only if  $R_0 > 1$ . The uniqueness of the solution is shown using Picard iterations of the birth rate function from the renewal equation [96]. As demonstrated in Theorem 6.5, this implies also a solution of the steady state (6.22) of the  $u$ -system (6.1). In the proof of Theorem 6.5, it was also shown that the condition (A.4)(iv) yields  $\tilde{\epsilon} = \frac{1}{I}$ , therefore the condition for the existence of the non-trivial solution reads  $R_0 = \frac{\epsilon_0}{\tilde{\epsilon}} = \epsilon_0 I > 1$ .

We guess the solution (6.23) and show that inserting (6.23) into (6.22)(i) solves the equation for  $\epsilon_0 I > 1$ :

$$\begin{aligned} \frac{d}{dw}(u(w)g(w)) &= R_{max} \left(1 - \frac{1}{\epsilon_0 I}\right) \frac{d}{dw} \left( e^{-\int_{w_0}^w \frac{\mu(\bar{w})}{g(\bar{w})} d\bar{w}} \right) \\ &= R_{max} \left(1 - \frac{1}{\epsilon_0 I}\right) \left( e^{-\int_{w_0}^w \frac{\mu(\bar{w})}{g(\bar{w})} d\bar{w}} \right) \left( -\frac{\mu(w)}{g(w)} \right) \\ &= -\mu(w)u(w) \end{aligned} \quad (6.24)$$

The prefactor  $R_{max} \left(1 - \frac{1}{\epsilon_0 I}\right)$  is determined by the boundary condition (6.22)(ii). It can be calculated by first inserting the general solution of (6.22)(i),

$$u(w) = u(w_0)g(w_0) \frac{1}{g(w)} e^{-\int_{w_0}^w \frac{\mu(\bar{w})}{g(\bar{w})} d\bar{w}} \quad (6.25)$$

into (6.22)(iii), yielding

$$\begin{aligned} SSB &= \int_{w_0}^{W_\infty} \beta(w)u(w, t)dw \\ &= u(w_0)g(w_0) \int_{w_0}^{W_\infty} w \psi_m(w) \frac{1}{g(w)} e^{-\int_{w_0}^w \frac{\mu(\bar{w})}{g(\bar{w})} d\bar{w}} dw = u(w_0)g(w_0)I. \end{aligned} \quad (6.26)$$

## 6 Mathematical analysis of the size structured population model

Inserting that into (6.22)(ii) yields an implicit equation for  $u(w_0)$ :

$$u(w_0) = \frac{1}{g(w_0)} \frac{\epsilon_0 u(w_0) g(w_0) I}{1 + \epsilon_1 u(w_0) g(w_0) I} = u(w_0) \frac{\epsilon_0 I}{1 + \frac{\epsilon_0}{R_{max}} u(w_0) g(w_0) I}. \quad (6.27)$$

If  $u(w_0) \neq 0$ , this is equivalent to

$$1 + u(w_0) \frac{g(w_0)}{R_{max}} \epsilon_0 I = \epsilon_0 I \quad (6.28)$$

The solution of that equation is

$$u(w_0) = \frac{1}{g(w_0)} R_{max} \left( 1 - \frac{1}{\epsilon_0 I} \right). \quad (6.29)$$

and it exists if  $\epsilon_0 I > 1$ . Otherwise, if  $\epsilon_0 I \leq 1$ , it follows from A.14 that the unique solution is the trivial solution,  $u(w) \equiv 0$ .  $\square$

### 6.3 Perturbations of the fleet selectivity

As we are interested in size based policies, an important question is whether a perturbation of the fleet selectivity (increasing the fishing mortality at some  $\hat{w}$ ) would increase or decrease the aggregate yield of the fishery in steady state. In other words, does the additional yield from more intensive fishing at size  $\hat{w}$  outweigh the negative effect of the decrease in the population, and hence of less yield at the larger sizes  $w > \hat{w}$ ? In this section we will develop a criterion from which it can be predicted whether increasing the exploitation of fish with size  $\hat{w}$  would increase or decrease the aggregate, steady state yield of the Nile perch fishery. First, we will develop the condition for finite increments, and second, for infinitesimally small increments, in the sense of small perturbations of the fleet selectivity. The second is helpful to policymakers as they are often interested in gradual changes around the current fishing pattern due to the lower risk of small changes.

Let us assume the policymakers can determine a size  $\hat{w}$  and get the fishers by some policy to increase the fishing intensity around that size  $\hat{w}$ . For the purpose of our consideration we can think of the limit case of perfect selectivity where fishers can perfectly target a single fish size. Then the policymaker's regulation would bring the fishers to increase the fishing mortality at size  $\hat{w}$ . Let the mortality rate  $\hat{F}$  determine the scale (amount) of the increase such that the additional term has the unit of a mortality rate, 1/yr. Let us model this with a  $\delta$ -distribution, such that

### 6.3 Perturbations of the fleet selectivity

the fishing mortality receives an additional summand  $\hat{F}\delta(w - \hat{w})$  so that it reads:

$$\mu_F(w) = F\psi_F(w) + \hat{F}\delta(w - \hat{w}) \quad (6.30)$$

Let us define the yield dependent on  $\hat{F}$  as  $\hat{Y}(\hat{F})$ . The general yield equation is

$$Y = \int_{w_0}^{W_\infty} wu(w)\mu_F(w)dw \quad (6.31)$$

and thus the yield in status quo is

$$Y_0 := \hat{Y}(0) = \int_{w_0}^{W_\infty} wu(w)F\psi_F(w)dw \quad (6.32)$$

Introducing the notation for the yield within the size range  $w \in [w_1, w_2]$  as

$$Y_0^{[w_1, w_2]} := \int_{w_1}^{w_2} wu(w)F\psi_F(w)dw, \quad (6.33)$$

we can state the following improvement condition.

#### Improvement condition

**Proposition 6.7.** *If the fishing mortality around the weight  $\hat{w}$  is increased by  $\hat{F}$  according to (6.30), then the new situation (in steady state) provides more yield than previously, if the following condition is fulfilled,*

$$\hat{F}u_0(\hat{w})\hat{w} > (1 - e^{-\frac{\hat{F}}{g(\hat{w})}})Y_0^{[\hat{w}, W_\infty]}. \quad (6.34)$$

*Proof.* Let us define the survival probability from  $w_0$  to  $w$ :

$$\Pi(w) = e^{-\int_{w_0}^w \frac{\mu(\sigma)}{g(\sigma)} d\sigma}. \quad (6.35)$$

Let this survival probability in status quo (before the additional mortality) be denoted by  $\Pi_0(w)$ .

The population density is related to the survival probability by

$$u(w) = \frac{R}{g(w)}\Pi(w). \quad (6.36)$$

## 6 Mathematical analysis of the size structured population model

Therefore the population density in status quo is

$$u_0(w) = \frac{R}{g(w)} \Pi_0(w). \quad (6.37)$$

We re-write (6.32):

$$Y_0 = \hat{Y}(\hat{F} = 0) = \int_{w_0}^{W_\infty} w \frac{R}{g(w)} \Pi_0(w) F \psi_F(w) dw. \quad (6.38)$$

The new population has the fishing mortality (6.30) and thus the survival probability from (6.35) becomes now

$$\hat{\Pi}(w) = e^{-\int_{w_0}^w \frac{\mu(\sigma) + \hat{F} \delta(w-\hat{w})}{g(\sigma)} d\sigma} = \begin{cases} \Pi_0(w), & \text{if } w < \hat{w} \\ \Pi_0(w) e^{-\frac{\hat{F}}{g(\hat{w})}}, & \text{if } w > \hat{w}. \end{cases} \quad (6.39)$$

Inserting this result into the yield equation (6.31) provides the new yield:

$$\begin{aligned} \hat{Y}(\hat{F}) &= \int_{w_0}^{W_\infty} w u(w) \mu_F(w) dw = \int_{w_0}^{W_\infty} \frac{R}{g(w)} \hat{\Pi}(w) w F \psi_F(w) dw \\ &= \int_{w_0}^{\hat{w}} \frac{R}{g(w)} \Pi_0(w) w F \psi_F(w) dw + u_0(\hat{w}) \hat{w} \hat{F} + \int_{\hat{w}}^{W_\infty} \frac{R}{g(w)} \Pi_0(w) e^{-\frac{\hat{F}}{g(\hat{w})}} w F \psi_F(w) dw. \end{aligned} \quad (6.40)$$

To understand the result, we compare it with the status quo yield, conveniently split at  $\hat{w}$ .

$$\begin{aligned} Y_0 &= Y_0^{[w_0, \hat{w}]} + Y_0^{[\hat{w}, W_\infty]} \\ &= \int_{w_0}^{\hat{w}} \frac{R}{g(w)} \Pi_0(w) w F \psi_F(w) dw + \int_{\hat{w}}^{W_\infty} \frac{R}{g(w)} \Pi_0(w) w F \psi_F(w) dw \end{aligned} \quad (6.41)$$

Comparing (6.40) with (6.41), it becomes clear that the new yield obeys the equation

$$\hat{Y}(\hat{F}) = Y_0^{[w_0, \hat{w}]} + \hat{F} u_0(\hat{w}) \hat{w} + e^{-\frac{\hat{F}}{g(\hat{w})}} Y_0^{[\hat{w}, W_\infty]}. \quad (6.42)$$

The first term simply states that the yield of sizes below  $w$  stays the same as these are not impacted by the additional mortality. The second term  $\hat{F} u_0(\hat{w}) \hat{w}$  is the yield that comes from the additional fishing mortality at size  $\hat{w}$ . And the third term  $e^{-\frac{\hat{F}}{g(\hat{w})}} Y_0^{[\hat{w}, W_\infty]}$  states that the yield of sizes larger than  $\hat{w}$  is decreased by a factor  $e^{-\frac{\hat{F}}{g(\hat{w})}}$  which is the impact of fishing at size  $\hat{w}$  leading to a decrease in the population

### 6.3 Perturbations of the fleet selectivity

density of all sizes  $w > \hat{w}$ . The higher the additional mortality value  $\hat{F}$ , the stronger is the effect on the population. A low value of  $g(\hat{w})$  means that the fish of size  $\hat{w}$  have a slow growth rate, indicating that they spend more time being subject to the additional fishing mortality, which implies a stronger impact on (decrease in) the population and thus the yield.

Now we can derive the general condition whether the perturbation of the fleet selectivity, i.e. the additional fishing mortality, increases or decreases the yield, compared to the status quo, by comparing (6.41) and (6.42).

$$\hat{Y}(\hat{F}) - Y_0 = \hat{F}u_0(\hat{w})\hat{w} + (e^{-\frac{\hat{F}}{g(\hat{w})}} - 1)Y_0^{[\hat{w}, W_\infty]} \quad (6.43)$$

This provides the improvement condition. □

**Remark 6.8.** *The improvement condition depends only on the size  $\hat{w}$ , the strength of the additional mortality  $\hat{F}$  and the growth rate  $g(\hat{w})$ .*

In order to illustrate the answer to the question, 'which sizes should be targeted more strongly?', also in another way, let us think of a sole-owner of the fishery who could decide to increase (or decrease) the fishing mortality at any size  $\hat{w}$  by an infinitesimally small value. To analyze the impact on the total yield, let us consider the derivative of  $\hat{Y}(\hat{F})$  in (6.42) with respect to  $\hat{F}$  around the status quo  $\hat{F} = 0$ , as a function of the target size  $\hat{w}$ .

$$\left. \frac{\partial \hat{Y}(\hat{F})}{\partial \hat{F}} \right|_{\hat{F}=0} = u_0(\hat{w})\hat{w} - \frac{1}{g(\hat{w})} \int_{\hat{w}}^{W_\infty} u(w)wF\psi_F(w)dw \quad (6.44)$$

$$= u_0(\hat{w})\hat{w} - \frac{1}{g(\hat{w})}Y_0^{[\hat{w}, W_\infty]} \quad (6.45)$$

We see that the derivative is positive if the benefit from getting more yield at size  $\hat{w}$  outweighs the loss from decreased yield of sizes larger than  $\hat{w}$ .

The numerical value of the derivative (6.45) is depicted in Fig. 6.2 for the standard Nile perch parameters (see Tables 3.1 and 3.2). For easier applicability in the context of Lake Victoria policies, we have transformed weight  $w$  to length  $L$ , using (3.17). The derivative is negative for a target size below  $L_d = 67.19$  cm. This means the total yield would decrease if the sizes below  $L_d$  were targeted more strongly. Correspondingly, the derivative is positive for sizes larger than  $L_d = 67.19$  cm. Targeting these sizes more strongly would increase the yield. It is important to remember that the derivative provides a 'local' information in the sense that it is valid for small

## 6 Mathematical analysis of the size structured population model

changes around the current fishing mortality. Larger changes require the use of the general improvement condition (6.34).

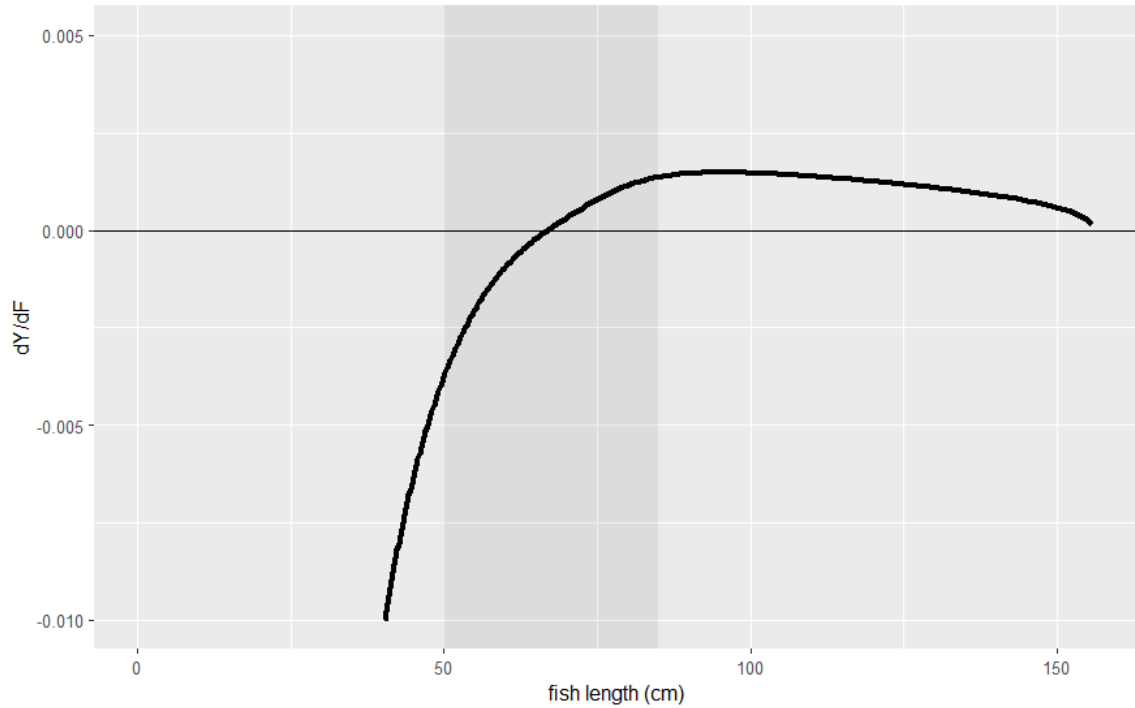


Figure 6.2: Derivative of yield with respect to the additional fishing mortality  $\hat{F}$  from (6.45), in dependence of the size  $\hat{w}$ , here converted to the equivalent fish length  $L$  using (3.17) for easier comparison to policies. The numerical value of the derivative is calculated for the standard parameters (see Tables 3.1 and 3.2). The gray shaded area indicates the slot size range 50-85 cm. The derivative is positive for  $L > 67.19$  cm.

## **Part II**

# **Application to the regulation of the Nile perch fishery**



# 7 Model validation and sensitivity analysis

With this chapter we begin the application of the size structured model to analyze the regulation of the Nile perch fishery. We start by validating the model against the van Bertalanffy growth curve and the measured population size structure.

## 7.1 Numerical procedure

The equilibrium of the McKendrick-von Foerster equation (6.22) is numerically solved with the following scheme. Starting from (6.22) and defining the flux

$$\phi(w) = g(w)u(w), \quad (7.1)$$

one arrives at the following equation for the flux in steady state:

$$\frac{d \ln \phi(w)}{dw} = -\frac{\mu(w)}{g(w)} \quad (7.2)$$

with the boundary condition

$$\phi(w_0) = R. \quad (7.3)$$

This can directly be solved, and the solution is

$$\frac{u(w)}{R} = \frac{1}{g(w)} \exp\left(-\int_{w_0}^{w_\infty} \frac{\mu(\sigma)}{g(\sigma)} d\sigma\right) = \frac{1}{g(w)} P_{w_0 \rightarrow w}, \quad (7.4)$$

where  $u(w)/R$  is the number density per recruit, which is necessary to calculate common quantities like the "yield-per-recruit". In the last step of the equation,  $P_{w_0 \rightarrow w}$  denotes the survival probability from  $w_0$  to  $w$ .

## 7 Model validation and sensitivity analysis

Solving for the survival function involves a numerical discretization scheme with the following steps [5, 2]:

1. The range  $[w_0, W_\infty)$  is discretized into  $m$  logarithmically distributed weight classes  $w_i$ ,

$$\begin{aligned} w_i &= \exp(\ln(w_0) + (i-1)\Delta), \quad \text{where} \\ \Delta &= \frac{\ln(W_\infty) - \ln(w_0)}{m-1}. \end{aligned} \quad (7.5)$$

In the simulations, the default value  $m = 1000$  is used.

2. At each grid point, the mortality  $\mu(w_i)$  is calculated and then the physiological mortality  $a_i$ :

$$a_i = \frac{\mu(w_i)}{g(w_i)} w_i \quad (7.6)$$

3. The survival probability is approximated

$$P_{w_0 \rightarrow w_i} \approx \exp\left(-\Delta \sum_{j=2}^i a_{j-1}\right) = \prod_{j=2}^i e^{-\Delta \cdot a_{j-1}}. \quad (7.7)$$

4. The population density can then be calculated from (7.4)

The scheme is implemented in the library `fishsizespectrum` [3] in R [173].

## 7.2 Validation

### 7.2.1 Growth curve

The numerical solution of the growth equation produces the curve of weight-at-age. This is compared to the classical van Bertalanffy growth curve for empirical parameters of Nile perch (Fig. 7.1). For young ages, both curves are flat because young fish are small and have a low growth rate. After around one year, the slope becomes steeper and reaches a maximum, where the growth rate is maximal due to large food consumption while still having moderate energy losses from reproduction and other sources. At higher ages, the curves become flatter again, until they converge to the asymptotic weight, where weight gains and losses are balanced. The biphasic growth curve predicts a lower weight until around 2.5 years and after

around 4 years. The van Bertalanffy curve has in its construction the parameter  $t_0$  that is interpreted as the “age at zero length” and has a negative value, such that the individuals’ growth curve actually starts before birth. The biphasic growth model avoids this construction.

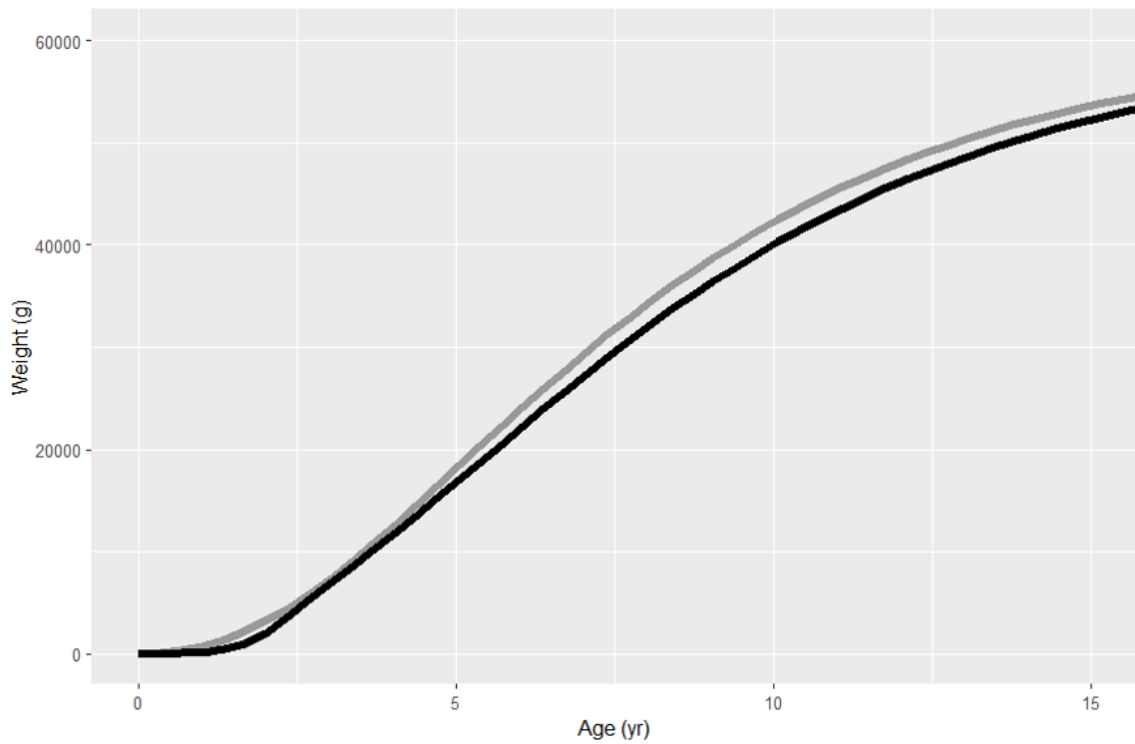


Figure 7.1: Van Bertalanffy growth curve (gray) vs integration of the differential equation  $dw/dt$  with biphasic growth (black).

This can also be illustrated with length instead of weight. Fig. 7.2 depicts the length-at-age curve with the van Bertalanffy equation and the integration of the biphasic growth model. Partly, the difference comes from the fact that in the van Bertalanffy equation, fish start at  $t = 0$  with a positive weight due to the negative value of “age at zero length”,  $t_0$ .

## 7.2.2 Size spectrum

To understand how the model functions and predicts the catch, the fishery was simulated in the steady state model for different levels of peak fishing mortality with the empirical fleet selectivity (Fig. 7.3) from [80]. As predicted from theory and observations [2], the biomass spectrum is similar to a flat spectrum in the unfished part of the spectrum (solid curves in Fig. 7.4). The upper black curve

## 7 Model validation and sensitivity analysis

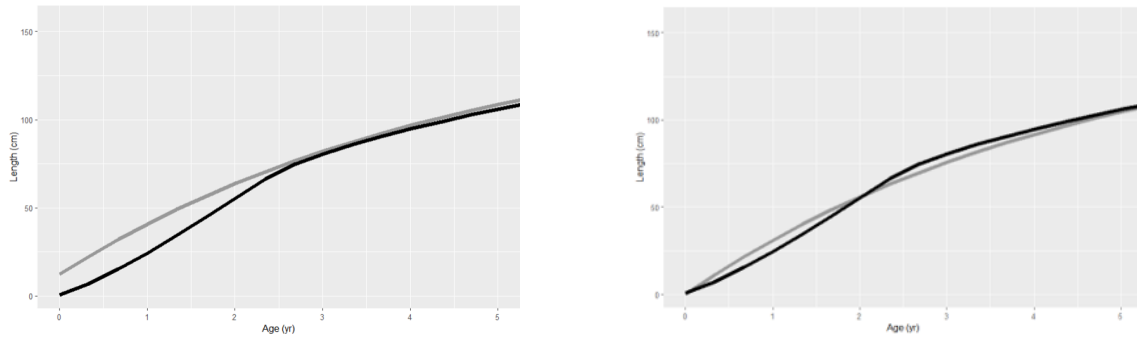


Figure 7.2: Van Bertalanffy growth curve (gray) vs integration of the differential equation  $dw/dt$  with biphasic growth (black). The left figure uses  $t_0 = -0.37yr$  [69], the right figure  $t_0 = 0$ .

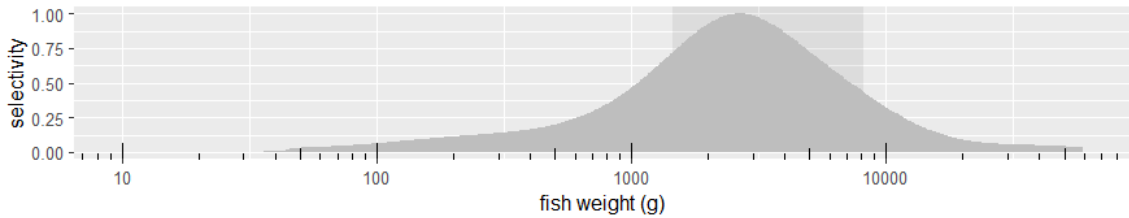


Figure 7.3: Empirical fleet selectivity (2020). The gray-shaded rectangle marks the legal slot size (50-85 cm).

represents the simulation with peak fishing mortality  $F=0.5/yr$  (i.e. the value of the fishing mortality at the maximum of the selectivity curve). At around 600 g, the fishing pressure becomes stronger, and the biomass spectrum begins to decline. It would further decline until and beyond the peak of the selectivity at 2000-3000 g. However, parallel to the increase in selectivity, fish start to mature in this range. As they become mature, they start to reproduce and put energy into reproduction which leaves less energy for growth, therefore the growth rate slows down. The fish “pile up” around the point of 50% maturity (70 cm or 4348 g). This counteracts the fishing pressure and leads to an increasing population density in the range 3000-8000 g. At around 8000 g, the growth rate has become so small that fish spend much time in each “weight bin”. Therefore, the mortality rate exceeds the growth rate and thus the spectrum decreases strongly.

As will be shown later, the results are sensitive to the uncertain parameter of physiological mortality  $a$  for which no direct experimental data exist. Therefore, we include the range of uncertainty of  $a$ , assuming  $a$  to be drawn randomly from a normal distribution with mean  $\mu = 0.3$  and standard deviation  $\sigma = 0.1$ . The

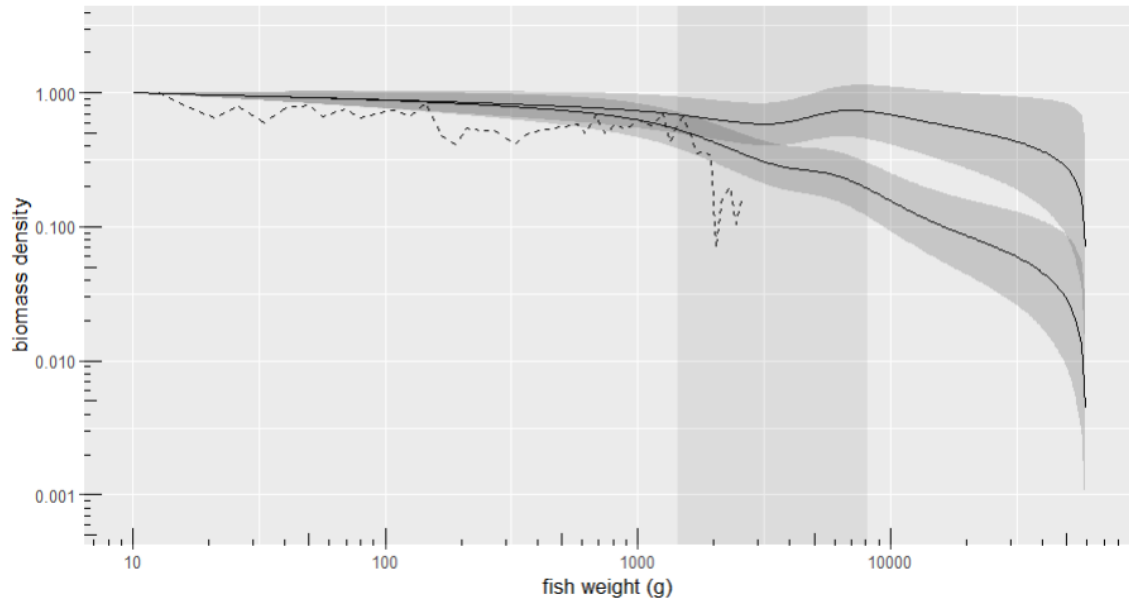


Figure 7.4: Bottom trawl survey (2019, dashed) compared to simulations of Nile perch biomass spectrum (solid) for  $F=0.5$  (upper solid curve) and  $1.5/\text{yr}$  (lower solid curve). The dark gray range indicates the sensitivity to the uncertainty in the value of physiological mortality (see text). The light gray shaded rectangle marks the legal slot size (50-85 cm).

gray uncertainty range in the figures shows the range between the 25th and 75th percentile from 100 simulations with  $a$  drawn from the normal distribution.

For a higher fishing mortality, the biomass density decreases faster the in fished range, i.e. the slopes are more negative. At  $F=1.5/\text{yr}$ , the fishing mortality counteracts the effect of fish “piling up” around maturation, resulting in a strictly monotonously decreasing curve. The bottom trawl survey is shown for comparison (dashed in Fig. 7.4). It has a small negative slope until around 50 cm (1451.75 g, begin of the gray rectangle that spans the range 50-85 cm), where it suddenly breaks down. At this point, two effects would coincide. First, the actual decreasing population density and, secondly, the impaired selectivity of bottom trawl surveys for larger fish. Currently, the exact selectivity of bottom trawl surveys, in particular the exact point at which the selectivity drops, is not studied well enough, but future studies could provide the selectivity curve and allow to disentangle the two effects.

In Fig. 7.5, the three simulations are compared with the hydroacoustic survey and the spectrum estimate from the CAS. The hydroacoustic curve shows a different behavior pattern than the other curves. For sizes above 200 g, the slope is more negative than for CAS and the simulations. This could relate to the TS-weight

## 7 Model validation and sensitivity analysis

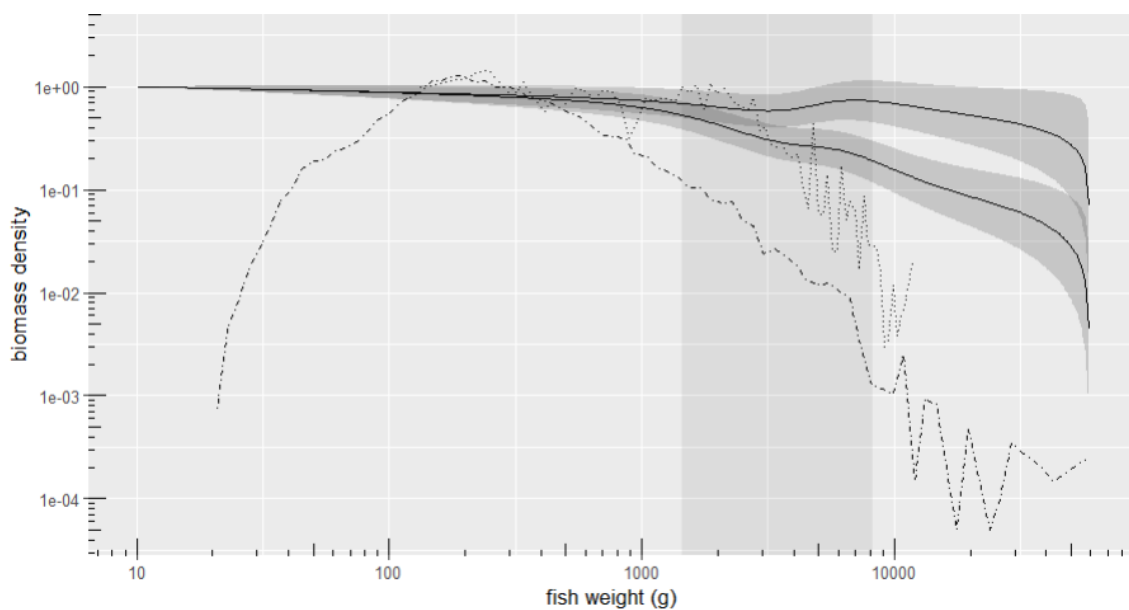


Figure 7.5: Hydroacoustic survey (2019, dotdash) and catch assessment survey (CAS, 2020, dotted) compared to simulations of Nile perch biomass spectrum (solid) for  $F=0.5$  (upper solid curve) and  $1.5/\text{yr}$  (lower solid curve). The dark gray range indicates the sensitivity to the uncertainty in the value of physiological mortality (see text). The light gray shaded rectangle marks the legal slot size (50-85 cm).

conversion (see section 5.1). The conversion could be the reason for a steeper slope. However, this needs further investigation and a re-analysis of the raw data of the hydroacoustic surveys. The curve of the CAS estimate is similar to the simulations until around 3000 g and afterwards it drops steeply. However, in the CAS data there were very few observations of larger fish (above 75 cm or 5444 g) from gillnets and few above 85 cm (8188 g) from longline hooks. Because of the few data points of larger fish, the right part of the CAS spectrum has lower confidence.

Table 7.1 shows the sum of squared residuals (SSR) (cf. Appendix A.4) between the logarithm of the simulated biomass spectrum ( $F=1.0/\text{yr}$ ) and the respective survey (normalized, linearly interpolated, logarithmic, 141 data points each) over the range 200 g-2500 g where all are comparable. A value of zero would indicate perfect agreement, and the larger the disagreement, the larger is the SSR. We use the logarithm because otherwise the SSR would be biased towards the lower part of the size range, as the biomass density drops over multiple orders of magnitude. The results confirm that the simulation, the bottom trawl survey and the catch assessment survey agree mutually, while the hydroacoustic survey describes a very different population structure.

Table 7.1: Sum of squared log-residuals over 200 g-2500 g between the simulated biomass spectrum ( $F=1.0/\text{yr}$ ) and the respective survey (normalized, linearly interpolated, 141 data points).

<b>survey</b>	<b>SSR-log</b>
BT2019	3.385286
HA2019	51.16156
CAS2020	2.979331

In Fig. 7.6, all three surveys are compared in one figure to the model simulation with  $F=1.0/\text{yr}$ . The observations described above also apply here. The (dis)agreement between the surveys can also be seen clearly, when depicting the length instead of the weigh density (Fig. 7.7). To corroborate the results, we also compare the slopes. The model predicts that in the part of the spectrum where fishing does not contribute to the total mortality, the slope should follow a power-law relation (for the parameters, see Chapter 3).

$$B(w) = \text{const} \cdot w^{-a-n+1} \quad (7.8)$$

7 Model validation and sensitivity analysis

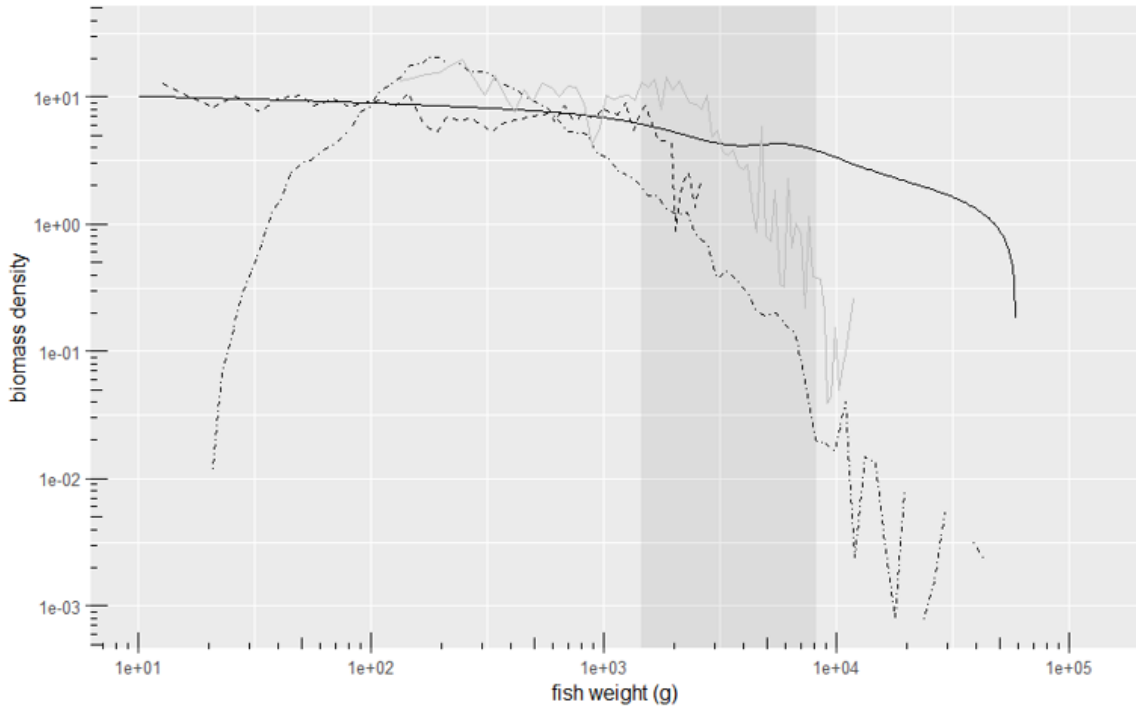


Figure 7.6: Three surveys together with the model simulation: bottom trawl survey (2019, dashed), hydroacoustic survey (2019, dotdash) and catch assessment survey (CAS, 2020, gray) compared to simulations of Nile perch biomass spectrum (solid) for  $F=1.0$ .

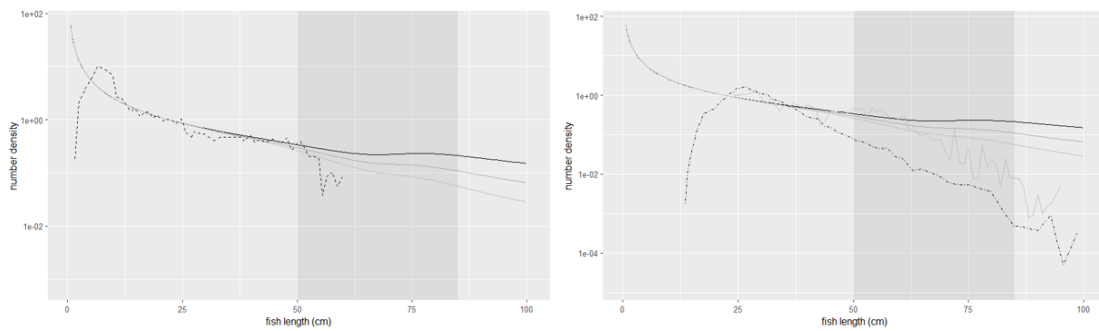


Figure 7.7: Left: bottom trawl survey (2019, dashed) compared to simulations of Nile perch biomass spectrum (solid) for  $F=0.5$  (black),  $1.0$  (dark gray) and  $1.5/\text{yr}$  (gray). Right: hydroacoustic survey (2019, dotdash) and catch assessment survey (CAS, 2020, gray).

In a double logarithmic diagram this should correspond to a linear relation, which can be measured with a linear regression. The model would predict a straight line with slope  $-a - n + 1$ . With  $n = 0.75$  and the estimates of the physiological mortality ranging from  $a = 0.244$  to  $a = 0.522$ , this would imply a slope in the range  $[-0.006, -0.272]$ . For each of the three surveys, the coefficients of the linear regression (cf. Appendix A.4) are compared in the part of the spectrum where (1) the length is smaller than 40 cm (here one can assume that the fishing mortality does not play a major role) and (2) where the slope is negative. The second condition is necessary because in the data of the hydroacoustic survey the number density increases up until around 30 cm which is biologically not meaningful. Table 7.2 shows the results. The bottom trawl survey and the CAS survey are in agreement with the predicted range, while the slope of the hydroacoustic survey is out of the range.

Table 7.2: The linear regression results concerning the slope in the range where the survey spectrum has negative slope and is not heavily influenced by the fishing mortality. Table shows the slope estimate together with the standard error (s.e.) and the residual standard error (i.e. weighted by number of data points).

<b>dataset</b>	range	slope	s.e.	residual s.e.
BT2019	10-40 cm	-0.141	0.026	0.072
HA2019	30-40 cm	-1.086	0.057	0.019
CAS2020	10-40 cm	-0.256	0.099	0.090

The residuals to the model, i.e. the difference between the (interpolated) survey data and the model prediction is depicted in Fig. 7.8. The reason for the deviation of the hydroacoustic survey both from the model prediction and the other surveys is not obvious. The analysis of the HA survey involves an intricate calibration which might be susceptible to errors. Apart from that, it is (again) visible that the spectrum of both BT and CAS drops suddenly after around 55 cm (BT) and around 60 cm (CAS). For the CAS, the data are not so reliable here due to sparse data for larger fish in the catch assessment survey and the BT survey has an unknown retention function after 40 cm (see above).

Summarizing, the validation indicates that with a high probability, the model replicates the size structure correctly because it agrees with the BT and the CAS

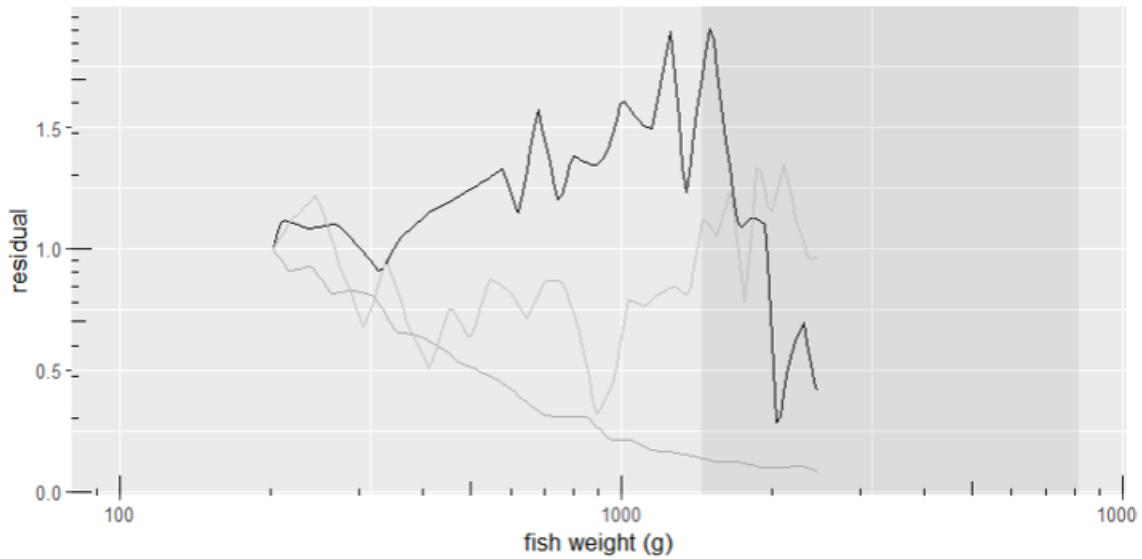


Figure 7.8: Distribution of residuals after subtracting model prediction from BT (black), HA (dark gray, bottom) and CAS (light gray, middle). For HA, residuals have a clear trend.

spectrum in the size range where the data are accurate. The HA surveys is incompatible with the BT, the CAS and the simulated spectrum.

### 7.3 Fishing mortality

In the literature, two distinct notions of the term “fishing mortality” are in use. Some use the term in the sense of the ratio between annual yield and biomass. It is important to emphasize that this notion is a mortality that is averaged, typically, over time (e.g. one year) and, more importantly, averaged across the population or at least across a major part of the population (e.g. all adults). We could refer to this notion as the *percent (annual) removal* as it is, in most cases, calculated from the ratio of annual yield (catch) to biomass.

The other notion of “fishing mortality” refers to an *instantaneous rate* and it depends, in general, on the size of the fish (e.g. in [196]). This is the notion of mortality rate that is used in this paper. It is important to note that the values of the two notions need not necessarily be the same or not even be similar to each other. As the second notion, the *instantaneous rate*, can vary across the fish population, some fish sizes could experience a very low or a very high mortality rate. Therefore, for comparison, the instantaneous rate can be translated to an annual mortality by building the ratio of annual catch to biomass. Here, the information on how

the mortality is distributed across the population, is completely lost. If the fishing mortality is applied equally across all fish sizes, then the two notions agree. Please note that the mortality that appears throughout the equations of Chapter 6, is the *instantaneous mortality rate*, as can be seen from its use in the McKendrick-von-Foerster equation (6.1).

Hence, in the case of the size structured model used in this paper, the actual fishing mortality rate is not the same for all fish, but depends on the fish size. For the purpose of comparing various fishing levels, therefore, it is necessary to define a reference fishing mortality. In the following this will be the “peak fishing mortality”, defined as the instantaneous mortality rate at the size of the maximum of the fleet selectivity curve, with the unit 1/yr.

To compare the results to estimates of the fishing mortality from the literature, the following approach is used. Across the range of admissible peak fishing mortality values, from  $F=0$  to the point, where the stock collapses, at  $F_{crash} = 5.52/yr$ , the ratio between annual yield and the stock biomass is calculated (Fig. 7.9). This ratio, equivalent to the widely used first definition of fishing mortality, and the peak fishing mortality are in direct relation to each other - and the mapping between the two quantities is unique in the range of admissible peak fishing mortality values. This means that the conductor of a survey, when he would observe the simulated stock in the reality, would interpret this yield/biomass ratio as the fishing mortality. Because of the unique mapping, the peak fishing mortality rates of the model simulations can uniquely be compared to conventional fishing mortality values.

With the mapping, the result of this paper - the value of  $F_{MSY}$  under the current fleet selectivity,  $F_{MSY} = 1.015/yr$  (see next chapter) - can be compared to empirical estimates from the literature and to other model simulations. In simulations of an Atlantis and an EwE model, the fishing mortality of Nile perch (approximated by the annual catch per biomass) was 0.312/yr (Atlantis) and 0.340/yr (EwE), respectively [145]. This value corresponds, in our model, to a peak fishing mortality of 1.05/yr and 1.11/yr, respectively, thus similar to our estimate. From an empirical analysis of commercial catch samples from two Kenyan landing sites, another study [196] estimates a fishing mortality of 0.54/yr, corresponding to a peak fishing mortality of 1.50/yr, somewhat higher than our finding. However, the value of the study [196] is likely to be biased, as it was derived not from the actual population in the lake, but only from catch samples, whose size structure differs systematically, due to the selectivity of the fishery.

## 7 Model validation and sensitivity analysis

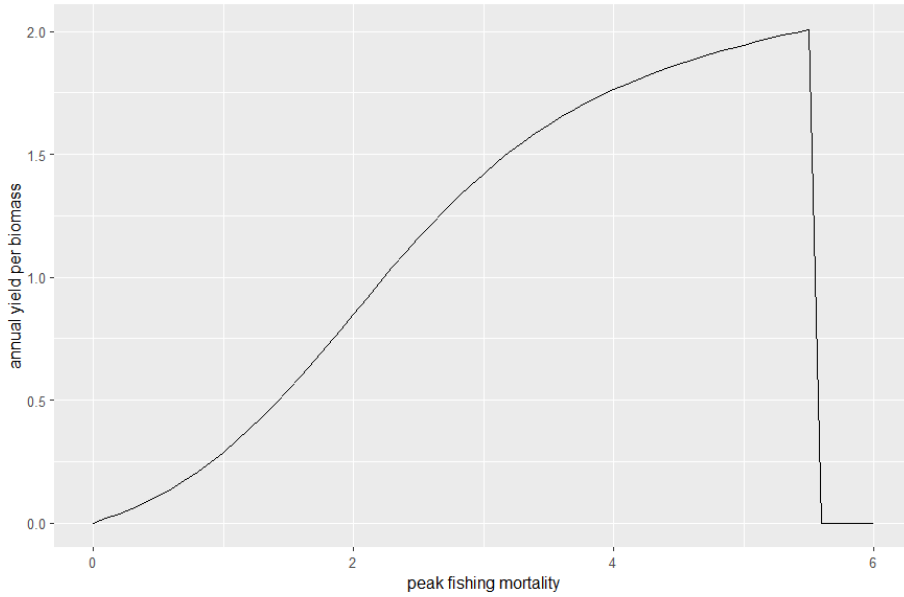


Figure 7.9: The relationship between the peak fishing mortality (an instantaneous mortality rate) and the annual fishing mortality (yield per biomass). The stock collapses at  $F_{crash} = 5.52/yr$ .

### 7.4 Sensitivity analysis

The sensitivity of the results to the input parameters is evaluated by quantifying the marginal effect of small parameter changes [171]. Two model results are considered here as most relevant: The fishing mortality that maximizes yield,  $F_{MSY}$ , and the relative recruitment, which denotes the recruitment relative to the maximal possible value,  $R^* = R/R_{max}$ .

The recruitment is a significant indicator of the state of the fish population. The smaller the value, the greater is the impairment of the stock from fishing. A value of  $R^* = 1$  means that there is no impairment at all (unfished case). Limit reference points indicate at which fishing mortality the recruitment is impaired (e.g. at  $R^* = \frac{1}{2}$  as used in [2]).

We calculate the sensitivity with respect to three parameters: the growth parameter  $A$ , the physiological mortality  $a$ , and the size at maturation  $w_m$ . The first two parameters can only be inferred, but not measured directly. The third parameter can be measured [160], but the measurement is costly, therefore it is not done frequently.

The evaluation is done in two ways: first, the change in absolute values:

- $\frac{\partial R^*}{\partial q_i}$  for  $q_i \in \{A, a, w_{mat}\}$

- $\frac{\partial F_{MSY}}{\partial q_i}$  for  $q_i \in \{A, a, w_{mat}\}$

Second, the relative change, which can be interpreted as the elasticity of the output variable with respect to the parameter:

- $\frac{\partial R^*}{\partial q_i} \bigg/ \frac{R^*}{q_i} = \frac{q_i}{R^*} \frac{\partial R^*}{\partial q_i}$  for  $q_i \in \{A, a, w_{mat}\}$
- $\frac{\partial F_{MSY}}{\partial q_i} \bigg/ \frac{F_{MSY}}{q_i} = \frac{q_i}{F_{MSY}} \frac{\partial F_{MSY}}{\partial q_i}$  for  $q_i \in \{A, a, w_{mat}\}$

The partial derivatives are approximated with the difference quotient using  $\Delta q_i = 0.01$ , the elasticity with  $\Delta q_i/q_i = 1\%$ . The basis parameter values are:  $A = 13.02g^{1/4}yr^{-1}$ ,  $a = 0.3$ ,  $w_{mat} = 4400 g$ . The results are given in Table 7.3. In each column, the largest (absolute) value is marked bold. The largest impact on  $R^*$  comes from the parameter  $a$ , both in absolute and relative terms.

Table 7.3: Relative and absolute sensitivity of  $R^*$  and  $F_{MSY}$  to the parameters  $A$ ,  $a$  and  $w_{mat}$ .

parameter ( $q_i$ )	$\frac{\partial R^*}{\partial q_i}(q_i)$	$\frac{q_i}{R^*} \frac{\partial R^*}{\partial q_i}(q_i)$	$\frac{\partial F_{MSY}}{\partial q_i}(q_i)$	$\frac{q_i}{F_{MSY}} \frac{\partial F_{MSY}}{\partial q_i}(q_i)$
$A$	0.00030	0.0038	0.078	<b>1.0</b>
$a$	<b>-0.049</b>	<b>-0.014</b>	<b>1.6</b>	0.48
$w_{mat}$	$2.8 \cdot 10^{-7}$	0.0012	$2.1 \cdot 10^{-5}$	0.089

For  $F_{MSY}$ , one sees that the elasticity is largest for the parameter  $A$  and is approximately one. This means that a faster growing population can tolerate a larger fishing mortality, in almost linear proportion to the growth rate. That implies that it is difficult to estimate both  $A$  and  $F$  simultaneously from an empirical population spectrum, as a linear scaling of both keeps the spectrum nearly unchanged which we also observed in the numerical simulations (not shown here). In absolute values, the crucial parameter for  $F_{MSY}$  is  $a$ . The table has to be interpreted in the sense that a change of 0.01 in  $a$  changes  $F_{MSY}$  by  $1.6/yr \cdot 0.01 = 0.016/yr$ . Because of the sensitivity of the results with respect to the physiological mortality  $a$ , in future research the important role of the physiological mortality should be considered, and more biological research and measurements are critical to determine the value accurately.

## 7.5 Catch size distribution

In addition to the population spectrum, the size distribution of the catch was simulated for three levels of fishing mortality (0.5, 1.0, 1.5/yr) which is shown in Fig. 7.10. The top

## 7 Model validation and sensitivity analysis

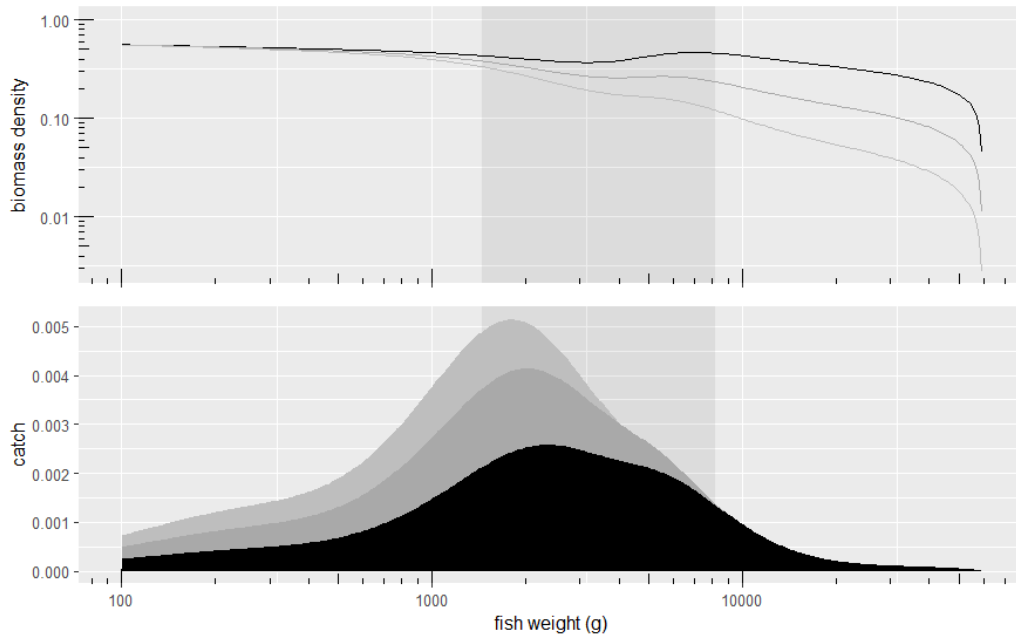


Figure 7.10: Simulations of Nile perch biomass spectrum (top) and catch distribution (bottom) with the empirical fleet selectivity (2020) for  $F=0.5$  (black), 1.0 (dark gray) and 1.5/yr (gray). The gray shaded rectangle indicates the slot size range (50-85 cm).

row shows the biomass spectrum, normalized at  $w = 1$  mg. The bottom row of Fig. 7.10 displays the spectrum of the catch for the three levels of fishing mortality. The major part of the selectivity curve left of the minimum legal size 50 cm reveals the non-compliance of fishers with the size regulation.

The following aspects can be observed: First, the peak of the catch curve is not equal to the peak of the selectivity curve, but is left of it. The reason is that the spectrum is declining, therefore the density of fish is higher at smaller sizes. The catch, being the product of biomass density and selectivity, is thus shifted to the left. For  $F=0.5/\text{yr}$ , where the biomass spectrum is almost flat in the legal range and even has a positive slope when fish pile up around maturation (70 cm), the catch curve has, next to the peak, a second hump right of it - at the position where the biomass density has a local maximum.

Second, the peak of the catch spectrum moves further to the left with increasing fishing intensity, from 2388.2 g (0.5/yr, black) to 1825.6 g (1.5/yr, light gray). The reason is found in the biomass spectrum: for  $F=0.5/\text{yr}$ , the spectrum is almost flat up until around 10,000 g. For  $F=1.0/\text{yr}$  and 1.5/yr, the spectrum declines earlier, already in the range of legal fishing, 50-85 cm. Therefore, the peak catch weight moves also towards lower sizes.

Third, the catch rates in the range up to around 4000 g increase with increasing fishing mortality. Beyond 4000 g, however, the catch rates with 1.5/yr (light gray) are lower than the rates with 1.0/yr (gray). The reason is: under the the higher fishing pressure less fish

## 7.5 Catch size distribution

survive such that the density of fish is now so low that it is not even compensated by the higher mortality. It is visible that a smaller fishing mortality can lead to higher catch rates of large fish (even in absolute numbers).

A full representation of the fishery includes both the selectivity  $\psi_F(w)$  and the level (intensity) of fishing,  $F$ . While the first one has been derived from the catch assessment survey [80], the level can be estimated by the yield to biomass ratio. From yield and biomass data from 2014 and 2015 [121, 120], the yield-to-biomass ratio is 0.304/yr, assuming the biomass of 2015,  $B=683.18\text{kt}$  [120]. This is similar to the results of the Atlantis (0.312/yr) and EwE (0.340/yr) simulations in the previously mentioned study [145] and it is lower than the value 0.44/yr, reported in [102] for the period 2005-2007. Given the empirical selectivity in the model, the yield-to-biomass 0.304/yr ratio is achieved with a peak fishing mortality  $F=1.036/\text{yr}$ .

The fishing level comes from fishers' decisions on their individual effort, and can therefore be subject to ongoing change. To predict how the fish stock and the yield would react to various fishing levels, the fishery is simulated for the range of peak fishing mortality from 0/yr to 6/yr (Fig. 7.11). Initially, from 0 to 1/yr, the yield increases rapidly, as fishing increases while the stock recruitment is not impaired yet. It is not impaired because the non-linearity buffers the additional fishing mortality, i.e. here fishing replaces the mortality early in life which is modeled by the non-linearity. At  $F=1.015/\text{yr}$ , the fishery reaches the maximum sustainable yield (MSY). Between 1/yr and 4.5/yr, the yield decreases almost linearly with fishing mortality. It is remarkable that the yield at  $F=2/\text{yr}$  is still high (around 85.2% of MSY), while the SSB has already decreased to 3.0% of the unfished state. This is possible because the recruitment is still at 98.9% and it demonstrates the enormous effect (and potential) of the non-linearity in recruitment which models the density-dependent effects early in life and which is particularly strong for large fish like Nile perch [2]. At  $F=4.83/\text{yr}$ , the recruitment is reduced to 50% or recruitment of the unfished population. Afterwards, the yield drops quickly, and at 5.52/yr, the stock is collapsed completely.

7 Model validation and sensitivity analysis

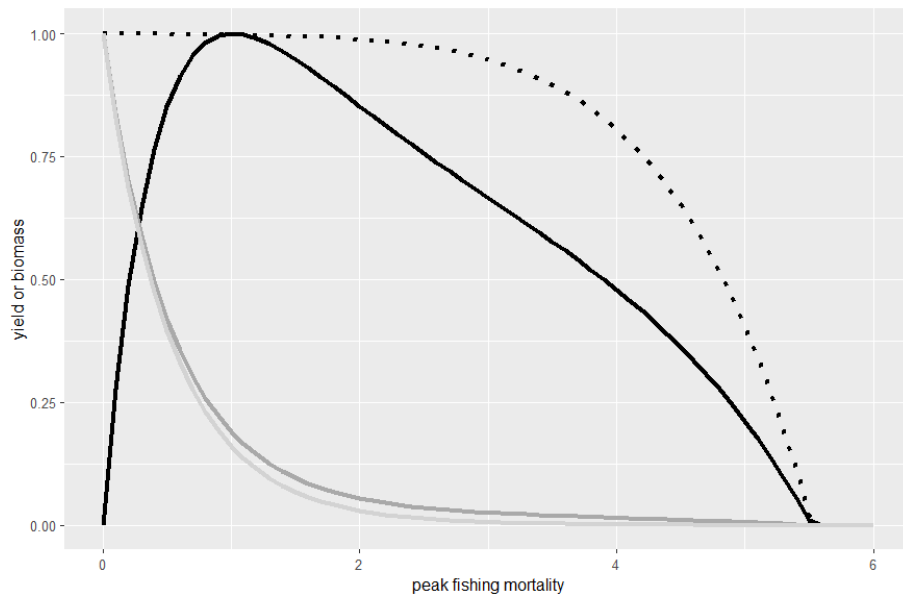


Figure 7.11: Steady state yield (black), stock biomass (dark gray), SSB (light gray) and recruitment (dotted) as a function of the peak fishing mortality up to 6/yr. The curves are normalized to the maximum.

# 8 Alternative fleet selectivity scenarios

While in the previous chapter we analyzed the actual situation of the fishery with fixed fleet selectivity, now we turn to possible alternatives in the exploitation pattern: Whereas in the previous chapter, only the level was free and the size selectivity was fixed, in this chapter we try to find better shapes of the fleet selectivity. To contribute to the management of the fishery, we orient this discussion along current proposals that are lively and controversially discussed by the fishery managers and fishery scientists of Lake Victoria. We seek to test and challenge the current understanding and question the narrative that harvesting should be "balanced" across all sizes, i.e. be proportional to the productivity at each size [147]. This would imply targeting smaller fish much stronger than larger ones. We will therefore simulate various alternative patterns of the selectivity inspired from the current proposals. Fishery managers want to achieve high yield without bringing the stock to deterioration or collapse, i.e. they want to keep the stock in an equilibrium. Therefore we assess the steady state solution and rank the scenarios by yield and income.

In the first section we test three scenarios around the current slot size regulation. In the second section we test whether a reduction in the number of vessels using small gears (targeting small fish) would decrease or increase the steady state yield of the fishery, which directly connects to the concerns of managers about lower yield from sparing young fish.

## 8.1 Slot size scenarios

We study the effect of three alternative fleet selectivities. The study is inspired by recent discussions about modifications of the legal fishing range. As we are interested only in how a given fleet selectivity translates into a stock size distribution, optimal fishing mortality ( $F_{MSY}$ ), annual yield, and catch size distribution, we exclude, for now, the effects of the re-distribution of fishing pressure in the respective range of legal fishing. This means that, in each scenario, inside the respective legal range the fishing selectivity is identical to the observed selectivity, and outside of the range it is zero. Due to the fact that the gears are not perfectly selective, a smooth transition is implemented at the edges of the fishing range. This helps to avoid sharp edges that would be unrealistic in the fishery setting.

## 8 Alternative fleet selectivity scenarios

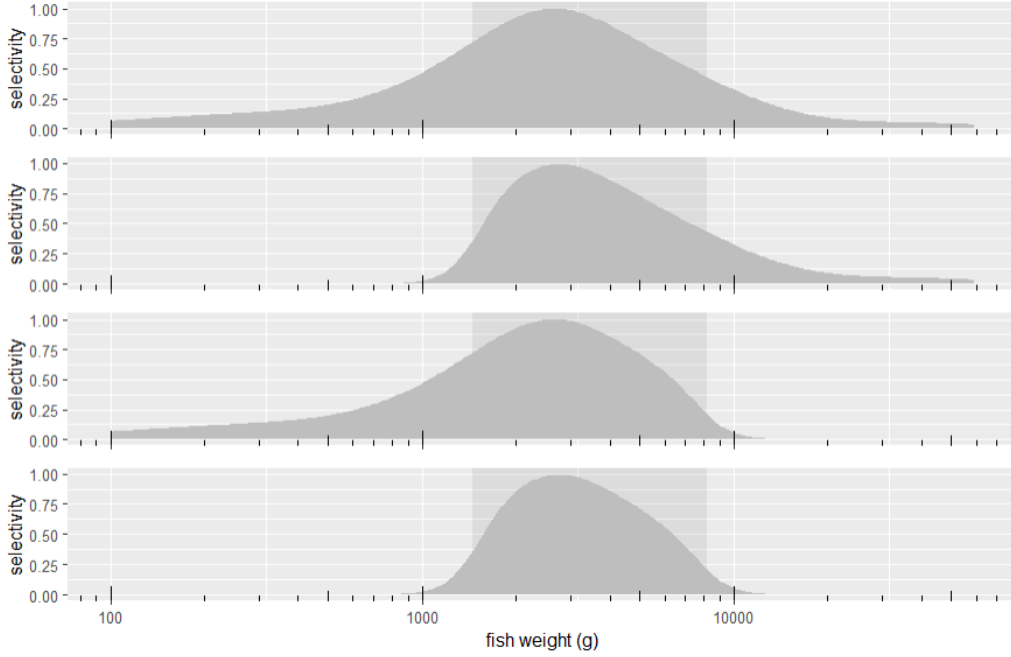


Figure 8.1: Top: empirical fleet selectivity. Second and third row: cropped fleet selectivities ( $>50$  cm and  $<85$  cm). Bottom: fleet selectivity within slot size (50-85 cm). Due to the imperfect selectivity of gears, a smooth transition around the edge is assumed in each case.

The fishing selectivity is thus multiplied with one switching function for each edge in the form

$$\psi_{sw}(L; L_0) = \frac{1}{1 + \left(\frac{L}{L_0}\right)^{-u}}, \quad (8.1)$$

where  $u = 25$  determines the sharpness of the transition,  $L$  is the fish length and  $L_0$  the position of the edge (length in cm). For the lower bound at  $L_l=50$  cm, the selectivity was multiplied with  $\psi_{sw}(L; L_l)$ , while for the upper bound at  $L_u=85$  cm, the selectivity was multiplied with  $1 - \psi_{sw}(L; L_u)$ .

The four scenarios (Fig. 8.1) are:

1. empirical fleet selectivity:  $\psi_1(w) = \psi_F(L(w))$
2. fishing only above 50 cm:  $\psi_2(w) = \psi_{sw}(L(w); L_l)\psi_F(L(w))$
3. fishing only below 85 cm:  $\psi_3(w) = (1 - \psi_{sw}(L; L_u))\psi_F(L(w))$
4. fishing only from 50-85 cm:  $\psi_4(w) = \psi_{sw}(L(w); L_l)(1 - \psi_{sw}(L; L_u))\psi_F(L(w))$

The results of this section should not be interpreted as predictions about how fishers would comply to various regulations. Rather, they are simulations how a *given* pattern

of the fleet selectivity translates to steady state yield and income. Under different policy regulations or under a stricter enforcement of the bounds of the slot size, fishers' would re-distribute their fishing effort to sizes that are more profitable to them, either because of higher yield, higher per-kilo price (for larger fish) or to avoid penalties for using illegal gear sizes, but this is not studied here. The response of fishers to the profit from fishing is investigated later in Chapter 10.

Like in the previous chapter, we keep the level (peak fishing mortality) variable, and therefore the four scenarios are simulated as the solution of (7.4) over the range of  $F=0$  to  $F=6/\text{yr}$ . From the population and the fishing mortality, the steady state yield (6.32) was calculated across the entire range (Fig. 8.2). The four scenarios can be compared from two perspectives.

First, they can be compared at the current level of fishing mortality (black vertical line in Fig. 8.2). This corresponds to a situation where the fishing level of the legal range 50-85 cm stays the same, but, depending on the scenario, there is no fishing below 50 cm, above 85 cm, or both.

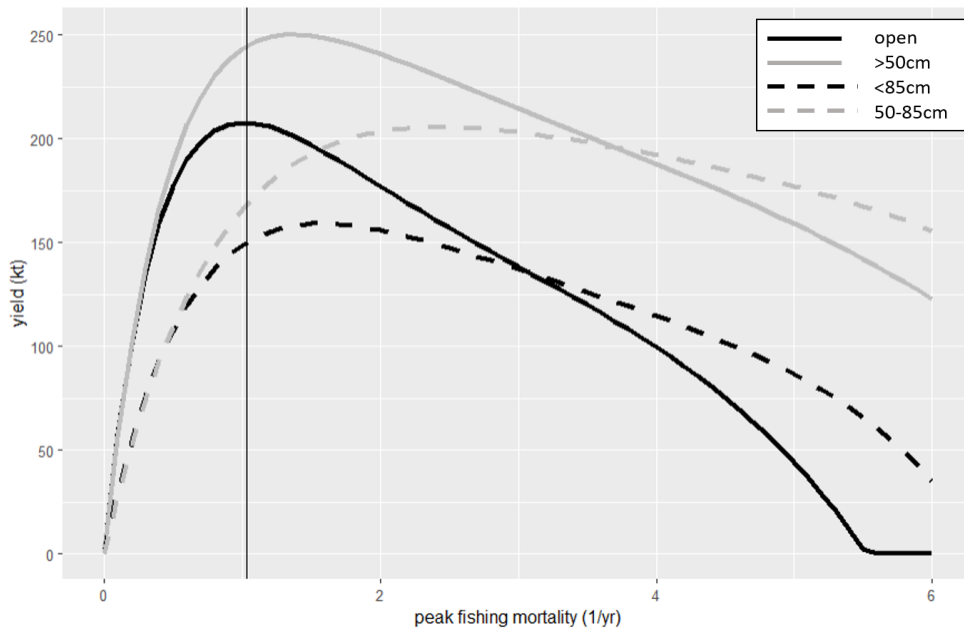


Figure 8.2: Yield dependent on fishing mortality for the four selectivity scenarios. The black vertical line is the empirical fishing mortality.

In the *open* scenario (with the empirical fleet selectivity), the annual steady state yield at the peak fishing selectivity  $F_{emp} = 1.036$  is 207.6 kt and the annual income is 532.6 million USD. The second scenario, catching no fish below 50 cm while keeping the fishing mortality above 50 cm the same, increases the annual yield by 17.7.% from 207.6 kt to 244.4 kt (Table 8.1). Catching not fish above 85 cm (scenario 3), however, decreases yield by 28.8% from 207.59 kt to 149.90 kt, with scenario 4 being somewhat better, but still

## 8 Alternative fleet selectivity scenarios

Table 8.1: Yield, percentage increase and yield and SSB at empirical peak fishing mortality  $F_{emp} = 1.036$  together with maximum sustainable yield MSY (kt) and best fishing mortality  $F_{MSY}$  (1/yr) for each of the four scenarios.

<b>scenario</b>	$Y_{F_{emp}}$ (kt)	$\pm\%$	$SSB_{F_{emp}}$ (kt)	$F_{MSY}$ (1/yr)	MSY (kt)
open	207.6	+0%	537.3	1.02	207.8
> 50 cm	244.4	+17.7%	708.4	1.37	250.3
< 85 cm	149.9	-27.5%	926.0	1.57	159.1
50 – 85 cm	168.2	-19.0%	1221.1	2.43	205.6

inferior to the open scenario. The SSB increases in each scenario because the fishing pressure, in total, is reduced.

Second, the scenarios can be compared at the fishing level that is optimal in each respective case. This MSY level is the point of the maximum in each curve in Fig. 8.2. At the empirical fleet selectivity, the MSY value is 207.8 kt (Table 8.1), which is similar to the predictions in [102, 143] (212 kt and 246 kt, respectively), and lower than earlier estimates from two to three decades ago [111, 168]. Again, the best scenario is fishing above 50 cm, where the maximum sustainable yield is 250.25 kt. Scenario 3 is inferior and scenario 4 has a similar MSY like the open scenario.

For small values of the peak fishing mortality, scenarios 1 and 2 are similar and have a steeper initial slope than scenarios 3 and 4. The reason is that the latter restrict from fishing large fish, which, at the unfished, “pristine” level of the fishing stock, are most abundant and therefore provide high yields. At the other end, for large values of the peak fishing mortality, scenarios 2 and 4 still provide moderate yield levels, because juveniles below 50 cm are spared and thus some individuals can still reach maturity and reproduce. Contrarily, in scenarios 1 and 3, juveniles are subject to fishing, which leads, for a high fishing mortality, to fewer survivors, very low yield, and eventually to the collapse of the stock.

An important result is that, under the empirical fleet selectivity, the  $F_{MSY}$  value is 1.015/yr and thus the empirical fishing mortality  $F_{emp} = 1.036/yr$  is only 2.0% above  $F_{MSY}$ , which would mean that the current (2020) fishing level is close to what is the best level, for the fleet selectivity being as it is. This is different from various other studies, who suggest an overfished, and hence unsustainable, state [196], but would explain the relatively stable population of Nile perch in the last decade [120, 145, 130, 127]. Of course, dynamical factors from the interaction with other species [199, 155] or the ecosystem or fluctuations in the fishing level can never be excluded, but at least this single species model hints towards a rather appropriate level of fishing mortality. Improvements in yield could, however, be achieved if the fishing pressure below 50 cm were reduced, as scenario

2 suggests. This case is also more stable in the sense that the curvature of the yield curve (Fig. 8.2) is smaller around the maximum, i.e. the maximum is broader and the curvature smaller which points toward a situation that is more resilient with respect to fluctuations in the level of fishing mortality.

Keeping fleet selectivity fixed, there is a trade-off between yield and the biomass. With increasing yield, the steady state biomass decreases. In the beginning this decrease follows roughly a straight line (Fig. 8.3). There is a second branch at the bottom, where the stock still exists, but is highly depleted. Note that for a broad range of yield values, two steady state SSB values, i.e. two different situations of the fish stock and the fishery exist, that would produce the same value of yield - either with a large stock (upper branch) or a heavily depleted stock (lower branch).

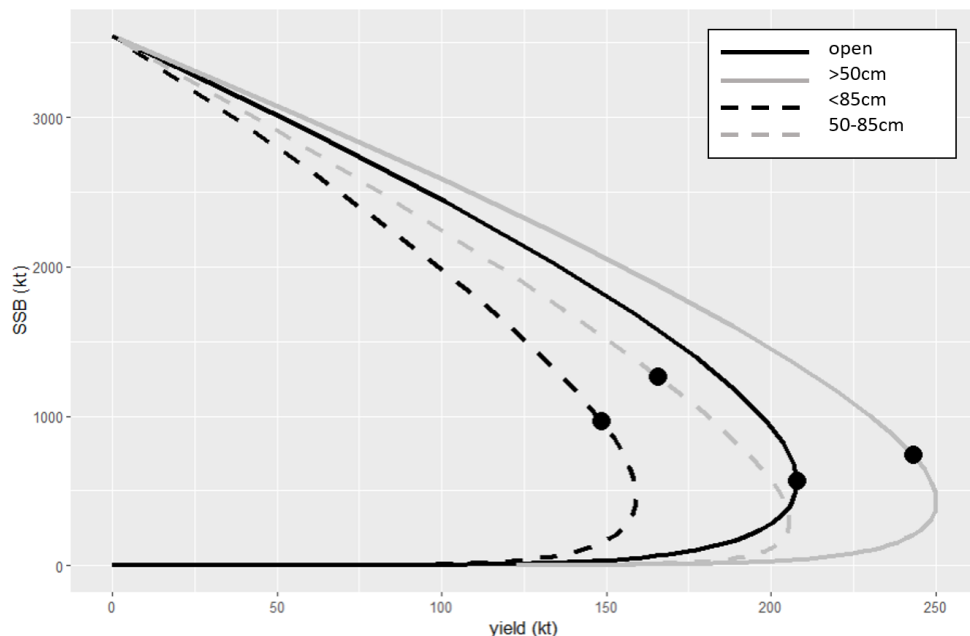


Figure 8.3: The figure depicts the SSB in steady state in dependence of the yield. Note the two "branches" in each curve, where the same yield value can be achieved in a situation with high or low SSB. Dots mark the situation at  $F_{emp} = 1.036/yr$  (current empirical peak fishing selectivity).

As the parameter  $a$  (physiological mortality) is rather uncertain and the results are sensitive to that parameter (cf. Section 7.4), it was tested to which degree the ranking of the four slot size scenarios with respect to the maximum sustainable yield depends on the parameter value (Table 8.2). The values  $a = 0.2$  and  $a = 0.3$  yield the same ranking of the scenarios, where the  $>50$  cm scenario produces the highest MSY, followed by the *open* scenario, the slot size and, finally, the  $<85$  cm scenario. In the cases  $a = 0.4$  and  $a = 0.5$ , the physiological mortality is so strong that the slot size scenario is superior to the *open*

## 8 Alternative fleet selectivity scenarios

scenario. Independently of the value of  $a$ , however, is the  $>50$  cm scenario always the best and  $<85$  cm the worst scenario.

Table 8.2: Maximum sustainable yield MSY in each scenario for four different values of the parameter  $a$ . Note that the unit here is not kt, but  $g/R_{max}$  (because the conversion to the unit of kt would itself depend on the scenario).

scenario	$a = 0.2$	$a = 0.3$	$a = 0.4$	$a = 0.5$
open	159.82	30.09	6.05	1.15
$> 50$ cm	190.12	36.22	7.26	1.35
$< 85$ cm	102.95	23.00	5.09	1.03
50 – 85 cm	135.03	29.78	6.43	1.24

To test the robustness, we additionally vary the three parameters  $a$ ,  $A$ ,  $F_{emp}$  ( $= Y_{emp}/B$ ) in the range  $a \in \{0.2, 0.3, 0.4\}$ ,  $A \in \{10, 13.02, 16\}$ ,  $F_{emp} \in \{0.1, 0.304, 0.5, 0.7\}$  and find that the magnitude of the increase/decrease in yield and income (at  $F_{emp}$ ) in the three alternative scenarios ( $>50$  cm,  $<85$  cm and slot size) compared to the *open* scenario varies, but the direction of change (increase/decrease) does not depend on the parameter values. Thus the ranking of the results is the same independent of the parameter values.

In addition, we test scenarios where the fishing mortality is increased or decreased by 50%, below 50 cm and analogously above 85 cm, and find that the direction of change (increase/decrease) in both yield and income at the current peak fishing mortality is the same independent of the values of the parameters  $a$ ,  $A$ ,  $F_{emp}$  ( $= Y_{emp}/B$ ) in a wide range ( $a \in \{0.2, 0.3, 0.4\}$ ,  $A \in \{10, 13.02, 16\}$ ,  $F_{emp} \in \{0.1, 0.304, 0.5, 0.7, 0.9\}$ ), such that we can conclude that the qualitative results are robust within these ranges of the parameter values.

## 8.2 Gillnet scenarios

From discussions with research partners at LVFO and the associated fisheries research institutes it became evident that, next to the slot size, it is of high importance to regard the mesh size of gillnets as a tool for regulation. The reason is that the usage of gillnets can be directly controlled on the lake, e.g. with control boats. This is corroborated by the fact that the mesh size restrictions play an important role both in the concrete enforcement of the fishery regulations and the everyday life of fishers as well as in the discussion in the general public regarding the legitimacy and efficiency of the regulations and of a potentially strict enforcement. This discussion is not only undertaken by scientists, but reaches into the general public with various reports on the typical "punishment" for using illegal mesh sizes, namely the destruction of the nets.

## 8.2 Gillnet scenarios

The regulation via gear sizes allows also, in principle, for other government inference apart from gear destruction, but in the form of taxes or subsidies which has e.g. been tested in a small-scale field experiment for dagaa nets [47]. This thesis restricts itself to studying the effect of a change in the fishing selectivity, instead of the tools to enforce a given regulation. In other words, the question is, which fleet selectivity should a regulation aim for. Therefore, for simplicity, the scenarios are simplified in the following manner:

First, the fishery in the model is assembled from a (generalized) longline hook and from gillnets with mesh sizes ranging from 3" to 8" in steps of 1", as described in chapter 4. Then in each of the five additional scenarios, some gears are not employed in the fleet, i.e. those gears are not included in the fleet selectivity. To test the robustness, we have also tested the case where fishers move to the next larger legal gear (see below).

In the first scenario, all gears with mesh size 3" drop out of the fishery, such that the fishing fleet is now composed only of longline hooks and the gillnets with mesh sizes 4" and above (in unaltered numbers). This scenario is referred to as "GN4-8" or, equivalently, "GN4+". In the second scenario, the 4" gillnet vessels drop out, so that the fleet is composed of longlines and mesh sizes  $\geq 5$ ". The scenarios three, four and five follow analogously such that in the fifth scenario only the 8" gillnets are left, again together with the longline hooks. It is important to emphasize that this study is primarily asking for the effect of a particular fleet selectivity on the steady state yield or income. A different question, which we cannot address here, is whether banning small gillnets would actually lead to those fishers exiting the market, whether they would leave or switch to larger gears, in general all topics concerning the compliance to restrictions and the reaction of fishers or boat owners to gear regulations. To some degree, these questions can be addressed with the coupled model from Chapter 10, but generally the compliance is out of the scope of this thesis because we focus on the impact of a given fleet selectivity on stock, yield and income.

It is also important to note that there exist two distinct effects: the effect of less vessels on the lake (from boats leaving) and the shift of the fleet selectivity. By letting the vessel exit the fishery, we disentangle the effects and have only a reduction, but no movement to larger nets. We study the combined effect afterwards in a setting where fishers will shift towards the next larger legal net. With this simplistic representation we want to show primarily that the idea of the previous section - a comparison of fleet selectivity alternatives - need not be restricted to the slot size, but can be studied with respect to gears as well.

In this chapter and throughout the thesis we assume that the price which the boat owners achieve on the fish market are fixed and do not depend on supply. Thus an

## 8 Alternative fleet selectivity scenarios

increase in supply of large Nile perch does not impact the price in our model<sup>1</sup>. This assumption comes from the consideration that Nile perch (especially the larger fish) are primarily exported to Europe and East Asia. Those markets are also supplied with fillets from many other fish species, whose stocks are independent of the fishery at Lake Victoria. If we can reasonably assume a certain substitutability between fillets from Nile perch and from other fish species, we can work, for the purpose of our model, with retail prices for large fillets independent of the supply.

Now for each scenario, the steady state yield and income are compared to the results of the standard model with the empirical fleet selectivity. The income is calculated by using the price per kg of Nile perch provided in Table 4.4. Table 8.3 shows the yield and income increase relative to the status quo, Table 8.4 the increase in biomass and SSB. The same data are depicted in Figures 8.4 and 8.5, respectively.

Table 8.3: Increase in steady state yield and income, relative to the current situation, in five selectivity scenarios.

scenario	yield increase	income increase
GN4-8	4.55 %	5.33 %
GN5-8	6.87 %	8.44 %
GN6-8	12.45 %	16.58 %
GN7-8	21.81 %	33.44 %
GN8-8	21.49 %	34.86 %

Table 8.4: Increase in steady state biomass and SSB, relative to the current situation, in five selectivity scenarios.

scenario	biomass increase	SSB increase
GN4-8	5.59 %	5.70 %
GN5-8	9.10 %	9.39 %
GN6-8	21.23 %	22.65 %
GN7-8	65.96 %	74.38 %
GN8-8	81.65 %	93.43 %

These results indicate that steady state yield, income, stock biomass and SSB increase in each of the scenarios, relative to the status quo. With a single exception (yield in GN8-8), each scenario produces higher values than the previous one. E.g. in scenario GN5+, yield is 6.87% higher than in status quo, income 8.44%, biomass 9.10% and SSB 9.39%. The highest increase between two scenarios is from GN6+ to GN7+, where in the

<sup>1</sup>However the price depends on the size of the fish: larger fish achieve a higher per-kg price than smaller ones, mainly because they can be better used for filleting (see Table 4.4).

latter yield is 21.81% higher than in status quo, income 33.44%, biomass 65.96% and SSB 74.38%. What is the reason for the jump from GN6+ to GN7+? It is caused by the fact that 6” is the gear with highest frequency in the fishery (see Table 4.3). When this gear drops out, the fishing mortality decreases strongly, leaving (in steady state) a higher fish stock with more adults that produces more yield and income. The increase in income is more pronounced than the increase in yield because the price per kg of Nile perch increases with the weight of the fish (Table 4.4).

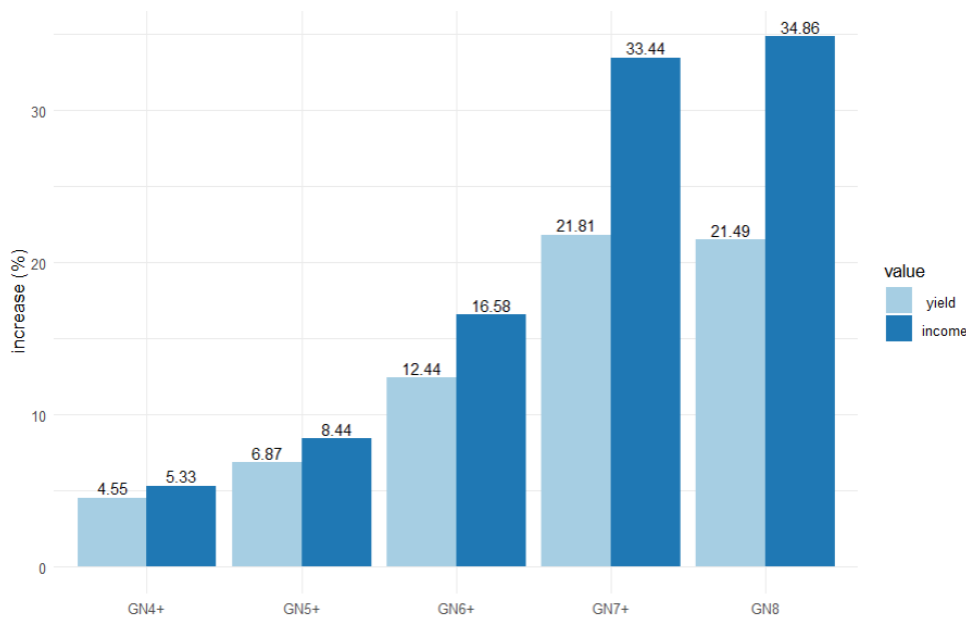


Figure 8.4: Increase in steady state yield and aggregate income of the fishery for five selectivity scenarios, relative to the current situation.

We have also tested variations of the three parameters  $a$ ,  $A$ ,  $F_{emp}$  ( $= Y_{emp}/B$ ) in the range  $a \in \{0.2, 0.3, 0.4\}$ ,  $A \in \{10, 13.02, 16\}$ ,  $F_{emp} \in \{0.1, 0.304, 0.5, 0.7\}$ , for the scenarios GN4+, GN5+, GN6+. We have found that the ranking of the scenarios did not change. In each case, the reduction of the lower-sized gears increases yield and income.

Now we test whether the results change if, from one scenario to the next, the fishers with the now illegal gear not simply exit the fishery, but rather switch to the next larger legal net. In the standard case (without senescent mortality), if fishers do not exit, but rather move to the next larger legal size, the yield increases stronger than otherwise, while the income increase is either stronger or less strong in GN7+ and GN8+. The conjecture about this observation is that the current fishing effort of large gears is currently lower than optimal (concerning yield).

## 8 Alternative fleet selectivity scenarios

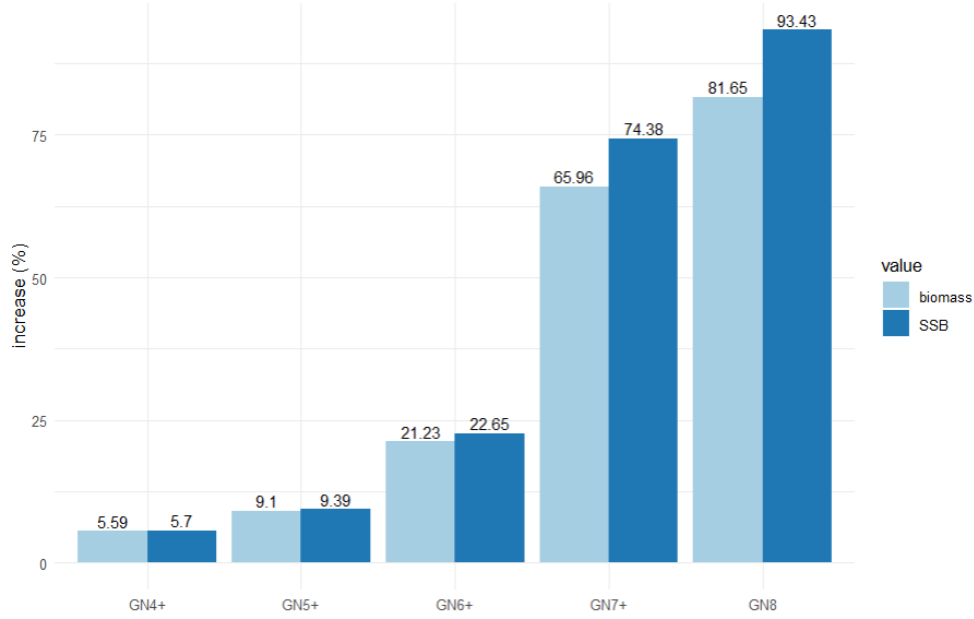


Figure 8.5: Increase in steady state biomass and SSB of the fish stock for five selectivity scenarios, relative to the current situation.

Furthermore, we test three different kinds of senescent mortality as described in 3.2.4. First, a mortality that increases linear in weight

$$\mu_s^1(w) = \frac{2w}{W_\infty}, \quad (8.2)$$

and second a hyperbolic shape

$$\mu_s^2(w) = \frac{\alpha_s}{a_\dagger - \text{age}(w)}, \quad (8.3)$$

where  $a_\dagger = 16yr$  is the maximum age [181] and  $\text{age}(w)$  the age at weight  $w$ , respectively. We test two different values of the parameter  $\alpha_s \in \{1, 3\}$ , which determines the strength of the mortality. The trend of increasing yield and income in each subsequent scenario also holds if fishers move, for all three senescent mortality cases. We conclude a robust trend that sparing small fish increases yield, income and spawning stock biomass. These results challenge a common perception among LV fishery managers that sparing small fish would only mean forgone harvest, neglecting the positive effects of fish surviving to larger sizes both because the growth potential is then fully utilized and because more fecund fish increase the reproduction of the stock.

## 9 Optimal fleet selectivity

In Section 6.3, a criterion was provided to compare the steady state yield of the current fishing pattern with the one from a modified fishing pattern, and an equation to analyze where (at which sizes) a higher fishing mortality would increase the steady state yield of the fishery. In the previous chapter we have studied how alternative shapes of the fleet selectivity would impact the steady state yield and income of the fishery. In this chapter, we address the question how yield and income can be maximized and which fishing pattern would be the one that maximizes yield or income, respectively, this means asking the question about the optimal fleet selectivity, using a numerical optimization.

Before taking the approach described below, we had first optimized the number of vessels of each gear, and had found that the solutions indicated that all available vessels would use 8" gillnets, i.e. the gear with the largest target size. Only if there was a cap on the number of vessels that can employ the same gear, then, to the remaining vessels, longlines were assigned and, consecutively, 7" gillnets.

Beyond this simple and straightforward result, we decided to go into more details because the gears with their large target range seem to be a rather coarse variable in the optimization, leading to a sort of corner solution where everybody uses 8" gillnets. To get a finer resolution, we decide to abstract from gears and instead optimize the size selectivity itself. To do so, we split the size range into 10 cm bins, where the optimization variables correspond to the fishing mortality in each of the bins. This corresponds to the assumption that a sole-owner of the fishery could effectively reach any size selectivity he wishes by an appropriate combination of perfectly selective gears in the fleet. What pattern should he then aim for?

## 9.1 Optimization problem

To reach a feasible maximization, the axis of fishing mortality is separated into 16 bins. There are correspondingly 16 optimization variables, which can be written as the vector

$$X = \begin{pmatrix} f_1 \\ f_2 \\ f_3 \\ \vdots \\ f_{16} \end{pmatrix}. \quad (9.1)$$

Each component determines the fishing mortality in a bin of width 10 cm. The first variable  $f_1$  indicates the value of the fishing mortality in the bin  $[0,10 \text{ cm}]$ , and the others analogously. The total fishing mortality is composed of the 16 bins. Formally, we can write this:

$$\psi_F(w(L)) = \sum_{i=1}^{16} f_i \delta_{i,\text{bin}(L)}, \quad (9.2)$$

where  $\delta_{i,\text{bin}(L)}$  is the characteristic function, that is 1 if  $L$  is in the bin  $i$  and 0 otherwise:

$$\delta_{i,\text{bin}(L)} = \begin{cases} 1, & \text{if } L \in [10(i-1), 10i) \\ 0, & \text{otherwise.} \end{cases} \quad (9.3)$$

The objective function is the steady state yield of the fish stock from the fishing mortality, given the variable vector  $X$ .

$$\max_X Y = \int_{w_0}^{W_\infty} wu(w; \psi_F(w)) F \psi_F(w) dw, \quad \text{s.t. (9.2)} \quad (9.4)$$

The optimization problem is solved using the function `optim` with the method `L-BFGS-B` (see A.5.4) in R [173]. In order to avoid that the optimization gets trapped in a local maximum, the optimization is repeated 100 times. Each optimization has random initial values of the 16 variables, independent and identically distributed in  $[0,1]$  with units of 1/yr.

## 9.2 Maximizing yield

Fig. 9.1 shows the outcome of the 100 optimization runs maximizing yield. The results are as follows: The fishing mortality is zero for  $L < 90 \text{ cm}$ . The peak of the fishing mortality is around 1.73/yr in the bin 110-120 cm. Between 0 and 120 cm, the variance across

## 9.2 Maximizing yield

optimization runs is extremely small (e.g.  $2.616 \cdot 10^{-4}/\text{yr}$  in the bin 110-120 cm). As the 100 optimization runs started from random initial conditions, it is therefore very likely that the results are globally optimal, as otherwise all runs would have converged to the same local maximum. Only beyond 130 cm, and especially in the two last bins in the range 140-160 cm, the variance becomes somewhat larger. The supposed reason is the fact the few fish left in this size range have a negligible impact on the total yield. The results corroborate the conclusion of the previous section, that the optimal fishing mortality is disproportionately targeting large fish while sparing the younger ones. If the fishery employed the median values of the 100 optimization runs, the steady state yield would be 404.87 kt/yr, which serves as a benchmark to assess the current situation. The optimal fishing pattern would hence provide a 94.6% increase in the steady state yield compared to the current situation (see Table 4.5).

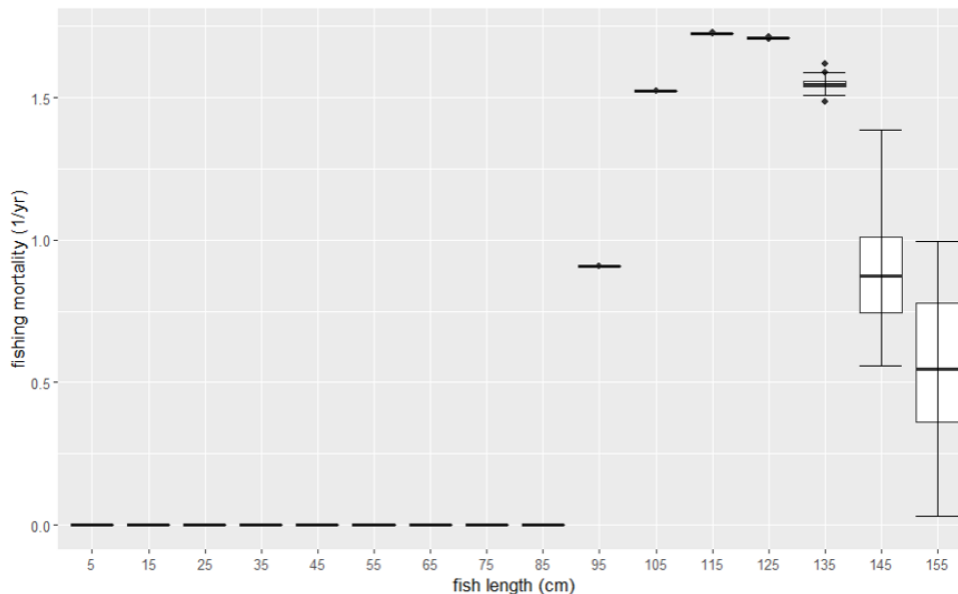


Figure 9.1: Maximizing steady state yield with 16 optimization variables, each one determining the fishing mortality in a bin of 10 cm width. The figure shows, for each bin, the result from 100 optimization runs with random initial conditions: the boxplots indicate the mean (center black line), the first and the third quartile (25th and 75th percentile, respectively) (hinges of the white box), the minimum and the maximum (besides outliers) (whiskers) and, if existent, outliers which are defined by being more than  $1.5 \cdot \text{IQR}$  from the hinge of the white box, where IQR denotes the inter-quartile range, i.e. distance between the first and the third quartile.

## 9 Optimal fleet selectivity

It was also tested whether the model with an additional senescent mortality for large fish would lead to different conclusions. The senescent mortality is linear in the fish weight

$$\mu_s(w) = \frac{2w}{W_\infty} \quad (9.5)$$

It was found that the optimal fishing mortality would then begin earlier, namely at 70 cm, which is still 20 cm more than the current lower bound of the slot size. The peak would be in the range 100-120 cm (Fig. 9.2). Note that the median optimal fishing mortality values are much higher than in the case without senescent mortality. Because of the additional mortality of large fish, it is necessary to harvest them at a higher rate, otherwise they would be lost due to the natural senescent mortality.

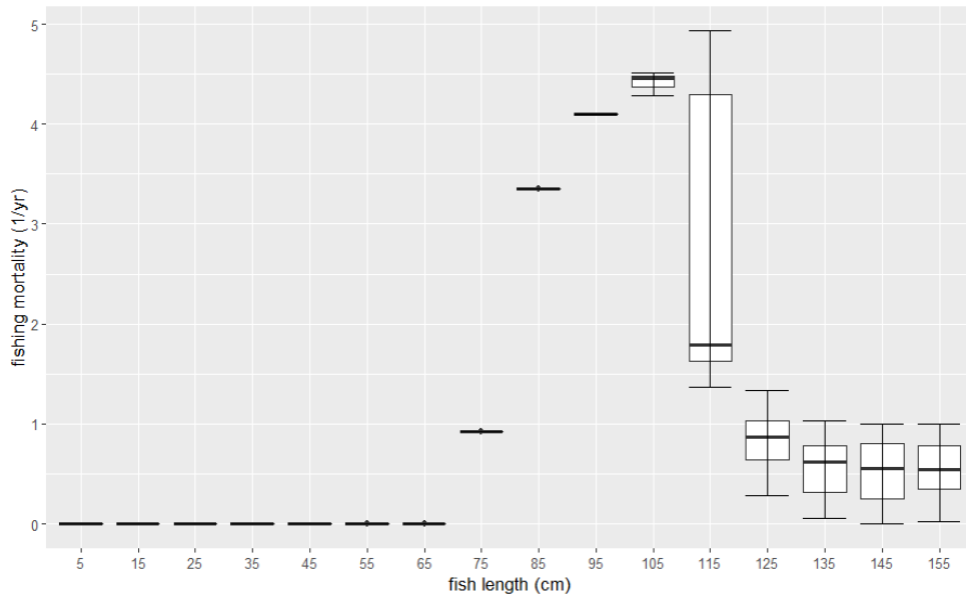


Figure 9.2: Maximizing steady state yield with 16 optimization variables, each one determining the fishing mortality in a bin of 10 cm width, in a model with an additional senescent mortality for large fish. The figure shows, for each bin, the result from 100 optimization runs with random initial conditions. For the meaning of the hinges, whiskers and outliers, see the caption of Fig. 9.1.

## 9.3 Maximizing income

The income was maximized from the optimization problem with the following objective function

$$\max_X I = \int_{w_0}^{W_\infty} p(w)wu(w; \psi_F(w))F\psi_F(w)dw, \quad \text{s.t. (9.2)} \quad (9.6)$$

### 9.3 Maximizing income

where  $p(w)$  is the per-kg price of Nile perch with size  $w$  (Table 4.4). The overall pattern is similar to the yield maximization, just the shape is slightly shifted towards the larger fish, due to their achieving a larger per-kg price at the market (Table 4.4). Here again, the fishing would start at 90 cm and the peak would be at  $F=1.72/\text{yr}$  in the bin 110-120 cm. Between 90 and 140 cm the variance of the 100 optimization runs with random initial conditions is almost non-existent, therefore one can conclude again with high confidence that the maximum is a global optimum. Between 140-160 cm, the results scatter for the same reason as before, because only few large fish are left such that the level of fishing has little influence on the total income. If one sets the fishing mortality in each bin to the median level of the optimization results, then the income is 1341.4 million USD/yr. This is 151.9% above the annual income with the empirical fleet selectivity (532.6 million USD), thus providing a substantial increase.

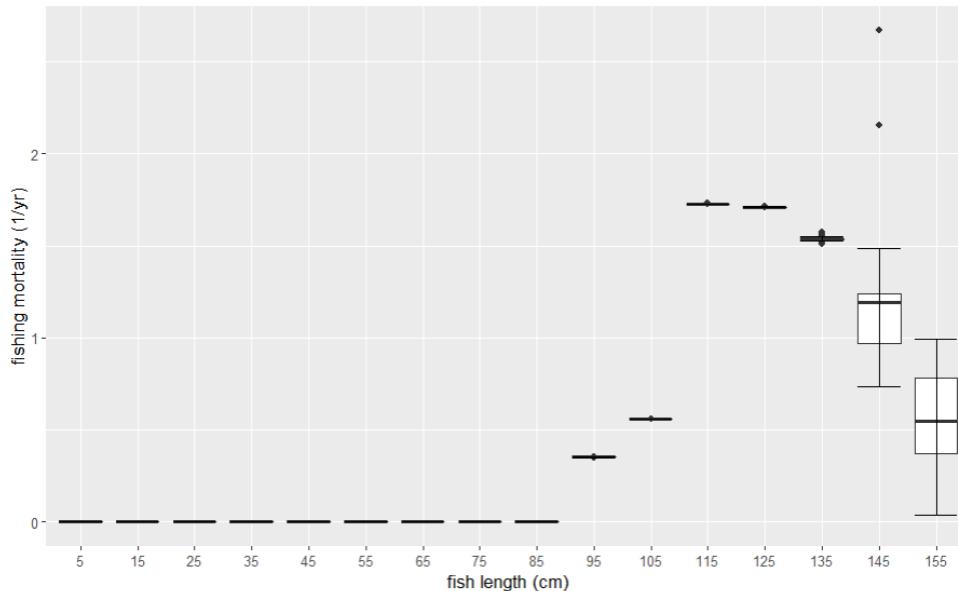


Figure 9.3: Maximizing steady state income with 16 optimization variables, each one determining the fishing mortality in a bin of 10 cm width. The figure shows, for each bin, the result from 100 optimization runs with random initial conditions. For the meaning of the hinges, whiskers and outliers, see the caption of Fig. 9.1.

Introducing a linear senescent mortality like previously in the yield maximization has a similar effect (Fig. 9.4). As the natural mortality is higher, the fish have to be caught earlier, otherwise they get lost from senescence. Therefore the fishing patterns shifts towards smaller fish and exerts a higher fishing mortality. The smallest fish in the catch have 80 cm length and the highest fishing mortality is experienced by fish in the size range 110-120 cm with 4.43/yr. The variance until 120 cm is very low and even beyond that comparably small.

## 9 Optimal fleet selectivity

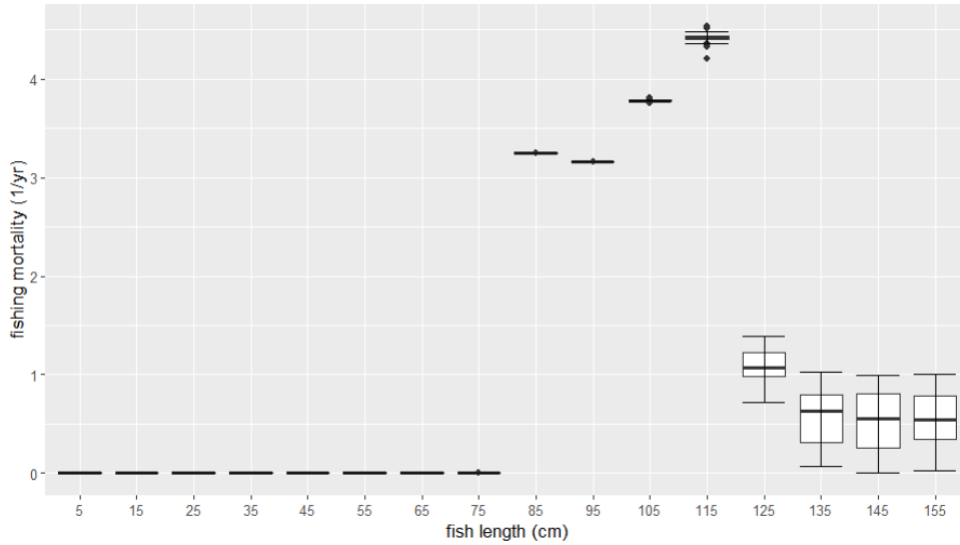


Figure 9.4: Maximizing steady state income with 16 optimization variables, each one determining the fishing mortality in a bin of 10 cm width, in a model with an additional senescent mortality for large fish. The figure shows, for each bin, the result from 100 optimization runs with random initial conditions. For the meaning of the hinges, whiskers and outliers, see the caption of Fig. 9.1.

## 9.4 Discussion

What is the interpretation of the result that the optimal fleet selectivity spares the juveniles? To understand this fact, one has to look at the curve of the cohort biomass (Fig. 9.5). A cohort is the group of fish that have been born in the same time period (in the continuous case this means fish that are born in the time interval  $[t; t + dt]$ ). The number of fish in a cohort is non-increasing with time, as the only relevant process is mortality which reduces the numbers. The cohort biomass, the sum of the biomass (weight) of all individuals in the cohort, however, has a more complex development. As long as the biomass increase from the growth of the individuals outweighs the biomass loss from mortality, the cohort biomass increases. At some point, typically beyond the maturation size, the mortality becomes so large that it dominates and the cohort biomass decreases. This gives a unimodal curve.

Fig. 9.5 shows the cohort biomass (3.16) across the lifespan for the case without fishing (black). The maximum of the cohort biomass lies at 100.9 cm (14318.6 g). It was pointed out in [50] for a similar scenario that under perfect selectivity (i.e. where the target size of fish can be selected with perfect accuracy and precision) the optimal management is to target the fish at the size where the cohort biomass peaks. This explains the optimization

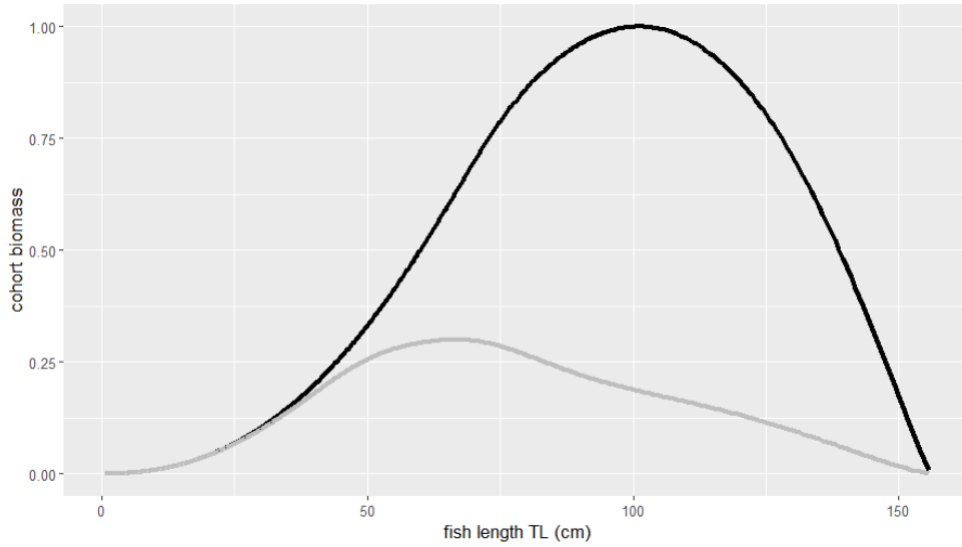


Figure 9.5: Cohort biomass (normalized to the maximum) in the case without fishing (black) and under the empirically observed fleet selectivity with  $F = 1.0/yr$ .

results of this section, as even with the not perfectly selective gears a range similar to the point of maximum cohort biomass is targeted.

Fig. 9.5 depicts also the cohort biomass of the population subject to the empirical fleet selectivity (gray) with  $F = 1.0/yr$  (similar to the empirical value). The maximum is at 66.8 cm. As derived in [50], a sole-owner with perfectly selective gear and zero costs would harvest all fish at the size of the maximum in the cohort biomass. In this sense, the location of the maximum at 66.8 agrees well with the results from section 6.3 where we have found that, given the current fleet selectivity, small increases in the fishing mortality increase the steady state yield if they target fish above 67.19 cm (Fig. 6.2).

We can conclude that large improvements are possible from an optimized size selectivity: Up to 94.6% increase in steady state yield and up to 151.9% increase in income compared to the current fishery. This demonstrates the high relevance of the size selectivity and emphasizes the importance to revise the paradigm among fishery stakeholders and managers that sparing small fish means only forgone harvest and that fishing should focus on targeting small fish with the highest intensity.



# 10 Simulations of the coupled dynamic stock-fishery model

Until now, we have considered steady state scenarios and compared the yield and income of the scenarios. This chapter introduces the time dimension and it includes the response of boat owners that adapt the number of vessels which they operate. Thus, this chapter "closes the loop" by including two mutual dependencies simultaneously in the model: how the temporal development of the fish stock depends on the actions of the fishers, and vice versa how the fishers adapt their fishing behavior to their profits, which depend on the fish stock. By closing the loop, the novel model opens up a new direction of research at LV as it provides the tool to simulate the economic side, the fishery, simultaneously with the ecological side, the stock.

## 10.1 Response of fishers in the dynamic model

We assemble the fishery from the sub-fleets, where each sub-fleet consists of the vessels using a particular gear. We use the economic model and the parameters from Chapter 4. The catchability factors  $q_j$  of each gear  $j$  are calibrated such that the catch per unit of effort (CPUE) of the simulation agrees with the empirical catch values [121]. After a burn-in period (100 years) with constant effort, sufficient to reach the steady state, we start the full model including the response of boat owners. The numerical simulation is implemented in R [173] using the library `deSolve` [101] which is specialized on solvers for initial value problems of differential equations. The function `ode.1D` is designed to integrate partial differential equations resulting from 1-dimensional reaction-transport problems with a method-of-lines approach after transforming the PDE to an ODE using finite differences. The simulation procedure is depicted in Fig. 10.1. The dynamic system is simulated for a period of 30 years with 0.1 yr time steps. After each time step with 0.1 yr, the sub-fleets evaluate their profit and adapt the effort in the next period accordingly.

Fig. 10.2 depicts the results of the simulation where each sub-fleet adapts the fishing effort (vessel-days) in relation to their profits (or losses). Due to the fast adaptation of vessels, the effort fluctuates strongly, until the amplitude of the oscillations decreases and the curves converge toward the equilibrium. The period of the oscillation is around 1.5 yr.

## 10 Simulations of the coupled dynamic stock-fishery model

The biomass follows the curve of the effort with around 1/4 period delay and it increases initially, then it converges. The amplitude of the oscillations in biomass is smaller than in effort.

Harvest (yield) is in phase with effort and income and shows a similar development of initial decrease, oscillations and eventual convergence (Fig. 10.3). The yield of each sub-fleet, i.e. disaggregated per gear, is given in Fig. 10.4. The figure features the same oscillations as seen before for the total yield. The vessels using 7" gillnets have the highest initial spike and the highest amplitude of the oscillations. After a short initial period of less than one year, only three gears have a substantial number of vessels on the lake, the gillnets with mesh sizes 6", 7" and 8". The sub-fleet with 7" gillnets achieves the highest aggregate yield at the end of the simulation, and it also has the highest income and most vessels. In accordance with the theory for an open access fishery, in the final state all rents are dissipated and each sub-fleet makes zero profit (Fig. 10.5).

These simulations explain the attractiveness to catch large fish that is observed around the lake in the form of a trend of fishers to shift to targeting larger fish. The simulations do not explain, why, at least currently still, the fishery is dominated by small gillnets. In a different version of the model with modified catchability factors and an equal sharing of revenue between boat owners and employed fishers (instead of fixed wage costs), we found that the current small gillnet dominated state can be reproduced. However, in that case, the small gillnets are so profitable that the observed tendency to target larger fish cannot be explained. For this chapter, we stick with the original model version that explains the profitability to catch large fish.

Why are longline vessels phased out rather quickly within the first years in the simulations, why are they not competitive? Vessels with longlines are the only ones that have bait costs - additional to the labor and fuel costs. The amount of bait costs depends on the species and the quality of the bait [134]. Self-reported values of bait costs from fishers in Uganda were in the range range of 17-58 USD/day and in the simulations we use the middle of the range, 37.5 USD/day (see Section 4.7). Now the vessels with longlines and with gillnets of mesh sizes 7" and 8" target fish in a similar size range (even though the range for longlines is broader) and have labor and fuel costs, but only the longline vessels have the additional bait costs. Therefore, they are not competitive with gillnets of the similar size range and their numbers decrease rapidly in the simulations.

10.1 Response of fishers in the dynamic model

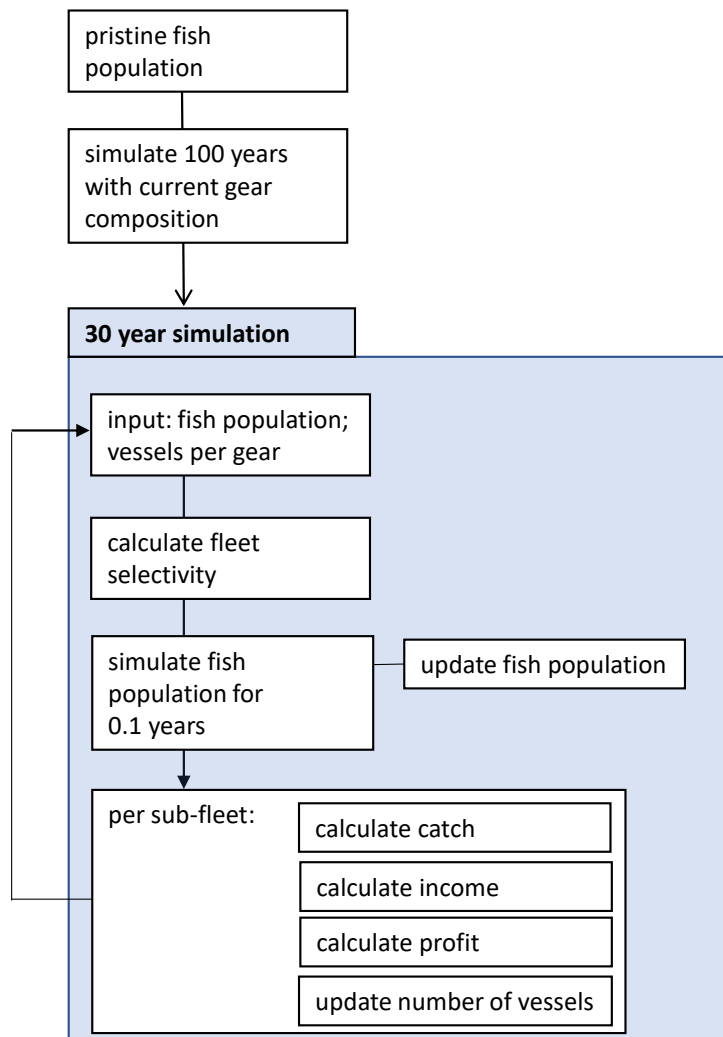


Figure 10.1: Sketch of the simulation procedure.

10 Simulations of the coupled dynamic stock-fishery model

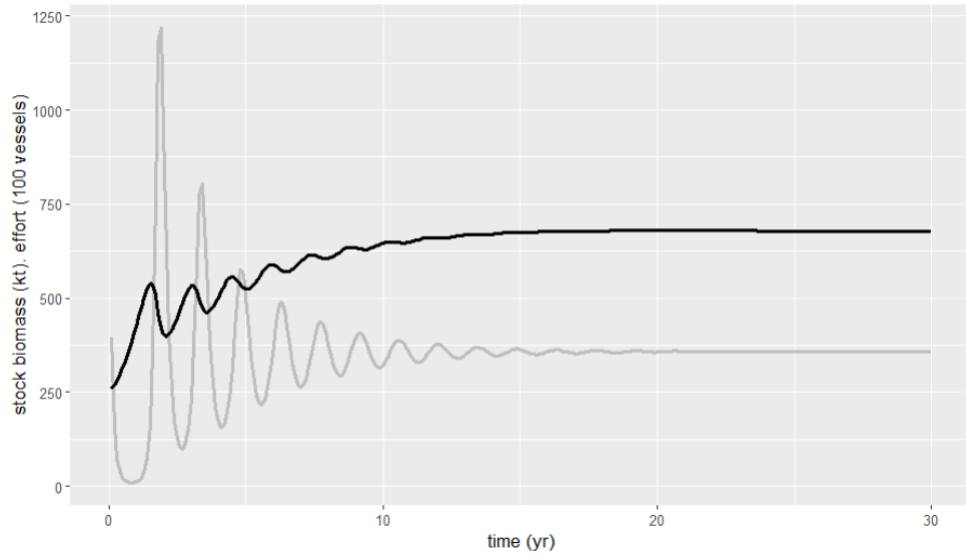


Figure 10.2: Stock biomass (black) and the effort (number of vessels, gray) in the simulation over a period of 30 years with the standard parameters.

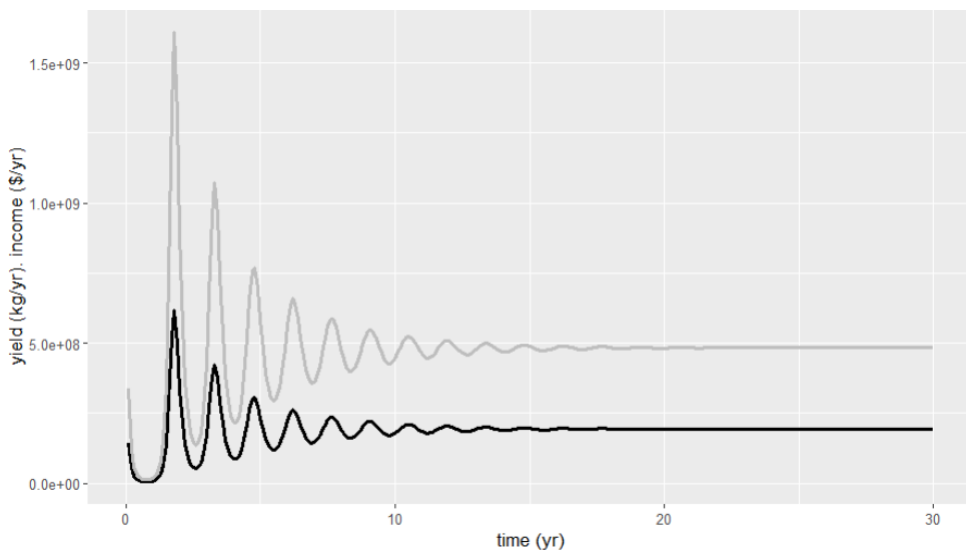


Figure 10.3: Total annual yield (black) and the income (gray) in the simulation over a period of 30 years with the standard parameters.

### 10.1 Response of fishers in the dynamic model

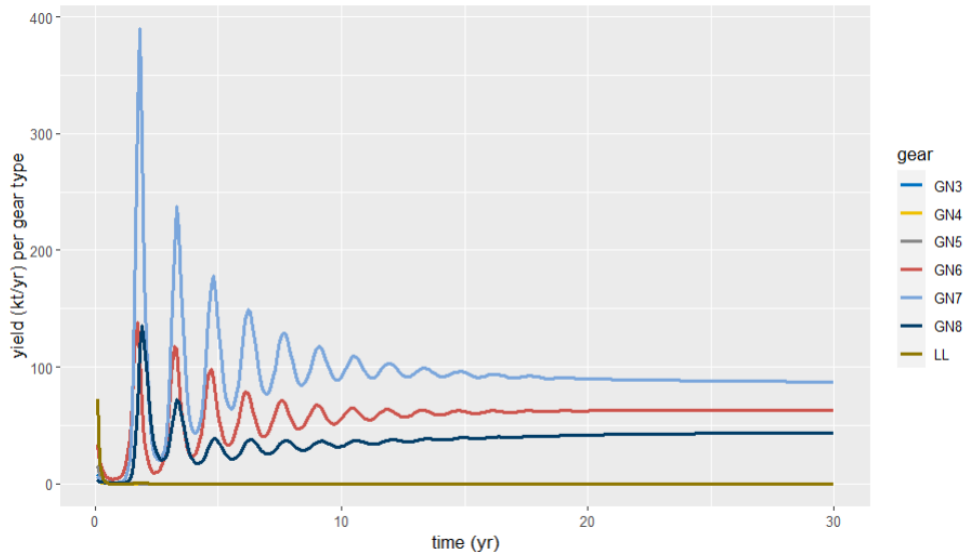


Figure 10.4: The yield, disaggregated per sub-fleet, for longline hooks (LL) and the gillnets with mesh sizes 3" (GN3) to 8" (GN8). The simulation runs over 30 years with the standard parameters.

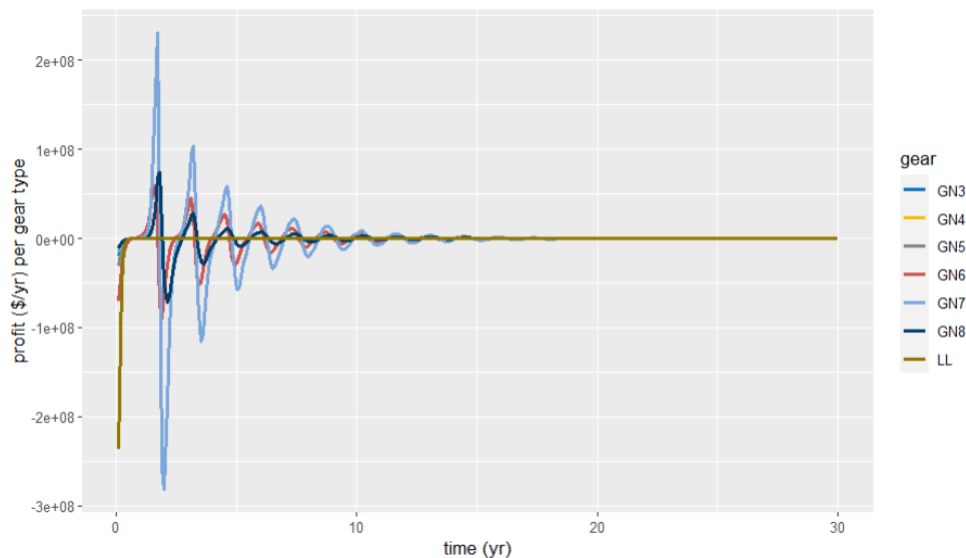


Figure 10.5: The profit, disaggregated per sub-fleet, for longline hooks (LL) and the gillnets with mesh sizes 3" (GN3) to 8" (GN8). The simulation runs over 30 years with the standard parameters.

## 10.2 Application: Impact of panelling and opportunity costs

### 10.2.1 Hypotheses

The analysis of this section aims to test three hypotheses: The first hypothesis is motivated by the ongoing discussion of Lake Victoria managers and stakeholders about the so-called "panelling" of gillnets where multiple nets are combined to increase the catchment area. In the model, this behavior can be represented by the multiplication of (4.13) with an additional panelling factor  $q_p$ .

$$\mu_F^j(w, E_j(t)) = q_p q_j E_j(t) \psi_F^j(w) \quad (10.1)$$

This model is designed to reveal the impact of panelling or from other ways to increase the catchability, e.g. by more efficient gears or techniques.

The second topic is the role of opportunity costs: More job opportunities in the region with a higher salary would increase the opportunity costs of fishing. We ask how this would impact the fishery and the outcomes of the fishery, the yield and the income (Hypothesis 2). We have identified the opportunity costs as a relevant variable as many people who are involved in the fishery also have additional jobs outside: In a surveys with BMU leaders and boat owners, more than 70% of the respondents stated to be involved in other income-generating activities [157].

The third aim is to understand the relationship between the number of boats employed in the fishery, the preference of fishers to target either small or large fish and the value of the fishery, measured through the total yield or the aggregated income of the fishery (Hypothesis 3). We seek to understand which properties of the stock and the fishery lead to a high or low values regime, respectively.

#### High and low value regime

**Definition 10.1.** The *high value regime* is a situation, where, given fixed parameter values, the response of the fishers to the stock, and the stock's development subject to fishing lead, without exogenous forces, to a state where the fishery achieves a high value, measured as high yield and high income. In the *low value regime*, the endogenous development leads to the opposite state of low yield and low income.

The case of less panels per boats is represented through a lower  $q_p$  factor in the model. Keeping the stock fixed, this would imply less catch per vessel and therefore less profits. As a consequence, the boat owners will decrease the total effort (number of vessel-days) (4.21). This reduces the fishing mortality further, leading to a higher stock. Due to the

## 10.2 Application: Impact of panelling and opportunity costs

reduced mortality, more fish survive to greater age and the percentage of large fish in the stock increases. This leads to a higher aggregate yield and income. However, the fishers are expected to adapt again by increasing the vessels until the equilibrium is reached. The hypothesis is that the equilibrium is still more valuable than the initial state. For a higher  $q_p$  value, the argument follows vice versa (Hypotheses 1).

Higher opportunity costs decrease the profits (4.20). As a consequence, the number of vessels decreases. Analogous to the previous case, the stock replenishes, the survival rate of fish increases, but, again, the fishers adapt. The hypothesis is that the yield and the income are still higher than in the status quo (Hypothesis 2). The opposite case with lower opportunity costs is vice versa, again.

Hypothesis 3 summarizes and generalizes those ideas. A low number of boats is expected to correlate with a high stock, high survival rate of fish (implying a larger fraction of large fish), more boats targeting large fish, and a higher total yield and income. Beside the desirable state concerning the economic aspect (the income) and the food security (yield), also the ecological state can be considered to be improved because of the higher biomass of the fish stock and in particular because of the stock being assembled of more large fish which increases the fecundity of the stock and also produces more robust eggs with a higher chance of survival [53, 13]. Therefore we hypothesize that the mentioned features characterize a "high value regime", both economically and ecologically. The high value regime is opposed by the "low value regime" with the opposite characteristics. We are also interested in the transition between the two regimes.

### Hypothesis 1

- (a) A higher panelling factor  $q_p$  leads to a lower stock biomass and a smaller average length of fish in the lake.
- (b) A higher panelling factor  $q_p$  leads to less total yield and income.

### Hypothesis 2

- (a) Higher opportunity costs lead to less boats on the lake.
- (b) Higher opportunity costs lead to a larger stock biomass with a higher average fish length in the population.
- (c) Higher opportunity costs lead to a higher total yield and income.

Hypothesis 3

The high value regime is characterized by

- (a) a high stock biomass,
- (b) a low number of boats,
- (c) which primarily target large fish.

The low value regime is characterized vice versa by a low stock biomass, less total yield and income, and a high number of boats which primarily target small fish.

### 10.2.2 Panelling

In the first simulation the panelling factor  $q_p$  was varied in the range 0.8 to 1.6 in steps of 0.2. Each point in the figures corresponds to the simulation state at the end of a 30 yr period. Over this range, the stock biomass (at the end of the 30 yr period in each simulation) decreases from 835.6 kt to 407.6 kt. The mean total length (TL) of the fish in the stock decreases from 16.8 cm to 13.5 cm (Fig. 10.6), together with the decrease in the abundance of large fish (Fig. 10.7).

The number of vessels decreases from 40,099 to 24,436 with the doubling of  $q_p$ , while the composition shifts from 0.03% of vessels targeting small fish to a majority of 67.8% (Fig. 10.8). From  $q = 0.8$  to  $q = 1.6$ , the yield decreases by 22.0% from 210.0 kt to 163.8 kt. Over the same range, the annual income decreases by 29.8% from 542.0 million USD to 380.8 million USD.

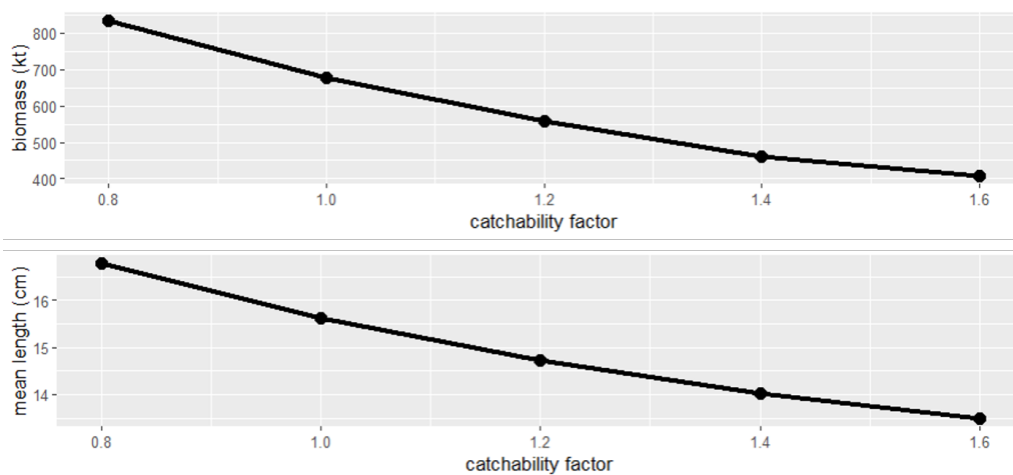


Figure 10.6: Stock biomass (top) and mean total length (TL) (bottom) after 30 years as a function of the panelling factor  $q_p$ .

10.2 Application: Impact of panelling and opportunity costs

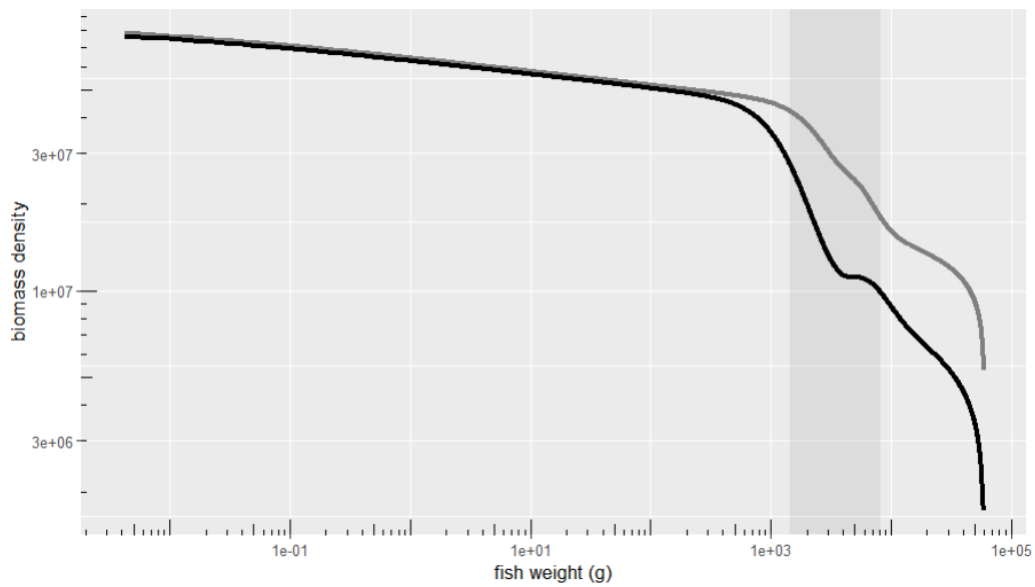


Figure 10.7: Biomass for  $q = 0.8$  (dark gray) and  $q = 1.2$  (black) after 30 years. The gray rectangle indicates the slot size range (50-85 cm).

10 Simulations of the coupled dynamic stock-fishery model

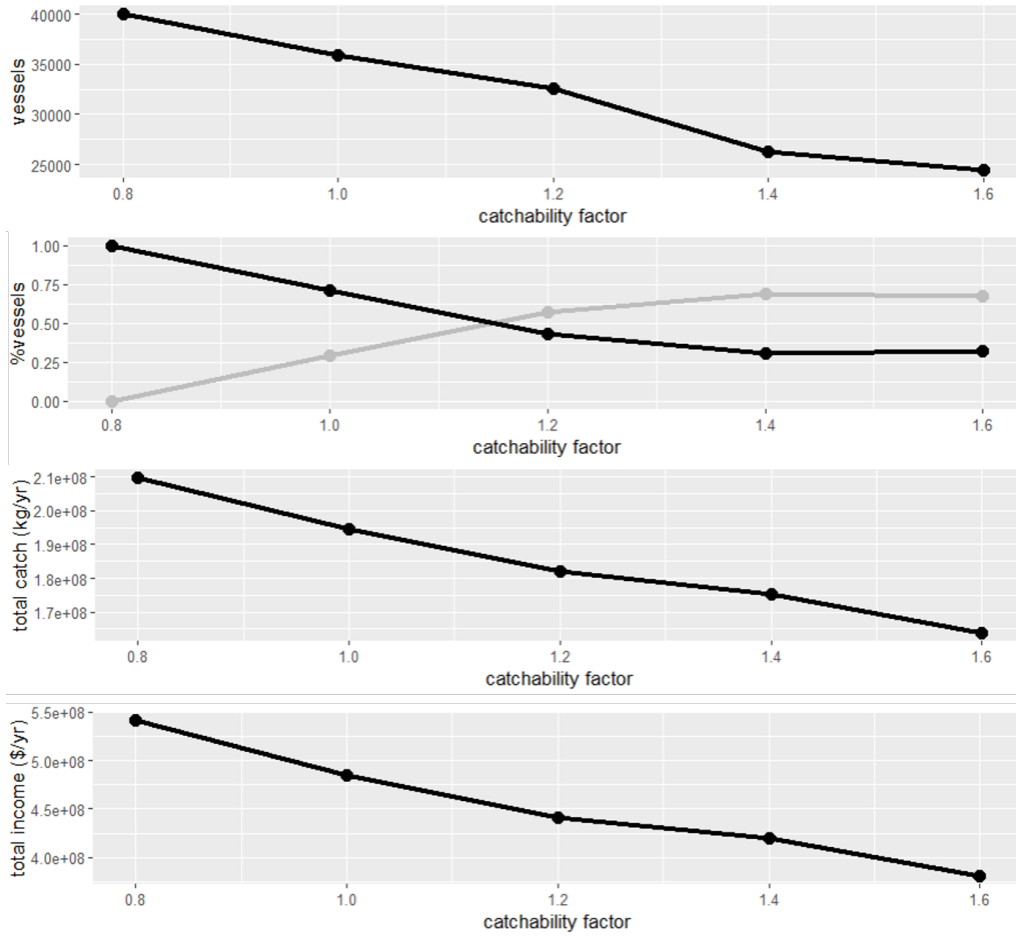


Figure 10.8: From top to bottom: (1) number of vessels, (2) percentage of vessels with mesh size 3-6" (gray) and vessels with mesh size 7-8" or longlines (black), (3) fishery yield and (4) fishery income. Each point in the figure is the final state of a 30 year simulation with the respective panelling factor.

### 10.2.3 Opportunity costs

Similarly, the influence of the opportunity costs was tested through six simulation runs, each one over a period of 30 yr, with the value of the opportunity cost ranging from 0 to 1250 USD/yr in steps of 250. This range is lower than the standard value of the opportunity costs, and was selected to include the transition between the high and the low value regime.

With opportunity costs going from 0 to 1250 USD/yr, the biomass increases by 10.7% from 565.8kt to 626.2kt and the mean total length slightly from 14.8 cm to 15.3 cm (Fig. 10.9) because the abundance of large fish is higher (Fig. 10.10). The total number of vessels decreases only slightly from 38,968 to 37,271 and a transition from targeting small fish to targeting large fish appears (Fig. 10.11), but the effect is less pronounced than in the simulations where the  $q_p$  factor is varied. The annual yield increases by 4.2% from 184.3kt to 192.0kt, and the income from 448.9 million USD to 475.9 USD (+6.0%).

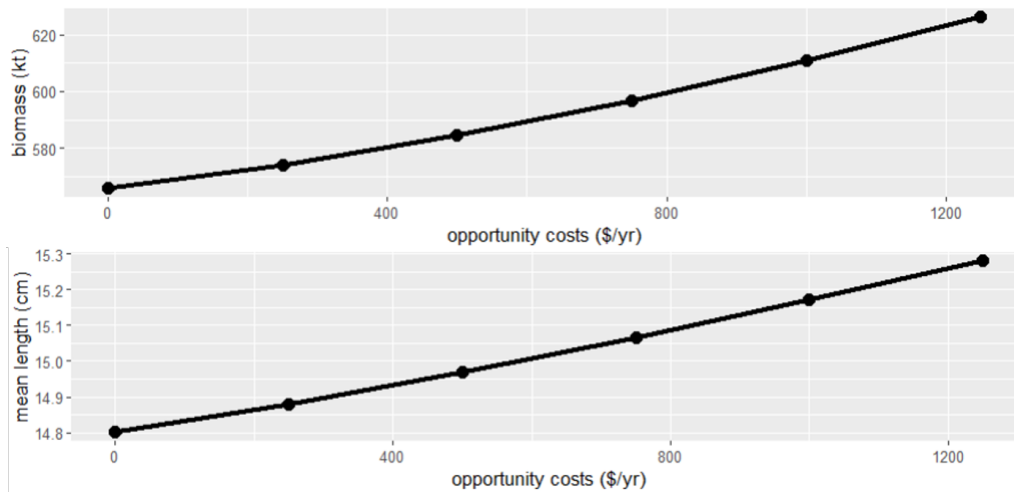


Figure 10.9: Stock biomass (top) and mean total length (TL) (bottom) after 30 years as a function of the opportunity costs.

10 Simulations of the coupled dynamic stock-fishery model

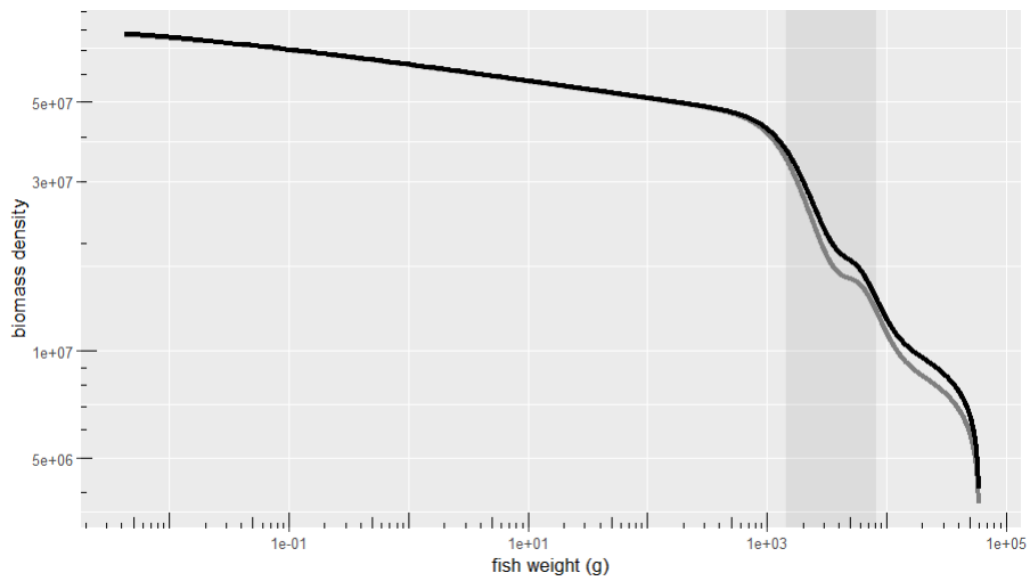


Figure 10.10: Biomass for opportunity costs 0 USD (dark gray) and 1250 USD (black) after 30 years. The gray rectangle indicates the slot size range (50-85 cm).

10.2 Application: Impact of panelling and opportunity costs

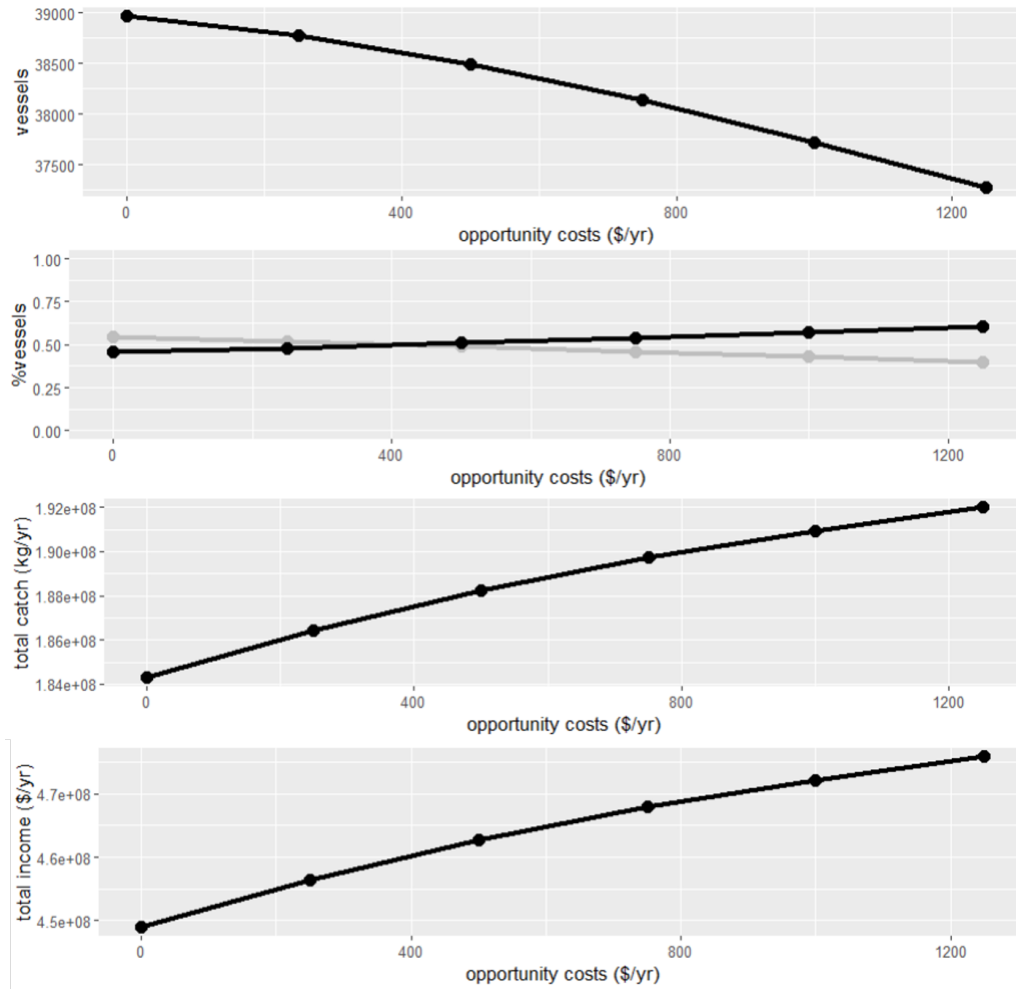


Figure 10.11: From top to bottom: (1) number of vessels, (2) percentage of mesh size 3-6" (gray) and mesh size 7-8" or longline (black), (3) fishery yield and (4) fishery income. Each point in the figures is the state after 30 years simulation with the respective value of opportunity costs.

## 10 Simulations of the coupled dynamic stock-fishery model

These results allow to confirm or reject the hypotheses.

### Review of hypothesis 1

- (a) *Confirmed.* The higher  $q_p$  factor leads to a smaller stock biomass which has on average smaller fish (Fig. 10.6).
- (b) *Confirmed.* The higher  $q_p$  factor leads to less total yield and a lower aggregate income (Fig. 10.8).

### Review of hypothesis 2

- (a) *Confirmed.* Higher opportunity costs lead to less vessels (Fig. 10.11). The magnitude of the effect is rather small.
- (b) *Confirmed.* Higher opportunity costs lead to a larger biomass and higher value of average length. The effect is only small or moderate (Fig. 10.9).
- (c) *Confirmed.* Higher opportunity costs lead to more total catch and income (Fig. 10.11). The magnitude of the effect is only moderate.

### Review of hypothesis 3

- (a) *Confirmed.* The high-value regime correlates with a higher stock biomass and a larger average length of the fish population in the lake.
- (b) *Rejected (not generally true).* The hypothesis is not generally valid, but it depends on the underlying causes. If the transition between the regimes is caused by a change in the catchability, then it is found: In the high value regime, there are more vessels on the lake, virtually all of which use large nets or hooks. If, on the other hand, the opportunity costs are the driver, then the high-value regime (under high opportunity costs) correlates with a lower total number of vessels.
- (c) *Confirmed.* The high-value regime correlates with a higher percentage of large nets.

### 10.2.4 Comparison to an agent-based model

In this section we will compare the results of the dynamic model with an agent-based model<sup>1</sup> [79, 87, 86]. That model shares the biological model with the one of the previous sections, but takes a structurally different modeling approach for the economic part. The fishery is modeled with an agent-based model (ABM), which constitutes a structurally different modeling approach compared to the more analytical approach of the previous sections based on differential equations (DEQ). In the ABM, the fishery consists not of sub-fleets, but the basis is the individual boat owner. The boat owners are modeled as individual agents, which, in each round, decide whether they exit the fishery (if they are active), whether they enter the fishery (if they are inactive), and which gear they will use in the following round (if active). They make their decisions based both on their individual profit as well as based on observations of other fishers' profits to decide which gear seems most profitable to them. In this model there are only two gears available to the fishers. The fishing selectivity of the first gear resembles the one of the 5" gillnet and the one of the second gear is similar to a (generalized) longline hook. The two gears are selected such that the first one targets smaller fish and the second gear targets larger fish (Fig. 4.4).

There were multiple scenarios simulated until a stationary state was reached, similar to the previous section. In the first case study the gear efficiency was multiplied with a factor from the range 1.0 to 3.0 in steps of 0.2, analogous to the previous panelling scenarios. Fig. 10.12 depicts the percentage of vessels targeting small or large fish, respectively, once the stationary state is reached. Between the values 1.4 and 1.6, a sharp transition happens between a majority of vessels targeting small fish (left of the transition) and the majority targeting large fish (right of the transition). Notably, the transition is much sharper than in Fig. 10.8, and also at a slightly higher value of the factor. The ABM has a more complex structure than the DEQ model: As the fishers can observe the other fishers' gears and profits, they adapt more quickly to the gears that are most profitable. The observation of others' behaviors and the deliberate gear choice based on observed profits induce a non-linear dynamic that leads to a rather abrupt transition.

Also in this model, the second case, the variation of the opportunity costs, induces a shift in the fishery (Fig. 10.13). The shift is less abrupt than for the variation of gear efficiency, but still more non-linear than in the DEQ model (Fig. 10.11). Also here, larger opportunity costs lead to a state with fewer vessel on the lake (Fig. 10.14).

Thus the results can be represented as a non-linear transition between two regimes (Fig. 10.15). The first regime is characterized by a high value of the fishery income (green curve in the figure), which correlates with a majority of vessels targeting large fish and, correspondingly, a minority targeting small fish (red curve). The second regime is marked

---

<sup>1</sup>The agent-based model was developed during the work on this thesis together with Santiago Gómez-Cardona, Grigori Shapoval and Hamsa Zazai.

## 10 Simulations of the coupled dynamic stock-fishery model

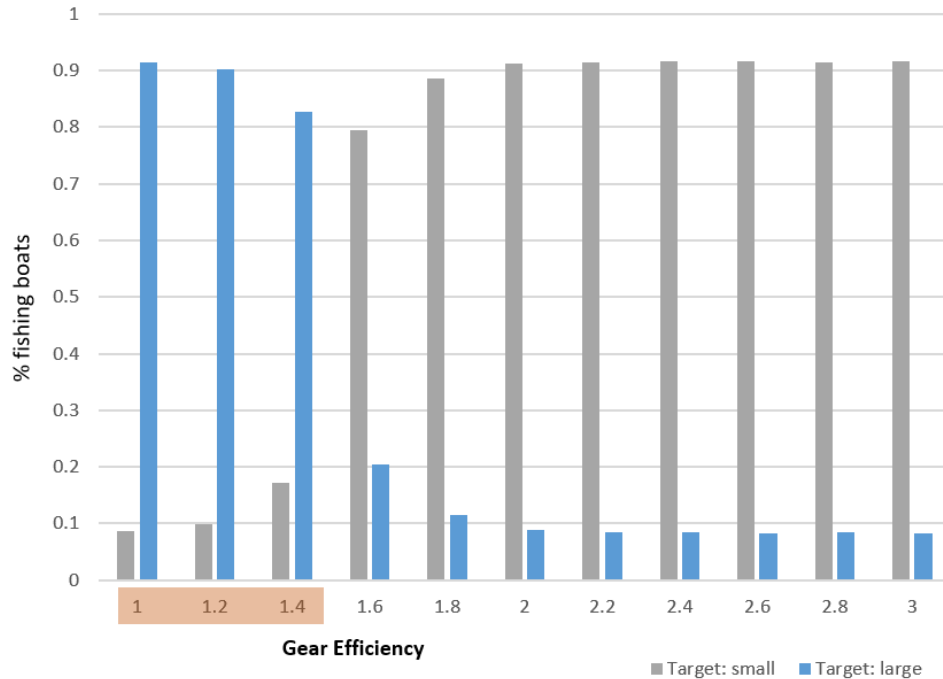


Figure 10.12: Each bar is the results of one simulation of the agent-based model, with the respective coefficient of gear efficiency, where the dynamics were simulated until no more change was observed (quasi-steady state). The bars show the percentage of vessels targeting large (blue) or small (gray) fish, respectively. From [86].

by a low income and more vessels targeting small fish than large fish. Between the two regimes, there is a non-linear transition. Note that the curves represent (quasi-)steady state points (i.e. after no more changes in the fishery were visible in the simulations). This means that the "instability" depicted in Fig. 10.15 is not an instability in time (each point of the curves is the end point of a simulation), but an instability with respect to variations in the number of gear on the lake. If for instance, the fishery is in a state in the blue shaded area, then a small variation in the number of gear on the lake can shift the system to a new steady state belonging to the other regime. This is a high risk and a chance at the same time: A high risk, because a small increase in vessels can strongly reduce the fishery income; a chance, because if a reduction in the number of vessels can be achieved, then the fishery becomes much more profitable and fishers switch to targeting larger fish, given the stock being more dominated by larger fish.

In the DEQ model, the transitions between the two regimes (both in the case of the panelling factor and of variations in opportunity cost) are not exactly linear, but visibly less abrupt than in the ABM. This is an important observation both for modellers and for policymakers. For modellers, because the agent-based structure, together with the

## 10.2 Application: Impact of panelling and opportunity costs

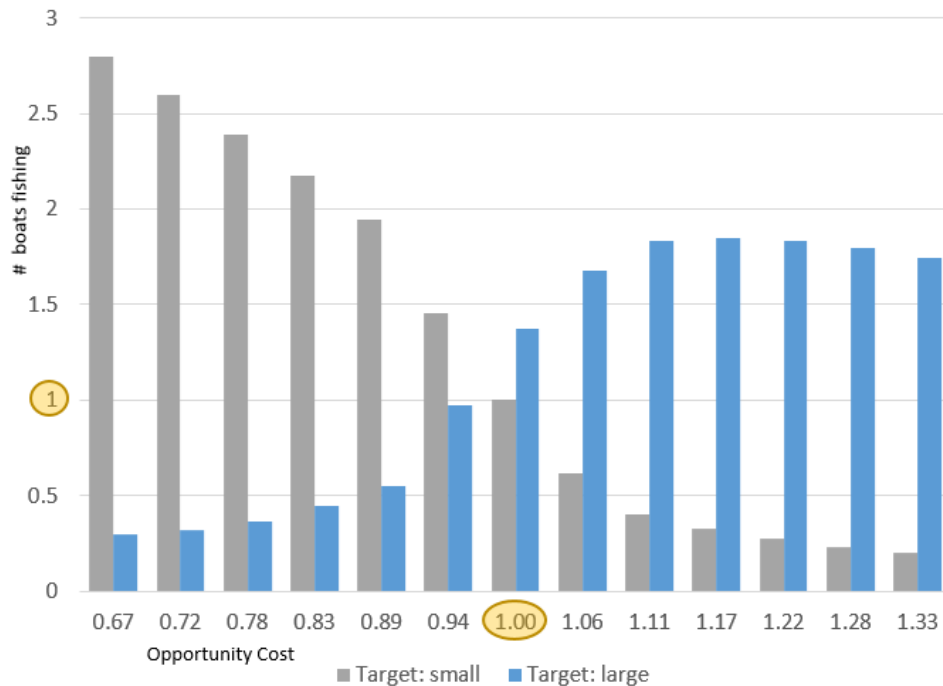


Figure 10.13: Each bar is the results of one simulation of the agent-based model with the respective factor of opportunity costs, where the dynamics were simulated until no more change was observed (quasi-steady state). The bars show the relative number of vessels targeting large (blue) or small (gray) fish, respectively. From [86].

swarm-like behavior of fishers (observing the others' behavior and, if successful, copying it) leads to similar situations, but a more abrupt transition between the two regimes, resembling more a "tipping point". For policymakers, it is important to know that the interaction between the fishers plays a major role for the transition between the states of the fishery and makes the situations more extreme. This is valid both in the aggravation case (towards the low value regime) as well as in the amelioration case (towards the high value regime).

### 10.2.5 Management implications

The two studies, using a DEQ model and an ABM, have policy-relevant implications for the management of the Lake Victoria Nile perch fishery, which are summarized in the following [87].

1. Two exploitation regimes of the Nile perch fishery can be distinguished, one with a high and one with a low value (income) of the fishery. The high value regime is characterized by a fish stock with a higher average fish size and by the majority of fishers targeting larger fish.

## 10 Simulations of the coupled dynamic stock-fishery model

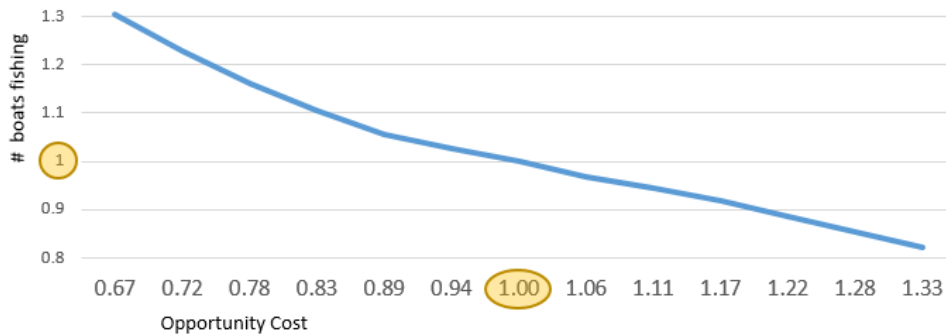


Figure 10.14: The number of fishing boats in quasi-steady state as a function of the opportunity costs. The values on the x-axis and the y-axis are normalized to the values of the standard scenarios (marked in yellow). From [86].

- At least two factors can induce a transition between the two regimes. If the fishers increase the net area by panelling, the consequence can be a shift from the high to the low value regime. If, on the other hand, fishers find more profitable job opportunities outside the fishery, the number of vessels and the lake is reduced, yielding more income, not only per vessel, but also in total.
- The model simulations suggest that the underlying dynamics are: A low fishing pressure decreases the mortality and lets fish survive longer and grow larger. With more large fish in the lake, the gears that target large fish become more profitable and more fishers choose to use these gears. This further decreases the mortality of juveniles. The fishery dominated by large fish in the catch is more profitable, as the increase in the average weight of fish outweighs the losses from reduced juvenile mortality. The fish stock dominated by larger fish is also more healthy because large fish lay more eggs, and eggs from large fish are more robust to adverse environmental conditions.
- Dependent on the dynamics of the fishers' behavior, the transition between the high and low value regimes can be more linear or more abrupt (non-linear). If the fishers are homogeneous such that average values are sufficient and if they make the decisions only based on their own profit in each period, then the transition between the high and low value regimes is more linear, meaning that small changes in the gear efficiency or in the opportunity costs have only small effects on the income. Otherwise, if the fishers observe their peers' behavior and profits, and if they make their decisions (whether to go fishing and which gear to use) based on the observed profit of other fishers, then the transition between the two regimes can be more sharply. A small change in the gear efficiency or the opportunity costs can bring

## 10.2 Application: Impact of panelling and opportunity costs

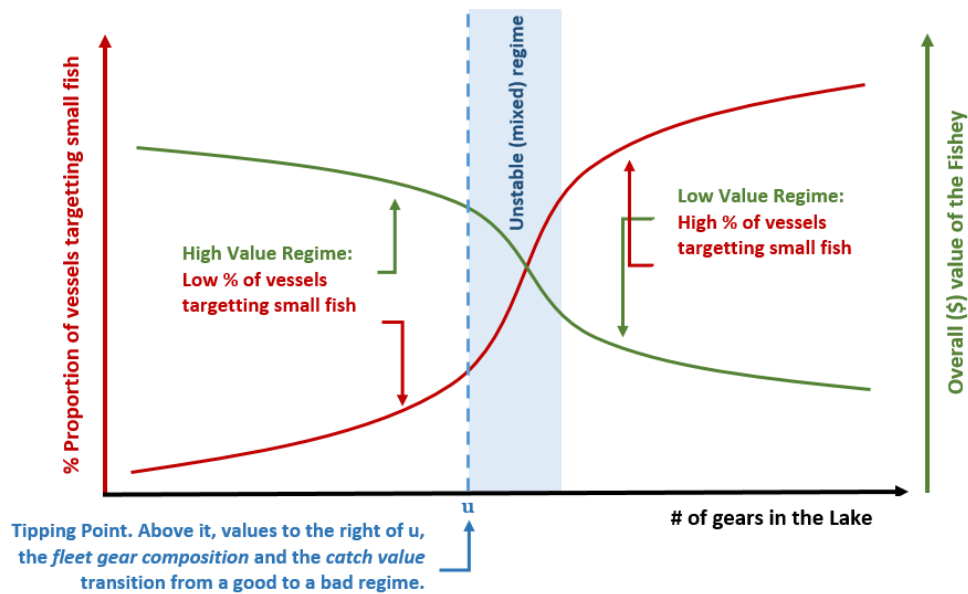


Figure 10.15: Summary of the simulations. With a low number of gears in the lake (left part), the quasi-steady state points of the simulations have a low proportion of vessels targeting small (red curve) fish and a high value of the fishery (green curve). In the scenarios with a high number of gears, the situation is reversed (right part). There is a sharp transition between the two regimes (blue shaded area). If the fishery is in the situation marked by the dashed vertical line (edge of blue area), it is in an unstable situation: a small increase in the number of gears brings about the transition to the low value regime. From [87].

the system from either regime to the other one - both in the beneficial and the deteriorating direction.

5. Therefore it is important to understand accurately how fishers make their economic decisions, how the boat owners decide on whether to stay in the fishery or not, and when to increase or reduce the number of boats, and which gears to use.
6. The simulations indicate that the percentage of fishers targeting large fish correlates strongly with the state of the fish stock (abundance in terms of biomass and structure in terms of the average fish size). Therefore the close monitoring of the composition of the gears in the fishery and the real-time analysis of the trend provides the decision makers with an indicator whether the fish stock is improving or deteriorating. Strict survey schemes could ensure regular data on the gear composition.
7. The situation of the fishery can be influenced by opportunity costs and by the gear efficiency. Profitable job opportunities outside the fishery would increase the opportunity costs, leading to less vessels and more fishery income. The effect of the

## *10 Simulations of the coupled dynamic stock-fishery model*

opportunity costs is, however, less pronounced than for case of the gear efficiency. A reduced number of gears on the lake can induce the transition toward the high value regime, which would provide higher income and yield of the fishery and, simultaneously, produce a larger fish stock with higher average fish size.

# 11 Integrating discussion and conclusions

## 11.1 Social-ecological systems modeling

The strongly interdependent system of the Nile perch stock and fishery at Lake Victoria poses a strong challenge for researchers to model the sub-systems and their interactions, to understand the drivers of the system and to find and characterize the conditions of a sustainable exploitation pattern. In this thesis, we make use of the *Social-ecological systems (SES)* framework. A social-ecological system (cf. Fig. 1.1) includes the societal and the ecological sub-systems and their interactions.

We have identified the following main components of the SES that the model must address: the resource units (individual fish in the stock), the resource system (how the development of the stock depends on ecological parameters), the resource users (how fishers respond to the fish stock level) and the governance system (restricting the use of gears and legal fish sizes).

The interaction between the resource units (fish) and the users (fishers) is defined by the size-resolved fishing mortality. The analysis of the regulations that are established in Lake Victoria (mesh size, hook size and slot size regulations) implied the requirement that the model must represent the complete size structure of both the stock and the fishery. Therefore we choose the approach of a size structured fish population model and develop, from catch data, the size selectivity of the main gears in the Nile perch fishery.

In order to model the *mutual* interaction between the fishery and the stock, we build a size structured model of the Nile perch fishery at Lake Victoria based on an advanced biological framework [2], together with a model describing how the fishers respond to the level of the fish stock. By dividing the vessels into sub-fleets according to the gear, the response of each sub-fleet is modeled as a function of the profit. In the dynamic effort model, we assume that the increase in fishing effort is proportional to the profit from fishing [182], such that in the steady state nobody makes profit, in line with the expected result of the dissipation of all rents in an open access resource system [81, 90]. Thus we "close the loop" between the stock and the fishery where the development of the stock and the fishery are modeled as *endogenous* variables of a single, coupled system.

## 11.2 Discussion of the results

### 1. Sustainability of the current exploitation

The model is used to understand the effect of the size selectivity of the fishery, and, with it, the potential of size-based policies. The existence of a unique, non-negative and regular solution of the stock model is proven for the time dependent case with constant fishing mortality and for the steady state case. Then the model is validated by comparing the emergent simulated growth curve with the van Bertalanffy curve and by comparison to the population size structure from three different experimental surveys.

Using the empirical fleet selectivity as an input into the model, the simulations of the size structure of the fish population in steady state are similar to the empirical size distribution from the bottom trawl and the catch assessment survey. The size distribution of the hydroacoustic survey, however, differs from the other surveys and from the model simulation. A potential reason could be the target-strength-to-size relationship in the calibration of the hydroacoustic survey, but more research is needed to investigate the cause.

We find that, under the current fleet selectivity, the empirical annual yield (207.6 kt) is close to the maximum sustainable yield (207.8 kt). Correspondingly, also the empirical peak fishing mortality rate,  $F=1.04/\text{yr}$ , is only 2.0% above the rate that leads to the maximum sustainable yield ( $F=1.02/\text{yr}$ ). This result is in line with the finding from an Atlantis model, where - in the scenario where the current fishing mortality is maintained (status quo) - the landings of Nile perch remain stable within the simulation period of 20 years [155], but the result differs from previous propositions that the stock is substantially overfished [135, 136].

The results of our model indicate that, contrary to a common perception among both fishers and policymakers of Lake Victoria, the fishery is not overfished, but the fishing pattern could be sustained over time as a steady state solution of the governing equation, and that, for fixed fishing pattern, the level of exploitation is almost optimal. However, this requires a stable ecological environment: The model assumes fixed parameters of predation mortality and growth, therefore the predictions are only valid as long as (1) the interaction between Nile perch and other species, (2) the interaction within the Nile perch population (cannibalism) and (3) other ecosystem parameters do not change. Extending the model for the cannibalistic behavior of Nile perch and for inter-species interactions (predation) would allow to extend the range of robust predictions.

We test the sensitivity of the results and find that the results are most sensitive to the parameter of physiological mortality. The value of the growth parameter and of the maturation size have less influence on the results. Future biological research is needed to determine the value of predation mortality more precisely and accurately.

## 2. Alternative size and gear based exploitation patterns

We develop a criterion to assess whether the increase of fishing mortality at a given size by a specific amount will increase or decrease the total fishery yield in steady state (Section 6.3). The additional mortality has two counteracting effects: Increasing the harvest at the specific size, but decreasing harvest of all larger sizes, because once a fish is caught, it cannot be harvested later at a larger size. The criterion depends only on the growth rate, the size and the amount of additional mortality. Furthermore, we calculate numerically the amount of increase or decrease of the total yield for a small perturbation in the fishing mortality around the current exploitation pattern.

In addition, we simulate eight hypothetical fleet selectivity shapes to predict the effect of selectivity on the fish stock and on steady state yield. For the comparison, each slot size scenario is simulated as the solution of the steady state of the McKendrick-von-Foerster equation across a wide range of fishing levels. We find that sparing all fish below 50 cm, while keeping the fishing mortality above 50 cm the same, increases the annual yield by 17.7% from 207.6 kt to 244.3 kt. Catching no fish above 85 cm, decreases yield by 28.0% from 207.6 kt to 149.5 kt. The maximum sustainable yield is highest in the scenario where only fish above 50 cm are harvested, and lowest in the scenario where only fish below 85 cm are caught.

Next to the slot size scenarios, five gear-related scenarios are simulated, where the scenarios sequentially exclude smaller gillnets, from the fishery with longlines and only gillnets with mesh size above 4" to the last scenario with longlines and only gillnets with 8" mesh size. In each case, it is assumed that the vessels with abandoned nets exit the fishery. We find that each scenario with less small nets increases steady state yield (up to 21.5%), income (up to 34.9%), stock biomass (up to 81.7%) and spawning stock biomass (SSB) (up to 93.4%). The effect comes from the reduced fishing pressure on small fish (exit of vessels with small nets), increasing the number of survivors and leading to a larger reproduction of the stock, therefore a higher stock level in total.

This result contests the common perception among stakeholders that sparing young fish would reduce the yield of the fishery. On the contrary, sparing small fish increases not only the catch from larger nets (in the short run) from the survivors, but (in the long run) also the whole stock level as the survivors increase the reproduction of the stock (SSB). Both effects are included in the modeled steady state. Assuming that fishers do not exit, but switch to the next larger legal gear in each scenario, does not change the results qualitatively. To test the robustness of the results, we compare the results additionally to the case with a senescent mortality. Only for the case where fishers do not switch and with a linear senescent mortality, we find that the scenario with mesh sizes at or above 6" produces the highest yield and income. This is plausible because with the high senescent

## 11 *Integrating discussion and conclusions*

mortality the fish would simply die naturally if they are not harvested early enough. In all other cases, the scenario with only 8" gillnets ranks highest.

Thus this thesis provides a study of the effect of one empirical and multiple hypothetical slot size and gear related scenarios of fleet selectivity. The results give an understanding of the relationship between fleet selectivity and steady state yield. Our study depicts the significant potential improvement in steady state yield that could emerge from reducing the fishing pressure on juvenile fish.

### 3. **Optimal fishing selectivity**

An overwhelming branch of literature about Lake Victoria emphasizes the importance of the catch for food provision and thus food security for the regional population [75, 74, 68, 38, 76, 10, 11]. Therefore, a part of the study was to find the fleet selectivity that maximizes the annual yield (catch weight) in steady state. As Nile perch is also to a significant share exported to other countries, creating monetary income beyond food supply, the maximization of income is analyzed, too.

Early in fishery economics, Scott distinguished between the case of competing fishers and the case of a single management of the fishery by a "sole owner" [178]. He showed that, particularly in the long-run, the single ownership is, in terms of efficiency, superior to the open access case. In his seminal textbook, Clark [31] further substantiated this distinction between the case of the open access fishery and the case of a sole-owner who has property rights of the whole resource. While the open access situation leads to the dissipation of all rents [81, 90], a sole-owner can enforce the level and the fleet size selectivity he wishes, so he is interested in the question of the optimal exploitation. We approach the question of the optimal fleet selectivity through numerical maximization of steady state yield and income, respectively.

In the optimization of the fleet selectivity to maximize steady state yield, we find that the fishing mortality would be focused only on the larger fish sizes: In the standard scenario without senescent mortality, there would be no fishing mortality below 90 cm. The same holds if the income is maximized. With additional senescent mortality, the lower bound of fishing is at 70 cm which is still 20 cm above the current lower bound of the slot size (50 cm) and above the range of selectivity of the lowest legal mesh size (5") which targets fish in the range  $47.69 \pm 7.90$  cm.

The yield from the optimal fleet selectivity is 94.6% above the current value, thus providing a substantial improvement. With an optimized fleet selectivity the income would be 151.9% above the current value. These findings are opposed to the common suggestion to aim for "balanced harvesting" (harvesting each size in proportion to its productivity), which would imply to force a strong fishing mortality on the smallest fish and a proportionally reduced one on the larger sizes [116, 112, 115, 113, 169, 170]. However, our

results are in line with the call to spare the "BOFFs" (big old female fish) in order to sustain a healthy population with a large SSB that is more robust to pernicious environmental events<sup>1</sup> [53, 94, 13, 72].

The theoretical basis for that result is developed in Section 6.3. There we shown that a small perturbation of the current fleet selectivity (a small increase in fishing mortality) above 67 cm would increase steady state yield, while a perturbation below 67 cm would decrease yield. To this "local" information (in the sense that it is only valid sufficiently close to the current fleet selectivity), Chapter 9 adds the "global" information about the optimal fleet selectivity.

#### 4. Fishers' response

In the final chapter, the previous model is coupled to an economic model of fishers' dynamic decisions about entry into or exit from the fishery, represented through the boat owners' decisions about the number of vessels they operate. The model is a gear related dynamic effort model, where the sign of the profit determines whether the number of vessels is increased or reduced, and the absolute value determines the rate at which new vessels are added or operating vessels exit.

After an extended burn-in period, we simulate 30 years of the coupled model. Within the first year, vessels with unprofitable gears exit the fishery, leaving a state where only gillnets with 6", 7" and 8" mesh size are employed. After an initial period of larger oscillations, these three sub-fleets approach constant catch levels. At the end of the simulation period, no sub-fleet makes profit, in line with the theoretical prediction for an open access fishery.

We find that panelling and the state of the non-fishery economy (through the level of opportunity costs) have an impact on the equilibrium of the fishery. Panelling would decrease yield, income, stock biomass and the average size of fish in the stock. Higher opportunity costs (favorable jobs outside the fishery) would increase yield, income, stock biomass and average length, but the magnitude of the effect is only small or moderate (compared to panelling). We find that the fishery can be either in a high value (high income and yield) or low value regime, and that e.g. panelling can induce a transition between the two. Whether the transition is rather abrupt or smooth, depends on specific characteristics of the behavior of fishers, for example how strongly their behavior is coupled (fishers imitating the behavior of their peers). We conclude that fishery managers should monitor the percentage of vessels targeting larger fish, and encourage the usage of nets and hooks that catch primarily large fish.

---

<sup>1</sup>Already in 1997 it was suggested from the simulation of a bio-energetic model, that a strictly regulated fishery of large mesh size gill nets provides the greatest fishery yield, while simultaneously reducing the predation pressure of Nile perch on other species like haplochromines and cannibalism of young Nile perch [105].

## 11.3 Limitations and future research

This thesis develops a size structured model of the Nile perch population together with the size selectivity of the relevant fishing gears. In order to keep the results tractable, we focus on Nile perch as a single species. Therefore, the model in this thesis assumes that Nile perch lives in a fixed environment and its feeding rates depend only on the size. However, the ecosystem is interdependent with multiple interactions between the species, mainly mediated through predator-prey relationships. The structure of our model has the advantage that, in future research, the predation can be neatly incorporated as a relationship that depends on the size ratio between predator and prey. In that way, one can include the cannibalistic behavior of Nile perch and, moreover, it is possible to connect multiple interdependent species within the same model. This would provide an advanced representation of the feeding processes in the ecosystem [117, 17, 179, 199, 194, 27].

Furthermore, this extension would comply with the "Ecosystem Approach to Fisheries Management" (EBFM) that has been suggested as the new paradigm for sustainable management of the African inland lakes [142, 118]. EBFM "considers the ecosystem in totality in order to maintain its resilience rather than advancing single species-specific management measures" [142]. The approach emphasizes that one must "manage target species in the context of the overall state of the system, habitat, protected species, and nontarget species. Single-species target and limit reference points are still appropriate, but will need to be modified in the context of these other factors." [167] The multispecies approach, where the predation is directly modeled through the size structure of the fish populations, would incorporate more of the ecosystem dynamics and could detect dependencies between the fish species [199].

The decision process of the fishers is modeled in this thesis in a simplistic matter as a gear based dynamic effort model, assuming free entry/exit in proportion to the profit/loss. Each sub-fleet, i.e. the vessels that employ the same gears, is modeled as a single actor that increases or decreases the number of boats on the lake dependent on the profits, hence the model averages over the boat owners in each sub-fleet. Extensions of the research of this thesis can apply more complex decision models of the boat owners that include more heterogeneities among the fishers and boat owners like in [79]. It has been suggested that simple adaptive decision rules might predict the behavior of fishers better than assuming perfectly rational profit-maximizing agents [28]. Furthermore, in the application to the panelling case there is no cost linked to panelling, which one should include in future simulations.

Another important factor, which is not included yet, is the strategic dimension between the three riparian countries Tanzania, Uganda, and Kenya. As the lake is shared as a

common pool resource among the countries, each of the countries' actions influences the resource availability for the other two countries. The international strategic situation of rational players (nations) can be analyzed as a non-cooperative exploitation [50]. In the strategic setting of an age or size structured fish population, each country has an incentive to harvest fish smaller than in the cooperative optimum, which can lead to serious loss of rents and deterioration of the fish stock. The concepts developed for other locations with a fish stock shared between multiple countries [52] can also be applied to Lake Victoria.

## 11.4 Conclusions

In this thesis we develop a size structured model of the Nile perch fishery. This involves the development of the size selectivity of each relevant gear in the fishery, together with a biological model and the economic model of the fishers' economic response to the profit. The results of the simulations suggest consistently that improvements in the value of the fishery (both for yield and for income) come from shifting the fishing pattern towards larger fish. Reducing smaller gillnets increases yield and income. Targeting large instead of small fish maximizes yield and income - a result which is robust with respect to the particularities of the model settings and parameters. In the coupled dynamic stock-fishery model we find that gillnets with 6", 7" and 8" mesh size provide positive profits and dominate the fishery after the 30 year simulation period. This state provides more yield and income than the current state of the fishery. Other factors like net panelling and the level of opportunity costs can induce a transition between a high value and a low value regime of the fishery.

The results of this thesis include the mathematical analysis of the new size structured Nile perch model, where the existence of a unique, non-negative and regular solution for the time dependent and the steady state fish stock model is proven. Additionally it provides concrete, decision-relevant research outputs. As the regulators at Lake Victoria tend to focus on determining the appropriate rules about *which* fish should be caught (and not *how many* vessels should be allowed or *how many* quotas be issued), the research of this thesis centers on assessing the value of the fishery (annual yield or income) under various fishing patterns and gear restrictions - answering the question, *which fish to catch*, i.e. *which fish size to target*. We find that optimizing the size dimension of the fishing effort can provide substantial increase in yield (up to 94.6%) and in income (up to 151.9%). Hence significant increases in the catch are possible from mere adaptation of the fishing selectivity, thus increasing the food supply while simultaneously making the fish stock more resilient to shocks or environmental fluctuations. These results are opposite to the overfishing hypothesis and to the supposed trade-off between increasing yield and stock

## *11 Integrating discussion and conclusions*

biomass, and challenge the notion of balancing harvest proportional to the productivity across the size dimension.

## 12 Summary

*Motivation:* Lake Victoria is the world's second largest freshwater lake and is widely understood to support the livelihood of three to four million people in the three neighboring countries Kenya, Uganda and Tanzania. The most profitable fish species is Nile perch, a top predator which has played a dominant role in the tipping point of the ecosystem in the 1980s, when the stocks of 500 native fish species collapsed. The fishery managers' discussions today center on restrictions of gears and fish size in the catch to regulate the exploitation of the stock. A ruling paradigm suggests to catch fish in proportion to their productivity, which implies targeting smaller fish more intensely than larger ones. This paradigm is controversially debated.

*Approach:* In this thesis a new bio-economic model of the Nile perch fishery is developed, analyzed and simulated. The key idea is the incorporation of the size structure of the fish population and of the gear selectivity. This is achieved through coupling a bio-energetic fish population model to a bio-economic model of the fishery with size selective gears. The model is based on the McKendrick-von Foerster equation and has the form of a first order hyperbolic partial differential equation with a non-local boundary condition.

*Results:* We show the existence of a unique, non-negative and regular solution to the model for the time dependent case with constant fishing mortality and for the steady state case. After validation of the model against the empirical population size structure and the van Bertalanffy growth curve, the assessment shows that the current state of the fishery is a steady state solution to the governing equation, indicating a "sustainable" fishing pattern, and that the effort is 2.0% above the optimal effort for fixed fleet selectivity.

Improvements of fishery yield and income come from modifications of the fleet selectivity, where we find from three alternative slot size related scenarios and five gear based scenarios that the scenarios which primarily target the largest possible fish rank highest with respect to steady state yield, income and stock biomass. Sparing fish below 50 cm increases, *ceteris paribus*, steady state yield by 17.7% and spawning stock biomass by 31.9%.

A numerical optimization study demonstrates that the sole-owner's optimal fleet selectivity spares fish below at least 70 cm, which is 20 cm above the minimum legal size of 50 cm. Optimizing the fleet selectivity increases yield and income substantially (by 94.6% and 151.9%, respectively).

## 12 Summary

Coupling the fish population to the dynamic model of fishers' response to the fish stock, mediated through profits, a 30 year simulation shows that boat owners shift to using 6", 7" and 8" gillnets because of the high profitability. An application to net panelling and changes in opportunity costs reveals two regimes of the fishery where changes in the use of panelling can induce a transition from the high value to the low value regime.

*Conclusions:* The results of this thesis highlight that a substantial gain in harvest and income of the Nile perch fishery is possible from a modified fishing pattern that spares small fish and instead primarily targets large fish. This, at the same time, conserves the reproductive potential of the stock and leads to an increase in stock biomass. The results challenge the current understanding in three ways: First, shifting the fishing pattern towards targeting larger fish increases both steady state yield and stock biomass, hence there is not necessarily a strict trade-off between harvest and stock biomass in steady state, as is often suggested. Second, sparing young fish and catching them only beyond the point of maximum cohort biomass utilizes the growth potential of fish and leads to a larger steady state stock from increased reproduction of large fish. Hence the interpretation of sparing small fish as simply forgone catch misses crucial positive short term and long term effects. Third, the ranking of alternative selectivity scenarios and the numerical optimization of the fleet selectivity to maximize yield or income, respectively, suggest that the fishery should spare small fish below at least 50 cm and primarily target large fish. This result questions the 'balanced harvesting' paradigm, where it is suggested to distribute fishing mortality across the widest possible range of species, functional groups, trophic levels and body sizes in proportion to biological productivity, which would imply harvesting smaller fish more intensely than large ones. The novel size structured bio-economic fishery model therefore challenges current paradigms and proposes new directions for modeling and analyzing the Nile perch fishery and its regulation in Lake Victoria.

# Bibliography

- [1] Mehiddin Al-Baali, Emilio Spedicato, and Francesca Maggioni. “Broyden’s quasi-Newton methods for a nonlinear system of equations and unconstrained optimization: a review and open problems”. In: *Optimization Methods and Software* 29.5 (2014), pp. 937–954.
- [2] Ken H Andersen. *Fish Ecology, Evolution, and Exploitation: A New Theoretical Synthesis*. Vol. 93. Princeton University Press, 2019.
- [3] Ken H. Andersen. *Fish Size Spectrum*. <https://github.com/Kenhasteandersen/FishSizeSpectrum>. 2022. (accessed: 15.02.2022).
- [4] Ken H. Andersen. *Fish Size Spectrum Parameters*. <https://github.com/Kenhasteandersen/FishSizeSpectrum/blob/master/R/baseparameters.R>. 2022. (accessed: 14.03.2022).
- [5] Ken H Andersen and Jan E Beyer. “Size structure, not metabolic scaling rules, determines fisheries reference points”. In: *Fish and Fisheries* 16.1 (2015), pp. 1–22.
- [6] Ken H Andersen et al. “When in life does density dependence occur in fish populations?” In: *Fish and Fisheries* 18.4 (2017), pp. 656–667.
- [7] Ken Haste Andersen et al. “How community ecology links natural mortality, growth, and production of fish populations”. In: *ICES Journal of Marine Science* 66.9 (2009), pp. 1978–1984.
- [8] KH Andersen. “Size-based theory for fisheries advice”. In: *ICES Journal of Marine Science* 77.7-8 (2020), pp. 2445–2455.
- [9] Ragnar Arnason. “Rents drain in fishery: the case of Lake Victoria Nile Perch fishery”. In: (2009).
- [10] Christopher Mulanda Aura et al. “Checking the pulse of the major commercial fisheries of Lake Victoria Kenya, for sustainable management”. In: *Fisheries Management and Ecology* 27.4 (2020), pp. 314–324.

## Bibliography

- [11] Christopher Mulanda Aura et al. “Consequences of calamities and their management: The case of COVID-19 pandemic and flooding on inland capture fisheries in Kenya”. In: *Journal of Great Lakes Research* 46.6 (2020), pp. 1767–1775.
- [12] Ananias Bagumire, Charles K Muyanja, and FW Kiboneka. “The value chain analysis of Nile perch maw trade in East Africa”. In: *The Responsible Fisheries Business Chains Project of Deutsche Gesellschaft für Internationale Zusammenarbeit (GIZ) under Contract 83285575* (2018), pp. 1–52.
- [13] Diego R Barneche et al. “Fish reproductive-energy output increases disproportionately with body size”. In: *Science* 360.6389 (2018), pp. 642–645.
- [14] Abdulrahman Ben-Hasan et al. “China’s fish maw demand and its implications for fisheries in source countries”. In: *Marine Policy* 132 (2021), p. 104696.
- [15] Eric Benoit and Marie-Joëlle Rochet. “A continuous model of biomass size spectra governed by predation and the effects of fishing on them”. In: *Journal of theoretical Biology* 226.1 (2004), pp. 9–21.
- [16] Raymond JH Beverton and Sidney J Holt. “On the dynamics of exploited fish populations, Fishery Investigations Series II, Vol. XIX, Ministry of Agriculture”. In: *Fisheries and Food* 1 (1957), p. 957.
- [17] Julia L Blanchard et al. “How does abundance scale with body size in coupled size-structured food webs?” In: *Journal of Animal Ecology* 78.1 (2009), pp. 270–280.
- [18] Hans Georg Bock. *Optimization with Differential Equations*. Lecture Notes Winter Semester 2015/16, Version 0.61. 2016.
- [19] Karlijn van den Broek. “Illuminating divergence in perceptions in natural resource management: A case for the investigation of the heterogeneity in mental models”. In: *Journal of Dynamic Decision Making* 4 (2018), pp. 2–8.
- [20] Karlijn L van den Broek. “Stakeholders’ perceptions of the socio-economic and environmental challenges at Lake Victoria”. In: *Lakes & Reservoirs: Research & Management* 24.3 (2019), pp. 239–245.
- [21] Karlijn L van den Broek et al. “Content and complexity of stakeholders’ mental models of socio-ecological systems”. In: *Journal of Environmental Psychology* 85 (2023), p. 101906.

- [22] Karlijn L van den Broek et al. “Evaluating the application of the mental model mapping tool (M-Tool)”. In: *Frontiers in Psychology* 12 (2021), p. 761882.
- [23] Charles G Broyden. “The convergence of a class of double-rank minimization algorithms: 2. The new algorithm”. In: *IMA journal of applied mathematics* 6.3 (1970), pp. 222–231.
- [24] Charles George Broyden. “The convergence of a class of double-rank minimization algorithms 1. general considerations”. In: *IMA Journal of Applied Mathematics* 6.1 (1970), pp. 76–90.
- [25] Richard H Byrd et al. “A limited memory algorithm for bound constrained optimization”. In: *SIAM Journal on scientific computing* 16.5 (1995), pp. 1190–1208.
- [26] Ed Camp et al. “Fish Population Recruitment: What recruitment means and why it matters: FA222, 3/2020”. In: *EDIS* 2020.2 (2020), pp. 6–6.
- [27] T Mariella Canales, Gustav W Delius, and Richard Law. “Regulation of fish stocks without stock–recruitment relationships: The case of small pelagic fish”. In: *Fish and Fisheries* 21.5 (2020), pp. 857–871.
- [28] Ernesto Carrella et al. “Simple adaptive rules describe fishing behaviour better than perfect rationality in the US West Coast Groundfish fishery”. In: *Ecological Economics* 169 (2020), p. 106449.
- [29] Dražen Cepić and Fiona Nunan. “Justifying non-compliance: The morality of illegalities in small scale fisheries of Lake Victoria, East Africa”. In: *Marine Policy* 86 (2017), pp. 104–110.
- [30] Villy Christensen and Carl J Walters. “Ecopath with Ecosim: methods, capabilities and limitations”. In: *Ecological modelling* 172.2-4 (2004), pp. 109–139.
- [31] Colin Clark. *Mathematical bioeconomics*. New York, NY (USA); John Wiley and Sons Inc., 1990.
- [32] Johan Colding and Stephan Barthel. “Exploring the social-ecological systems discourse 20 years later”. In: *Ecology and Society* 24.1 (2019).
- [33] Jon M Conrad. *Resource economics*. Cambridge University Press, 1999.
- [34] Christopher Costello et al. “Economic incentives and global fisheries sustainability”. In: *Annu. Rev. Resour. Econ.* 2.1 (2010), pp. 299–318.

## Bibliography

- [35] Marine Stewardship Council. *Bottom trawls*. <https://www.msc.org/what-we-are-doing/our-approach/fishing-methods-and-gear-types/demersal-or-bottom-trawls>. 2023. (accessed: 24.05.2023).
- [36] Marine Stewardship Council. *Gillnets*. <https://www.msc.org/what-we-are-doing/our-approach/fishing-methods-and-gear-types/gillnets>. 2023. (accessed: 24.05.2023).
- [37] Marine Stewardship Council. *Longlines*. <https://www.msc.org/what-we-are-doing/our-approach/fishing-methods-and-gear-types/longlines>. 2023. (accessed: 24.05.2023).
- [38] Ian G Cowx and Richard Ogutu-Owhayo. “Towards sustainable fisheries and aquaculture management in the African Great Lakes”. In: *Fisheries Management and Ecology* 26.5 (2019), pp. 397–405.
- [39] Diana-Patricia Danciu. “Mathematical Modelling of Stem Cell Dynamics during Post-embryonic Organ Growth”. PhD thesis. Thesis, Heidelberg University, 2019.
- [40] Diana-Patricia Danciu et al. “Identifying stem cell numbers and functional heterogeneities during postembryonic organ growth”. In: *Iscience* 25.2 (2022).
- [41] Diana-Patricia Danciu et al. “Mathematics of neural stem cells: Linking data and processes”. In: *Cells & Development* (2023), p. 203849.
- [42] Astrid Dannenberg, Florian Diekert, and Philipp Händel. “The effects of social information and luck on risk behavior of small-scale fishers at Lake Victoria”. In: *Journal of Economic Psychology* 90 (2022), p. 102493.
- [43] Samik Datta, Gustav W Delius, and Richard Law. “A jump-growth model for predator–prey dynamics: derivation and application to marine ecosystems”. In: *Bulletin of Mathematical Biology* 72 (2010), pp. 1361–1382.
- [44] Samik Datta et al. “A stability analysis of the power-law steady state of marine size spectra”. In: *Journal of Mathematical Biology* 63 (2011), pp. 779–799.
- [45] Florian Diekert. “Appreciating the value of age: An evaluation of efficiency gains from controlling gear selectivity under various scenarios”. In: *International Institute of Fisheries Economics and Trade* (2012).

- [46] Florian Diekert, Timo Goeschl, and Christian König-Kersting. “Social risk effects: The” experience of social risk” factor”. In: *AWI discussion paper series* (2021).
- [47] Florian Diekert et al. “Subsidizing Compliance: A Multi-Unit Price List Mechanism for Legal Fishing Nets at Lake Victoria”. In: *AWI discussion paper series* (2022).
- [48] Florian Diekert et al. “The creation of social norms under weak institutions”. In: *Journal of the Association of Environmental and Resource Economists* 9.6 (2022), pp. 1127–1160.
- [49] Florian K Diekert. “Fisheries management in a dynamic setting”. In: *PhD thesis, University Oslo* (2011).
- [50] Florian K Diekert. “Growth overfishing: the race to fish extends to the dimension of size”. In: *Environmental and Resource Economics* 52.4 (2012), pp. 549–572.
- [51] Florian K Diekert. “The growing value of age: exploring economic gains from age-specific harvesting in the Northeast Arctic cod fishery”. In: *Canadian journal of fisheries and aquatic sciences* 70.9 (2013), pp. 1346–1358.
- [52] Florian K Diekert et al. “Non-cooperative exploitation of multi-cohort fisheries—The role of gear selectivity in the North-East Arctic cod fishery”. In: *Resource and Energy Economics* 32.1 (2010), pp. 78–92.
- [53] Florian K Diekert et al. “Spare the young fish: optimal harvesting policies for North-East Arctic cod”. In: *Environmental and Resource Economics* 47.4 (2010), pp. 455–475.
- [54] O. Diekmann, M. Gyllenberg, and J.A.J. Metz. *The Dynamics of Physiologically Structured Populations: A Mathematical Framework and Modelling Explorations*. <https://www.math.mun.ca/~zhao/ARRMSschool/FifthDraft.pdf>. 2012. (accessed: 08.08.2023).
- [55] R Documentation. *General-purpose Optimization*. <https://stat.ethz.ch/R-manual/R-devel/library/stats/html/optim.html>. 2023. (accessed: 14.06.2023).
- [56] Andrea S Downing. “Assembling the pieces of Lake Victoria’s many food webs: Reply to Kolding”. In: *Ecological Applications* 236 (2013), pp. 671–675.

## Bibliography

- [57] Andrea S Downing et al. “Collapse and reorganization of a food web of Mwanza Gulf, Lake Victoria”. In: *Ecological Applications* 22.1 (2012), pp. 229–239.
- [58] Andrea S Downing et al. “Coupled human and natural system dynamics as key to the sustainability of Lake Victoria’s ecosystem services”. In: *Ecology and Society* 19(4): 31 (2014).
- [59] Andrea S Downing et al. “Effects of resources and mortality on the growth and reproduction of Nile perch in Lake Victoria”. In: *Freshwater Biology* 58.4 (2013), pp. 828–840.
- [60] Andrea S Downing et al. “Was Lates late? A null model for the Nile perch boom in Lake Victoria”. In: *PloS one* 8.10 (2013).
- [61] Echoview Software Pty Ltd. “Echoview version 8.0. Hobart, Australia (8.0)”. In: *Echoview Software Pty Ltd.* (2016).
- [62] Leah Edelstein-Keshet. *Mathematical models in biology*. SIAM, 2005.
- [63] Andrew M Edwards et al. “Accounting for the bin structure of data removes bias when fitting size spectra”. In: *Marine Ecology Progress Series* 636 (2020), pp. 19–33.
- [64] Andrew M Edwards et al. “Testing and recommending methods for fitting size spectra to data”. In: *Methods in Ecology and Evolution* 8.1 (2017), pp. 57–67.
- [65] Håkan Eggert and Razack B Lokina. “Regulatory compliance in Lake Victoria fisheries”. In: *Environment and Development Economics* 15.2 (2010), pp. 197–217.
- [66] Inigo Everson, Anthony Taabu-Munyaho, and Robert Kayanda. “Acoustic estimates of commercial fish species in Lake Victoria: Moving towards ecosystem-based fisheries management”. In: *Fisheries research* 139 (2013), pp. 65–75.
- [67] Laurence Fauconnet and Marie-Joëlle Rochet. “Fishing selectivity as an instrument to reach management objectives in an ecosystem approach to fisheries”. In: *Marine Policy* 64 (2016), pp. 46–54.
- [68] Kathryn J Fiorella et al. “Small-scale fishing households facing COVID-19: The case of Lake Victoria, Kenya”. In: *Fisheries Research* 237 (2021), p. 105856.

- [69] fishbase.se. *Life History Data on Lates niloticus*. [https://www.fishbase.se/popdyn/KeyfactsSummary\\_1.php?ID=347&GenusName=Lates&SpeciesName=niloticus&vStockCode=361&fc=631](https://www.fishbase.se/popdyn/KeyfactsSummary_1.php?ID=347&GenusName=Lates&SpeciesName=niloticus&vStockCode=361&fc=631). 2022. (accessed: 19.10.2022).
- [70] Roger Fletcher. “A new approach to variable metric algorithms”. In: *The computer journal* 13.3 (1970), pp. 317–322.
- [71] Heinz von Foerster. “Some remarks on changing populations”. In: *The Kinetics of Cellular Proliferation, Grune and Stratton* (1959), pp. 382–407.
- [72] Rainer Froese et al. “A critique of the balanced harvesting approach to fishing”. In: *ICES Journal of Marine Science* 73.6 (2016), pp. 1640–1650.
- [73] Elizabeth A Fulton et al. “Lessons in modelling and management of marine ecosystems: the Atlantis experience”. In: *Fish and fisheries* 12.2 (2011), pp. 171–188.
- [74] Simon Funge-Smith and Abigail Bennett. “A fresh look at inland fisheries and their role in food security and livelihoods”. In: *Fish and Fisheries* 20.6 (2019), pp. 1176–1195.
- [75] Kim Geheb et al. “Nile perch and the hungry of Lake Victoria: Gender, status and food in an East African fishery”. In: *Food policy* 33.1 (2008), pp. 85–98.
- [76] Sarah M Glaser et al. “Armed conflict and fisheries in the Lake Victoria basin”. In: *Ecology and Society* 24.1 (2019).
- [77] Donald Goldfarb. “A family of variable-metric methods derived by variational means”. In: *Mathematics of computation* 24.109 (1970), pp. 23–26.
- [78] Santiago Gómez-Cardona. “Spatial structure effects on fisheries management for Lake Victoria’s Nile Perch”. In: *AWI discussion paper series* (2022).
- [79] Santiago Gómez-Cardona and Johannes Kammerer. “Impact of Gear Choice on Open Access Fisheries: A Study on Fishery Regimes”. In: *AWI discussion paper series* (2023).
- [80] Santiago Gómez-Cardona, Johannes Kammerer, and Hillary Mrosso. “Fishing Fleet Selectivity in Lake Victoria’s Nile Perch Fishery”. In: *AWI discussion paper series* (2022).
- [81] H Scott Gordon. “The economic theory of a common-property resource: the fishery”. In: *Classic Papers in Natural Resource Economics*. Springer, 1954, pp. 178–203.
- [82] Damodar N Gujarati. *Basic econometrics*. Prentice Hall, 2022.

## Bibliography

- [83] Piotr Gwiazda, Grzegorz Jamroz, and Anna Marciniak-Czochra. “Models of discrete and continuous cell differentiation in the framework of transport equation”. In: *SIAM Journal on Mathematical Analysis* 44.2 (2012), pp. 1103–1133.
- [84] Piotr Gwiazda, Thomas Lorenz, and Anna Marciniak-Czochra. “A nonlinear structured population model: Lipschitz continuity of measure-valued solutions with respect to model ingredients”. In: *Journal of Differential Equations* 248.11 (2010), pp. 2703–2735.
- [85] Piotr Gwiazda et al. “Analysis of particle methods for structured population models with nonlocal boundary term in the framework of bounded Lipschitz distance”. In: *Numerical Methods for Partial Differential Equations* 30.6 (2014), pp. 1797–1820.
- [86] Santiago Gómez-Cardona et al. “A high-value Nile Perch fishery through limits on fishing pressure. Supplementary Material (Unpublished)”. In: *MultiTip Policy Briefs Series* (2023).
- [87] Santiago Gómez-Cardona et al. “A high-value Nile Perch fishery through limits on fishing pressure (Unpublished draft)”. In: *MultiTip Policy Briefs Series* (2023).
- [88] Aria Haghighi. *Numerical Optimization: Understanding L-BFGS*. <https://aria42.com/blog/2014/12/understanding-lbfgs>. 2023. (accessed: 14.06.2023).
- [89] Bruce Hansen. *Econometrics*. Princeton University Press, 2022.
- [90] Garrett Hardin. “The tragedy of the commons”. In: *science* 162.3859 (1968), pp. 1243–1248.
- [91] Richard Harrington et al. “Ecosystem services and biodiversity conservation: concepts and a glossary”. In: *Biodiversity and conservation* 19 (2010), pp. 2773–2790.
- [92] Paul JB Hart and John D Reynolds. *Handbook of fish biology and fisheries, Volume 1: Fish Biology*. Blackwell Publishing, 2002.
- [93] Martin Hartvig, Ken H Andersen, and Jan E Beyer. “Food web framework for size-structured populations”. In: *Journal of theoretical Biology* 272.1 (2011), pp. 113–122.

- [94] Mark A Hixon, Darren W Johnson, and Susan M Sogard. “BOFFFFs: on the importance of conserving old-growth age structure in fishery populations”. In: *ICES Journal of Marine Science* 71.8 (2014), pp. 2171–2185.
- [95] Mimmo Iannelli. “Mathematical theory of age-structured population dynamics”. In: *Giardini editori e stampatori in Pisa* (1995).
- [96] Mimmo Iannelli and Fabio Milner. “The basic approach to age-structured population dynamics”. In: *Lecture Notes on Mathematical Modelling in the Life Sciences. Springer, Dordrecht* (2017).
- [97] ICES. *Acoustic trawl surveys*. <https://www.ices.dk/data/data-portals/Pages/acoustic.aspx>. 2023. (accessed: 24.05.2023).
- [98] Chaning Jang and John Lynham. “Where do social preferences come from?”. In: *Economics Letters* 137 (2015), pp. 25–28.
- [99] Thomas C Johnson, Kerry Kelts, and Eric Odada. “The holocene history of Lake Victoria”. In: *Ambio* (2000), pp. 2–11.
- [100] Guido Kanschat and Robert Scheichl. *Numerical Analysis of Ordinary Differential Equations*. 2018.
- [101] Karline Soetaert, Thomas Petzoldt, and R. Woodrow Setzer. “Solving Differential Equations in R: Package deSolve”. In: *Journal of Statistical Software* 33.9 (2010), pp. 1–25. DOI: 10.18637/jss.v033.i09.
- [102] Robert Kayanda et al. “Status of the major commercial fish stocks and proposed species-specific management plans for Lake Victoria”. In: *African Journal of Tropical Hydrobiology and Fisheries* 21 (2009), pp. 15–21.
- [103] Robert Kayanda et al. “Target strength measurements of Nile perch (*Lates niloticus*: Linnaeus, 1758) in Lake Victoria, East Africa”. In: *Fisheries Research* 113.1 (2012), pp. 76–83.
- [104] Thomas Kiørboe, André Visser, and Ken H Andersen. “A trait-based approach to ocean ecology”. In: *ICES Journal of Marine Science* 75.6 (2018), pp. 1849–1863.
- [105] James F Kitchell et al. “The Nile perch in Lake Victoria: interactions between predation and fisheries”. In: *Ecological Applications* 7.2 (1997), pp. 653–664.
- [106] Sina A Klein et al. “How knowledge acquisition shapes system understanding in small-scale fisheries”. In: *Current Research in Ecological and Social Psychology* 2 (2021), p. 100018.

## Bibliography

- [107] Jeppe Kolding. “Incredible evolution or incredulous application?” In: *Ecological applications: a publication of the Ecological Society of America* 23.3 (2013), pp. 670–671.
- [108] Jeppe Kolding et al. “Are the Lake Victoria fisheries threatened by exploitation or eutrophication? Towards an ecosystem based approach to management”. In: *The ecosystem approach to fisheries* (2008), pp. 309–354.
- [109] Jeppe Kolding et al. “Status, trends and management of the Lake Victoria fisheries”. In: *Inland fisheries evolution and management - case studies from four continents. FAO Fisheries and Aquaculture Technical Paper 579* (2014).
- [110] Lone Grønbaek Kronbak, Dale Squires, Niels Vestergaard, et al. “Recent developments in fisheries economics research”. In: *International Review of Environmental and Resource Economics* 7.1 (2014), pp. 67–108.
- [111] Peter Kyomuhendo. “A bioeconomic model for Uganda’s Lake Victoria Nile Perch fishery”. MA thesis. Universitetet i Tromsø, 2002.
- [112] Richard Law, Jeppe Kolding, and Michael J Plank. “Squaring the circle: reconciling fishing and conservation of aquatic ecosystems”. In: *Fish and Fisheries* 16.1 (2015), pp. 160–174.
- [113] Richard Law and Michael J Plank. “Balanced harvesting could reduce fisheries-induced evolution”. In: *Fish and Fisheries* 19.6 (2018), pp. 1078–1091.
- [114] Richard Law and Michael J Plank. “Fishing for biodiversity by balanced harvesting”. In: *Fish and fisheries* 24.1 (2023), pp. 21–39.
- [115] Richard Law, Michael J Plank, and Jeppe Kolding. “Balanced exploitation and coexistence of interacting, size-structured, fish species”. In: *Fish and Fisheries* 17.2 (2016), pp. 281–302.
- [116] Richard Law, Michael J Plank, and Jeppe Kolding. “On balanced exploitation of marine ecosystems: results from dynamic size spectra”. In: *ICES Journal of Marine Science* 69.4 (2012), pp. 602–614.
- [117] Richard Law et al. “Size-spectra dynamics from stochastic predation and growth of individuals”. In: *Ecology* 90.3 (2009), pp. 802–811.
- [118] Jason S Link et al. “Changing how we approach fisheries: a first attempt at an operational framework for ecosystem approaches to fisheries management”. In: *Fish and Fisheries* 21.2 (2020), pp. 393–434.

- [119] Joseph Luomba, Ratana Chuenpagdee, and Andrew M Song. “A bottom-up understanding of illegal, unreported, and unregulated fishing in Lake Victoria”. In: *Sustainability* 8.10 (2016), p. 1062.
- [120] LVFO. “A report of the lake-wide hydroacoustic survey”. In: *Hydro-acoustics Regional Working Group* (2019).
- [121] LVFO. “Regional catch assessment survey synthesis report, June 2005 to November/December 2015”. In: *LVFO* (2016).
- [122] LVFO. “REGIONAL STATUS REPORT ON LAKE VICTORIA BI-ENNIAL FRAME SURVEYS BETWEEN 2000 AND 2016”. In: *Regional Frame Survey Report* (2017).
- [123] LVFO. “Revised Standard Operating Procedures for Hydro-acoustics surveys on Lake Victoria”. In: *LVFO* (2018).
- [124] LVFO. “The Nile Perch Fisheries Management Plan-III for Lake Victoria 2021-2025”. In: *LVFO* (2021).
- [125] Uganda LVFO Secretariat Jinja. “REGIONAL SYNTHESIS REPORT ON THE ECONOMIC AND FINANCIAL IMPACT ASSESSMENT OF LAKE VICTORIA FISHERIES”. In: *LVFO* (2020).
- [126] Anna Marciniak-Czochra et al. “Modeling of asymmetric cell division in hematopoietic stem cells—regulation of self-renewal is essential for efficient repopulation”. In: *Stem cells and development* 18.3 (2009), pp. 377–386.
- [127] Brian E Marshall. “Guilty as charged: Nile perch was the cause of the haplochromine decline in Lake Victoria”. In: *Canadian Journal of Fisheries and Aquatic Sciences* 75.9 (2018), pp. 1542–1559.
- [128] Michael D McGinnis and Elinor Ostrom. “Social-ecological system framework: initial changes and continuing challenges”. In: *Ecology and society* 19.2 (2014).
- [129] AG McKendrick. “Applications of mathematics to medical problems”. In: *Proceedings of the Edinburgh Mathematical Society* 44 (1925), pp. 98–130.
- [130] Yunus D Mgaya and Shigalla B Mahongo. “Lake Victoria Fisheries Resources”. In: *Springer* (2017).
- [131] Russell B Millar and Robert J Fryer. “Estimating the size-selection curves of towed gears, traps, nets and hooks”. In: *Reviews in Fish Biology and Fisheries* 9 (1999), pp. 89–116.

## Bibliography

- [132] Russell B Millar and René Holst. “Estimation of gillnet and hook selectivity using log-linear models”. In: *ICES Journal of Marine Science* 54.3 (1997), pp. 471–477.
- [133] OC Mkumbo and BE Marshall. “The Nile perch fishery of Lake Victoria: current status and management challenges”. In: *Fisheries Management and Ecology* 22.1 (2015), pp. 56–63.
- [134] Oliva C Mkumbo and Enock Mlaponi. “Impact of the baited hook fishery on the recovering endemic fish species in Lake Victoria”. In: *Aquatic Ecosystem Health & Management* 10.4 (2007), pp. 458–466.
- [135] Eliaza Mkuna and Lloyd JS Baiyegunhi. “Determinants of Nile perch (*Lates niloticus*) overfishing and its intensity in Lake Victoria, Tanzania: a double-hurdle model approach”. In: *Hydrobiologia* 835.1 (2019), pp. 101–115.
- [136] Eliaza Mkuna and Lloyd JS Baiyegunhi. “Impact of Nile perch (*Lates niloticus*) overfishing on fishers’ income: Evidence from Lake Victoria, Tanzania”. In: *African Journal of Agricultural and Resource Economics* 15.311-2020-1790 (2020), pp. 213–229.
- [137] Veronica Mpomwenda et al. “Adaptation Strategies to a Changing Resource Base: Case of the Gillnet Nile Perch Fishery on Lake Victoria in Uganda”. In: *Sustainability* 14.4 (2022), p. 2376.
- [138] Veronica Mpomwenda et al. “Fisheries management on Lake Victoria at a crossroads: Assessing fishers’ perceptions on future management options in Uganda”. In: *Fisheries Management and Ecology* 29.2 (2022), pp. 196–211.
- [139] BS Msuku, HDJ Mrosso, and PE Nsinda. “A critical look at the current gillnet regulations meant to protect the Nile Perch stocks in Lake Victoria”. In: *Aquatic Ecosystem Health & Management* 14.3 (2011), pp. 252–259.
- [140] Johannes Müller and Christina Kuttler. “Methods and models in mathematical biology”. In: *Lecture Notes on Mathematical Modelling in Life Sciences*, Springer, Berlin (2015).
- [141] Jonathan Munguti et al. “Nutritive value and availability of commonly used feed ingredients for farmed Nile tilapia (*Oreochromis niloticus* L.) and African catfish (*Clarias gariepinus*, Burchell) in Kenya, Rwanda and Tanzania”. In: *African Journal of Food, Agriculture, Nutrition and Development* 12.3 (2012), pp. 6135–6155.

- [142] Laban Musinguzi, Vianny Natugonza, and Richard Ogutu-Ohwayo. “Paradigm shifts required to promote ecosystem modeling for ecosystem-based fishery management for African inland lakes”. In: *Journal of Great Lakes Research* 43.1 (2017), pp. 1–8.
- [143] Laban Musinguzi, Mark Olokotum, and Vianny Natugonza. “Status and targets for rebuilding the three major fish stocks in Lake Victoria”. In: *BioRxiv* (2020), pp. 2020–10.
- [144] Vianny Natugonza et al. “Ecosystem modelling of data-limited fisheries: How reliable are Ecopath with Ecosim models without historical time series fitting?” In: *Journal of Great Lakes Research* 46.2 (2020), pp. 414–428.
- [145] Vianny Natugonza et al. “Ecosystem models of Lake Victoria (East Africa): can Ecopath with Ecosim and Atlantis predict similar policy outcomes?” In: *Journal of Great Lakes Research* 45.6 (2019), pp. 1260–1273.
- [146] Vianny Natugonza et al. “Exploring the structural and functional properties of the Lake Victoria food web, and the role of fisheries, using a mass balance model”. In: *Ecological modelling* 342 (2016), pp. 161–174.
- [147] Vianny Natugonza et al. “Spatiotemporal variation in fishing patterns and fishing pressure in Lake Victoria (East Africa) in relation to balanced harvest”. In: *Fisheries Research* 252 (2022), p. 106355.
- [148] M Njiru, OC Mkumbo, and M Van der Knaap. “Some possible factors leading to decline in fish species in Lake Victoria”. In: *Aquatic Ecosystem Health & Management* 13.1 (2010), pp. 3–10.
- [149] M Njiru et al. “Are fisheries management, measures in Lake Victoria successful? The case of Nile perch and Nile tilapia fishery”. In: *African Journal of ecology* 45.3 (2007), p. 315.
- [150] M Njiru et al. “Management of Lake Victoria fishery: Are we looking for easy solutions?” In: *Aquatic Ecosystem Health & Management* 17.1 (2014), pp. 70–79.
- [151] Jorge Nocedal and Stephen J Wright. *Numerical optimization*. Springer, 1999.
- [152] Fiona Nunan and Paul Onyango. “Inter-sectoral governance in inland fisheries: Lake Victoria”. In: *Inter-sectoral governance of inland fisheries. Too Big To Ignore-WorldFish, St. John’s, Newfoundland, Canada* (2017), pp. 48–57.

## Bibliography

- [153] Chrispine Nyamweya et al. “Exploring Lake Victoria ecosystem functioning using the Atlantis modeling framework”. In: *Environmental modelling & software* 86 (2016), pp. 158–167.
- [154] Chrispine Sangara Nyamweya et al. “A century of drastic change: Human-induced changes of Lake Victoria fisheries and ecology”. In: *Fisheries Research* 230 (2020), p. 105564.
- [155] Chrispine Sangara Nyamweya et al. “Prediction of Lake Victoria’s response to varied fishing regimes using the Atlantis ecosystem model”. In: *Fisheries research* 194 (2017), pp. 76–83.
- [156] Chrispine Sangara Nyamweya et al. “Response of fish stocks in Lake Victoria to enforcement of the ban on illegal fishing: Are there lessons for management?” In: *Journal of Great Lakes Research* (2023).
- [157] Kevin O Obiero et al. “The challenges of management: Recent experiences in implementing fisheries co-management in Lake Victoria, Kenya”. In: *Lakes & Reservoirs: Research & Management* 20.3 (2015), pp. 139–154.
- [158] Eric O Odada et al. “Mitigation of environmental problems in Lake Victoria, East Africa: causal chain and policy options analyses”. In: *Ambio: A journal of the human environment* 33.1 (2004), pp. 13–23.
- [159] Richard Ogutu-Ohwayo. “Adjustments in fish stocks and in life history characteristics of the Nile perch, *Lates niloticus* L. in lakes Victoria, Kyoga and Nabugabo”. In: *PhD thesis, University of Manitoba* (1994).
- [160] Richard Ogutu-Ohwayo. “Reproductive potential of the Nile perch, *Lates niloticus* L. and the establishment of the species in Lakes Kyoga and Victoria (East Africa)”. In: *Hydrobiologia* 162.3 (1988), pp. 193–200.
- [161] Willis Okumu. *Chinese markets deplete Lake Victoria’s Nile perch*. <https://issafrica.org/iss-today/chinese-markets-deplete-lake-victorias-nile-perch>. 2023. (accessed: 22.11.2023).
- [162] Horace Owiti Onyango et al. “The Lost Coin: Redefining the economic and financial value of small-scale fisheries, the case of Lake Victoria, Kenya”. In: *Social Sciences & Humanities Open* 4.1 (2021), p. 100221.
- [163] Elinor Ostrom. “A general framework for analyzing sustainability of social-ecological systems”. In: *Science* 325.5939 (2009), pp. 419–422.

- [164] Nicholas Otieno Outa et al. “A review on the status of some major fish species in Lake Victoria and possible conservation strategies”. In: *Lakes & Reservoirs: Research & Management* 25.1 (2020), pp. 105–111.
- [165] Daniel Pauly. “On the interrelationships between natural mortality, growth parameters, and mean environmental temperature in 175 fish stocks”. In: *ICES journal of Marine Science* 39.2 (1980), pp. 175–192.
- [166] Roger Perman et al. *Natural resource and environmental economics*. Pearson Education, 2003.
- [167] Ellen K Pikitch et al. “Ecosystem-based fishery management”. In: *Science* 305.5682 (2004), pp. 346–347.
- [168] Tony J Pitcher and Alida Bundy. “Assessment of the Nile perch fishery in Lake Victoria”. In: *The impact of species changes in African lakes*. Springer, 1995, pp. 163–180.
- [169] Michael J Plank. “Balanced harvesting is the bioeconomic equilibrium of a size-structured Beverton-Holt model”. In: *ICES Journal of Marine Science* 74.1 (2017), pp. 112–120.
- [170] Michael J Plank et al. “Balanced harvesting can emerge from fishing decisions by individual fishers in a small-scale fishery”. In: *Fish and fisheries* 18.2 (2017), pp. 212–225.
- [171] John G Pope et al. “Comparing the steady state results of a range of multispecies models between and across geographical areas by the use of the jacobian matrix of yield on fishing mortality rate”. In: *Fisheries Research* 209 (2019), pp. 259–270.
- [172] Raúl Prellezo et al. “A review of EU bio-economic models for fisheries: the value of a diversity of models”. In: *Marine Policy* 36.2 (2012), pp. 423–431.
- [173] R Core Team. *R: A Language and Environment for Statistical Computing*. R Foundation for Statistical Computing. Vienna, Austria, 2023. URL: <https://www.R-project.org/>.
- [174] Rolf Rannacher. *Numerik 1: Numerik gewöhnlicher Differentialgleichungen*. Heidelberg University Publishing, 2017.
- [175] David B Sampson. “Fishery selection and its relevance to stock assessment and fishery management”. In: *Fisheries Research* 158 (2014), pp. 5–14.

## Bibliography

- [176] Milner B Schaefer. “Some aspects of the dynamics of populations important to the management of the commercial marine fisheries”. In: *Inter-American Tropical Tuna Commission Bulletin* 1.2 (1954), pp. 23–56.
- [177] Maja Schlueter et al. “New horizons for managing the environment: A review of coupled social-ecological systems modeling”. In: *Natural Resource Modeling* 25.1 (2012), pp. 219–272.
- [178] Anthony Scott. “The fishery: the objectives of sole ownership”. In: *Journal of political Economy* 63.2 (1955), pp. 116–124.
- [179] Finlay Scott, Julia L Blanchard, and Ken H Andersen. “mizer: an R package for multispecies, trait-based and community size spectrum ecological modelling”. In: *Methods in Ecology and Evolution* 5.10 (2014), pp. 1121–1125.
- [180] David F Shanno. “Conditioning of quasi-Newton methods for function minimization”. In: *Mathematics of computation* 24.111 (1970), pp. 647–656.
- [181] BA Shinkafi, LN Ukoha, and NA Tukur. “Some Aspects of Growth and Reproduction in the Nile Perch (*Lates niloticus*, Linne 1762) From River Rima, North-western Nigeria”. In: *Niger J Fish Aquac* 1 (2013), pp. 31–41.
- [182] Vernon L Smith. “On models of commercial fishing”. In: *Journal of political economy* 77.2 (1969), pp. 181–198.
- [183] William Gary Sprules and Lauren Emily Barth. “Surfing the biomass size spectrum: some remarks on history, theory, and application”. In: *Canadian Journal of Fisheries and Aquatic Sciences* 73.4 (2016), pp. 477–495.
- [184] Olli Tahvonen. “Economics of harvesting age-structured fish populations”. In: *Journal of Environmental Economics and Management* 58.3 (2009), pp. 281–299.
- [185] Olli Tahvonen, Martin F Quaas, and Rüdiger Voss. “Harvesting selectivity and stochastic recruitment in economic models of age-structured fisheries”. In: *Journal of Environmental Economics and Management* 92 (2018), pp. 659–676.
- [186] Hannes Uecker. “Optimal harvesting and spatial patterns in a semiarid vegetation system”. In: *Natural Resource Modeling* 29.2 (2016), pp. 229–258.
- [187] Hannes Uecker and Thorsten Upmann. “Optimal fishery with coastal catch”. In: (2016).

- [188] Ludwig Von Bertalanffy. “Quantitative laws in metabolism and growth”. In: *The quarterly review of biology* 32.3 (1957), pp. 217–231.
- [189] Wolfgang Walter. *Gewöhnliche Differentialgleichungen: Eine Einführung*. Springer-Verlag, 2013.
- [190] Carl J Walters and Francis Juanes. “Recruitment limitation as a consequence of natural selection for use of restricted feeding habitats and predation risk taking by juvenile fishes”. In: *Canadian Journal of Fisheries and Aquatic Sciences* 50.10 (1993), pp. 2058–2070.
- [191] ICES Website. *ICES Glossary*. <https://www.ices.dk/lists/glossary/ices%20glossary.aspx>. 2023. (accessed: 21.06.2023).
- [192] David A Wileman et al. *Manual of methods of measuring the selectivity of towed fishing gears*. ICES Cooperative Research Report No. 215. pp. 126, 1996. DOI: <https://doi.org/10.17895/ices.pub.4628>.
- [193] Frans Witte, JH Wanink, and M Kische-Machumu. “Species distinction and the biodiversity crisis in Lake Victoria”. In: *Transactions of the American Fisheries Society* 136.4 (2007), pp. 1146–1159.
- [194] Jia Wo et al. “Modeling the dynamics of multispecies fisheries: A case study in the coastal water of North Yellow Sea, China”. In: *Frontiers in Marine Science* 7 (2020), p. 946.
- [195] Karen E van de Wolfshaar et al. “Nile perch (*Lates niloticus*, L.) and cichlids (*Haplochromis* spp.) in Lake Victoria: could prey mortality promote invasion of its predator?” In: *Theoretical ecology* 7.3 (2014), pp. 253–261.
- [196] Edwine Yongo et al. “Growth, mortality and recruitment of Nile perch (*Lates niloticus*) in Lake Victoria, Kenya”. In: *Lakes & Reservoirs: Research & Management* 23.1 (2018), pp. 17–23.
- [197] L Zakharova, KM Meyer, and M Seifan. “Trait-based modelling in ecology: a review of two decades of research”. In: *Ecological Modelling* 407 (2019), p. 108703.
- [198] Ciyou Zhu et al. “Algorithm 778: L-BFGS-B: Fortran subroutines for large-scale bound-constrained optimization”. In: *ACM Transactions on mathematical software (TOMS)* 23.4 (1997), pp. 550–560.

## *Bibliography*

- [199] Paul AM van Zwieten et al. “The Nile perch invasion in Lake Victoria: cause or consequence of the haplochromine decline?” In: *Canadian Journal of Fisheries and Aquatic Sciences* 73.4 (2016), pp. 622–643.

# List of Figures

1.1	Social-Ecological Systems . . . . .	3
1.2	Outline of the thesis . . . . .	7
2.1	Map of the Lake Victoria region . . . . .	10
2.2	The two main gears in the Nile perch fishery . . . . .	11
3.1	The maximum ingestion rate as a function of the body weight . . . . .	21
3.2	The van Bertalanffy growth curve . . . . .	23
3.3	The percentage of mature male and female Nile perch in Lake Kyoga . . . . .	24
3.4	Recruitment survival probability . . . . .	26
4.1	Unimodal selectivity curves . . . . .	35
4.2	Sigmoidal selectivity curves . . . . .	36
4.3	Average length of the catch for gillnets and hooks . . . . .	42
4.4	The fishing selectivity curves of gillnets and longline hooks . . . . .	43
4.5	The aggregated selectivity of longlines, gillnets and the fleet selectivity . . . . .	45
5.1	Bottom trawl technique and the hydroacoustic method . . . . .	51
6.1	Model concept . . . . .	53
6.2	Derivative of yield . . . . .	66
7.1	Van Bertalanffy growth curve vs integration of the differential equation (weight-at-age) . . . . .	71
7.2	Van Bertalanffy growth curve vs integration of the differential equation (length-at-age) . . . . .	72
7.3	Empirical fleet selectivity (2020) . . . . .	72
7.4	Bottom trawl survey compared to simulations . . . . .	73
7.5	Hydroacoustic and CAS survey compared to simulations . . . . .	74
7.6	Three surveys together with the model simulation . . . . .	76
7.7	Surveys and simulations (number density as function of length) . . . . .	76
7.8	Distribution of residuals . . . . .	78
7.9	Peak fishing mortality and annual fishing mortality . . . . .	80

*List of Figures*

7.10	Simulations of Nile perch biomass spectrum and catch distribution . . .	82
7.11	Steady state yield, stock biomass, SSB and recruitment . . . . .	84
8.1	Fleet selectivity scenarios . . . . .	86
8.2	Yield dependent on fishing mortality for the four selectivity scenarios . .	87
8.3	SSB in steady state in dependence of the yield . . . . .	89
8.4	Increase in steady state yield and aggregate income of the fishery for five selectivity scenarios . . . . .	93
8.5	Increase in steady state biomass and SSB of the fish stock for five selectivity scenarios . . . . .	94
9.1	Maximizing yield . . . . .	97
9.2	Maximizing yield with senescent mortality . . . . .	98
9.3	Maximizing income . . . . .	99
9.4	Maximizing income with senescent mortality . . . . .	100
9.5	Cohort biomass . . . . .	101
10.1	Sketch of the simulation procedure . . . . .	105
10.2	Stock biomass and the effort in the simulation over a period of 30 years .	106
10.3	Total annual yield and the income in the simulation over a period of 30 years	106
10.4	The yield, disaggregated per sub-fleet . . . . .	107
10.5	The profit, disaggregated per sub-fleet . . . . .	107
10.6	Stock biomass and mean total length after 30 years as a function of the panelling factor . . . . .	110
10.7	Biomass after 30 years (panelling) . . . . .	111
10.8	State after 30 years simulation with the respective panelling factor . . . .	112
10.9	Stock biomass and mean total length after 30 years as a function of the opportunity costs . . . . .	113
10.10	Biomass after 30 years (opportunity costs) . . . . .	114
10.11	State after 30 years simulation with the respective value of opportunity costs	115
10.12	Percentage of vessels from simulations of the agent-based model . . . . .	118
10.13	Relative number of vessels from simulations of the agent-based model . .	119
10.14	The number of fishing boats in quasi-steady state as a function of the op- portunity costs . . . . .	120
10.15	Summary of the ABM simulations . . . . .	121
A.1	Length-weight relationship for two fish species . . . . .	170

# List of Tables

3.1	Species specific standard parameters . . . . .	29
3.2	Species independent parameters . . . . .	29
4.1	Selectivity parameters of gillnets . . . . .	44
4.2	Fraction of the area under the selectivity curve that is below 50cm . . . . .	44
4.3	Numbers of vessels in the standard model . . . . .	46
4.4	Fish price of Nile perch . . . . .	47
4.5	Standard values of biomass, catch and recruitment . . . . .	47
7.1	Sum of squared log-residuals . . . . .	75
7.2	The linear regression results concerning the slope . . . . .	77
7.3	Relative and absolute sensitivity of $R^*$ and $F_{MSY}$ . . . . .	81
8.1	Best fishing mortality . . . . .	88
8.2	Maximum sustainable yield (parameter a) . . . . .	90
8.3	Increase in steady state yield and income in five selectivity scenarios. . . . .	92
8.4	Increase in steady state biomass and SSB in five selectivity scenarios . . . . .	92



# List of publications

- Kammerer, J., Gómez-Cardona, S. and Nyamweya, C. (2022). Size selective fishing: The effect of size selectivity on the equilibrium yield in the Nile perch fishery of Lake Victoria. AWI Discussion Paper 720, Heidelberg University.  
*This publication studies the impact of the fleet selectivity on the stock and the fishery outcomes.*
- Gómez-Cardona, S., Kammerer, J. and Mrosso, H. (2022). Fishing Fleet Selectivity in Lake Victoria. AWI Discussion Paper 712, Heidelberg University.  
*This publication describes the derivation of the gear selectivity curves.*
- Gómez-Cardona, S. and Kammerer, J. (2023). Impact of Gear Choice on Open Access Fisheries: A Study on Fishery Regimes. AWI Discussion Paper 732, Heidelberg University.  
*This publication analyzes an agent-based model of the Nile perch fishery based on the biological model of this thesis.*



# Appendices



# A Mathematical methods

## A.1 Ordinary differential equations

### A.1.1 Existence

In the following we give a very brief primer on the theory of ordinary differential equations. For more details, the reader is referred to the introductions [174, 100, 189].

**Definition A.1** (Ordinary Differential Equation (ODE), [100]). Let  $u(t)$  be a function defined on an interval  $I \subset \mathbb{R}$  with  $u : I \rightarrow \mathbb{R}$ .

An (implicit) ordinary differential equation (ODE) of order  $n$  is an equation for  $u(t)$  of the form  $F(t, u(t), u'(t), \dots, u^{(n)}(t)) = 0$ .

If it can be formulated as  $u'(t) = f(t; u(t))$ , it is called an explicit ODE. If the right hand side  $f$  does not explicitly depend on  $t$ , so  $u'(t) = f(u)$ , the equation is called autonomous.

**Definition A.2** (Initial value problem (IVP) (Definition 1.2.7 in [100])). Given an initial point  $(t_0, u_0) \in \mathbb{R} \times \mathbb{R}^d$  and the function  $f(t, u)$ , defined in a neighbourhood of  $(t_0, u_0)$ ,  $I \times U \in \mathbb{R} \times \mathbb{R}^d$ , with the values of  $f$  in  $\mathbb{R}^d$ . The task to find a function  $u(t)$  such that  $u'(t) = f(t, u(t))$  and  $u(t_0) = u_0$ , is called an initial value problem.

**Theorem A.3** (Peano's local existence theorem, [174]). *Let  $\alpha, \beta > 0$  and let the function  $f(t; x)$  be continuous on the  $(d+1)$ -dimensional cylinder  $D = \{(t, x) \in \mathbb{R} \times \mathbb{R}^d : |t - t_0| \leq \alpha, \|x - u_0\| \leq \beta\}$ . Then there exists a solution  $u(t)$  of the IVP on the interval  $I := [t_0 - T, t_0 + T]$ , where  $T := \min(\alpha, \beta/M)$ ,  $M := \max_{(t,x) \in D} \|f(t, x)\|$ .*

The proof is given in [174, Satz 1.1].

**Remark A.4.** *Note that the Peano existence theorem guarantees only local existence of the solution, but not the uniqueness.*

**Theorem A.5** (Peano's continuation theorem, [100, 174]). *Let the function  $f(t, x)$  be continuous on some set  $D \subset \mathbb{R} \times \mathbb{R}^d$  that contains the point  $(t_0, u_0)$ . Let  $u$  be a local solution of the IVP in the neighbourhood of  $t_0$ , then there exists an interval  $I = (t_-, t_+)$  such that the local solution  $u$  can be extended to the left and the right of  $t_0$  to a continuously differentiable solution  $u \in C^1(I)$ , as long as the graph of  $u$  does not touch the boundary*

## A Mathematical methods

of  $D$ . The interval  $I$  may be unbounded and the graph  $(u) := \{(t, u(t)), t \in I\}$  may be unbounded for  $t \rightarrow t_+$  or  $t \rightarrow t_-$ .

The proof is given in [100, Theorem 1.2.15] and [174, Satz 1.2].

**Corollary A.6** (Global Existence, [174]). *Let the function  $f(t, x)$  of the IVP (Definition A.2) be defined on  $\mathbb{R} \times \mathbb{R}^d$  and continuous. If, for each local solution  $u(t)$  from Theorem A.3, it holds that  $\|u(t)\| \leq \beta(t)$ ,  $t \in [t_0 - T, t_0 + T]$ , with some fixed continuous function  $\beta : \mathbb{R} \times \mathbb{R}$ , then one can extend  $u$  to a global solution on  $\mathbb{R}$ .*

The proof is given in [174, Korollar 1.19].

### A.1.2 Uniqueness

**Definition A.7** (Lipschitz condition, [174, 100]). The function  $f(t, x)$  satisfies a uniform Lipschitz condition on the domain  $D \subset \mathbb{R} \times \mathbb{R}^d$ , if it holds with a continuous function  $L(t) > 0$  that:  $\|f(t, x) - f(t, x')\| \leq L(t)\|x - x'\|$ ,  $(t, x), (t, x') \in D$ .  $f(t, x)$  is said to satisfy a local Lipschitz condition, if the inequality holds for all compact subsets of  $D$ .

**Lemma A.8** (Grönwall's Lemma, [174]). *Let the piecewise continuous function  $w(t) \geq 0$  satisfy, with two constants  $a, b \geq 0$ , the integral inequality  $w(t) \leq b + a \int_{t_0}^t w(s) ds$ ,  $t \geq t_0$ . Then it holds:  $w(t) \leq be^{a(t-t_0)}$   $t \geq t_0$ .*

The proof is given in [174, Hilfssatz 1.19].

**Corollary A.9** (Uniqueness, [174]). *An IVP with Lipschitz continuous function  $f(t, \cdot)$  has at most one solution. If Peano's theorem guarantees the existence of a solution, the solution is then unique.*

The proof is given in [174, Korollar 1.2].

**Theorem A.10** (Existence theorem of Picard-Lindelöf, [100]). *Let  $f(t, x), f : D \rightarrow \mathbb{R}^d$  be continuous and satisfy a local Lipschitz condition on a domain  $D$  which contains the closed set  $D_0 = \{(t, x) \in D : |t - t_0| \leq \alpha, |y - y_0| \leq \beta\}$ , there exists a  $T > 0$  and a unique, local solution  $u : I = [t_0 - T, t_0 + T] \rightarrow \mathbb{R}^d$  of the IVP  $u'(t) = f(t, u(t))$ ,  $t \in I = [t_0 - T, t_0 + T]$ ,  $u(t_0) = u_0$ . The function  $f$  is then also bounded on  $D_0$  with  $M := \max_{(t,x) \in D_0} |f(t, x)| < \infty$  and  $T = \min(\alpha, \beta/M)$ .*

The proof is given in [100, Theorem 1.4.6].

**Definition A.11** (Well-posedness of an IVP, [100]). An initial value problem is well-posed if the three Hadamard conditions are fulfilled:

1. A solution exists.
2. The solution is unique.
3. The solution depends continuously on the data.

## A.2 Solution to the age structured population model

Let us consider the following age structured model [96],

$$\left\{ \begin{array}{l} \frac{\partial}{\partial t} p(a, t) + \frac{\partial}{\partial a} p(a, t) + \tilde{\mu}(a)p(a, t) = 0 \quad \text{on } [0, a_+] \times [0, T], \\ p(a, 0) = p_0(a) \quad \text{on } [0, a_+], \\ p(0, t) = R_0 \Phi(S(t)) \int_0^{a_+} \tilde{\beta}_0(a)p(a, t) da \quad \text{on } [0, T], \\ S(t) = \int_0^{a_+} \tilde{\gamma}(a)p(a, t) da, \end{array} \right. \quad (\text{A.1})$$

where  $p(a, t) : [0, a_+] \times [0, T] \rightarrow \mathbb{R}_+$  is the population density dependent on age  $a$  and time  $t$  with maximum age  $a_+ < \infty$ ,  $\tilde{\mu} : [0, a_+] \rightarrow \mathbb{R}_+$  is the mortality rate,  $R_0 \in \mathbb{R}_+$  the *intrinsic net reproduction number*,  $\tilde{\beta}_0 : [0, a_+] \rightarrow \mathbb{R}_+$  the baseline fertility, and  $p_0$  the initial population density. The recruitment depends on the density of the population, characterized by the *reproductive population*  $S : [0, T] \rightarrow \mathbb{R}_+$ . The impact of the size of the reproductive population on the fertility is modeled through the function  $\Phi : [0, \infty) \rightarrow \mathbb{R}_+$ , continuous on  $[0, \infty)$  and continuously differentiable on  $(0, \infty)$ , that decreases the reproduction with increasing population, with the following properties:

$$\Phi(0) = 1, \quad \Phi(x) \geq 0, \quad \Phi'(x) < 0, \quad \lim_{x \rightarrow \infty} \Phi(x) = 0. \quad (\text{A.2})$$

In the following the term *baseline* means without the effect of the density dependence, i.e. at  $S = 0$ . Defining the baseline survival probability

$$\Pi_0(a) = e^{-\int_0^a \tilde{\mu}(\sigma) d\sigma}, \quad (\text{A.3})$$

we have then the following basic assumptions:

$$\left\{ \begin{array}{l} i) \quad \tilde{\beta}_0 \in C_b((0, a_+)), \quad 0 \leq \tilde{\beta}_0(a) \leq \tilde{\beta}_+ \text{ a.e. in } [0, a_+], \\ ii) \quad \int_0^{a_+} \tilde{\beta}_0(a) \Pi_0(a) da = 1, \\ iii) \quad p_0 \in L^\infty(0, a_+), \quad p_0(a) \geq 0 \text{ a.e. in } [0, a_+], \\ iv) \quad \tilde{\mu} \in L^1_{loc}([0, a_+]); \quad \tilde{\mu}(a) \geq 0 \text{ a.e. in } [0, a_+]; \quad \int_0^{a_+} \tilde{\mu}(a) da = +\infty, \\ v) \quad \tilde{\gamma} \in C_b((0, a_+)), \quad 0 \leq \tilde{\gamma}(a) \leq \tilde{\gamma}_+ \text{ a.e. in } [0, a_+]. \end{array} \right. \quad (\text{A.4})$$

Further we require the *compatibility condition* between the initial age density and the fertility function [96]:

$$p_0(0) = R_0 \Phi(S(0)) \int_0^{a_+} \tilde{\beta}_0(a)p(a, 0) da. \quad (\text{A.5})$$

**Proposition A.12** (Existence of a unique, non-negative solution with regularity). *Under the assumptions (A.2)-(A.5), there exists a unique, non-negative solution  $p$  that satisfies the logistic model (A.1). The solution is continuous and the partial derivatives  $p_t$  and  $p_a$  exist a.e. in  $[0, a_+] \times [0, T]$ .*

*Proof.* The proof is given in [96, Theorem 5.2, Proposition 5.2 and Section 5.4].  $\square$

**Remark A.13.** *The compatibility condition (A.5) is only necessary to guarantee that the solution  $p$  is continuous across the characteristic line  $a = t$ , where the initial condition and the boundary condition concur [96].*

**Proposition A.14** (Steady state solution). *Under the assumptions (A.2)-(A.5), the logistic model (A.1) has a unique non-trivial steady state solution, if and only if  $R_0 > 1$ .*

*Proof.* The proof is given in [96, Theorem 5.4].  $\square$

### A.3 Convergence of the growth function

The growth rate of fish is given by

$$g(w) = Aw^n \left( 1 - \frac{1}{1 + \left(\frac{w}{w_m}\right)^{-\kappa}} \left(\frac{w}{W_{\dagger}}\right)^{1-n} \right) \quad \text{in } [0, \infty) \quad (\text{A.6})$$

with the parameters from Chapters 3 and 6. The growth curve  $w(a)$  of the individual fish is the solution to the ordinary differential equation

$$\begin{cases} \frac{dw(a)}{da} = g(w(a)) = Aw(a)^n \left( 1 - \frac{1}{1 + \left(\frac{w(a)}{w_m}\right)^{-\kappa}} \left(\frac{w(a)}{W_{\dagger}}\right)^{1-n} \right) & \text{in } [0, \infty), \\ w(0) = w_0 \end{cases} \quad (\text{A.7})$$

with the growth function  $g(w)$  and the other parameters and variables from the Chapters 3 and 6. Let us define the maximal weight  $W_{\infty} > 0$  as the positive weight where the growth function vanishes, such that  $g(W_{\infty}) = 0$ . We will now show that this maximal weight is not reached in finite time, i.e. not at a finite age of the fish.

**Lemma A.15.** *The maximal weight  $W_{\infty}$  with  $w_0 < W_{\dagger} < W_{\infty} < \infty$ , where the growth rate from (A.6) vanishes, is not reached at finite age  $a$ .*

*Proof.* From the definition of  $W_{\infty}$ ,

$$g(W_{\infty}) = AW_{\infty}^n \left( 1 - \frac{1}{1 + \left(\frac{W_{\infty}}{w_m}\right)^{-\kappa}} \left(\frac{W_{\infty}}{W_{\dagger}}\right)^{1-n} \right) = 0, \quad (\text{A.8})$$

### A.3 Convergence of the growth function

we can directly derive that

$$W_{\dagger} = \frac{W_{\infty}}{\left(1 + \left(\frac{W_{\infty}}{w_m}\right)^{-\kappa}\right)^{\frac{1}{1-n}}}. \quad (\text{A.9})$$

Introducing the new variable  $x = \frac{w}{w_m}$  allows to re-write  $g(w)$  in the following way:

$$\begin{aligned} g(x) &= Aw_m^n x^n \left(1 - \frac{1}{1+x^{-\kappa}} \left(\frac{w_m x}{W_{\dagger}}\right)^{1-n}\right) \\ &= Aw_m^n x^n \left(1 - \frac{x^{1-n}}{1+x^{-\kappa}} \left(\frac{w_m}{W_{\infty}}\right)^{1-n} \left(1 + \left(\frac{W_{\infty}}{w_m}\right)^{-\kappa}\right)\right) \\ &= Aw_m^n x^n \left(1 - \frac{x^{1-n}}{1+x^{-\kappa}} \left(\frac{w_m}{W_{\infty}}\right)^{1-n} w_m^{\kappa} (W_{\infty}^{-\kappa} + w_m^{-\kappa})\right). \end{aligned} \quad (\text{A.10})$$

Next we introduce

$$f(x) = 1 - \frac{x^{1-n}}{1+x^{-\kappa}} \left(\frac{w_m}{W_{\infty}}\right)^{1-n} w_m^{\kappa} (W_{\infty}^{-\kappa} + w_m^{-\kappa}) \quad (\text{A.11})$$

such that

$$g(x) = Aw_m^n x^n f(x). \quad (\text{A.12})$$

Now, using separation of variables we can write for the solution of (A.7):

$$\int_{w_0}^{W_{\infty}} \frac{dw}{g(w)} = \int_0^{a_{\infty}} da = a_{\infty}, \quad (\text{A.13})$$

where the maximal age  $a_{\infty}$ , defined as the age when the maximal weight  $W_{\infty}$  is reached, could, until now, be finite or infinite. In order to prove that  $a_{\infty} = \infty$ , we have to show that

$$\int_{w_0}^{W_{\infty}} \frac{dw}{g(w)} = \infty. \quad (\text{A.14})$$

As it holds for the prefactor  $Aw_m^n x^n$  that

$$0 < Aw_0^n < Aw_m^n x^n < Aw_{\infty}^n < \infty, \quad (\text{A.15})$$

we know that

$$\int_{x_0}^{x_{\infty}} \frac{dx}{f(x)} = \infty \implies \int_{w_0}^{W_{\infty}} \frac{dw}{g(w)} = \infty, \quad (\text{A.16})$$

## A Mathematical methods

where  $x_0 = \frac{w_0}{w_m}$  and  $x_\infty = \frac{W_\infty}{w_m}$ . The first integral can (if at all) only diverge around its pole  $x_\infty$ , where  $f(x_\infty) = 0$ , and it is sufficient to prove the divergence in a neighborhood of the pole. Therefore, one has to find a function  $p(x)$  with  $p(x) > f(x)$  around the pole, for which it holds that

$$\int_{x_0}^{x_\infty} \frac{dx}{p(x)} = \infty. \quad (\text{A.17})$$

This would be a lower bound for  $\int_{x_0}^{x_\infty} \frac{dx}{f(x)}$  and hence imply the divergence of the latter. Let us define

$$\zeta = \left( \frac{w_m}{W_\infty} \right)^{1-n} w_m^\kappa (W_\infty^{-\kappa} + w_m^{-\kappa}), \quad (\text{A.18})$$

where  $0 < \zeta < \infty$ . Then

$$f(x) = 1 - \frac{x^{1-n}}{1 + x^{-\kappa}} \zeta, \quad (\text{A.19})$$

and the derivative of  $f(x)$  is

$$f'(x) = -\zeta \frac{(1-n)x^{-n} + (1-n+\kappa)x^{-n-\kappa}}{(1+x^{-\kappa})^2}. \quad (\text{A.20})$$

With the values  $n = 0.75$  and  $\kappa = 5$ , the fraction is strictly positive at the pole  $x_\infty$ . As  $\zeta$  and the fraction are bounded, it follows that  $f'(x)$  is negative and bounded from above and below in a neighborhood of  $x_\infty$ :

$$-\infty < -C_1 \leq f'(x) \leq -C_2 < 0. \quad (\text{A.21})$$

Let us define the function

$$h(x) := f(x) - \epsilon(W_\infty - w) \quad (\text{A.22})$$

in some neighborhood of  $x_\infty$ . As

$$h'(x) = f'(x) + \epsilon \quad (\text{A.23})$$

and  $f'(x)$  is bounded from above and below in the neighborhood of  $x_\infty$ , we can surely find some  $0 < \epsilon < \infty$ , such that

$$h'(x) = f'(x) + \epsilon > 0 \quad (\text{A.24})$$

## A.4 Ordinary least squares

As  $h(x_\infty) = f(x_\infty) = 0$  and  $f'(x) < 0$  near the pole, this implies that

$$h(x) = f(x) - \epsilon(W_\infty - w) < 0 \quad (\text{A.25})$$

in some neighborhood of  $x_\infty$ . Then

$$p(x) := f(x) - h(x) = \epsilon(x_\infty - x) > f(x) \quad (\text{A.26})$$

in the neighborhood. At the same time, it holds with some point  $x_\infty - \delta$  in the neighborhood for  $x_\infty$  that

$$\int_{x_\infty - \delta}^{x_\infty} \frac{dx}{p(x)} = \int_{x_\infty - \delta}^{x_\infty} \frac{dx}{\epsilon(x_\infty - x)} = \left[ -\frac{1}{\epsilon} \log(\epsilon(x_\infty - x)) \right]_{x_\infty - \delta}^{x_\infty} = \infty. \quad (\text{A.27})$$

Therefore it follows that

$$\int_{x_0}^{x_\infty} \frac{dx}{f(x)} > \int_{x_0}^{x_\infty} \frac{dx}{p(x)} = \infty \implies \int_{w_0}^{W_\infty} \frac{dw}{g(w)} = \infty, \quad (\text{A.28})$$

thus the maximal age from (A.13) is infinite:

$$a_\infty = \infty. \quad (\text{A.29})$$

□

## A.4 Ordinary least squares

Consider a data set of  $N$  data pairs, where  $x_i$  is the independent variable (the *predictor*) and  $y_i$  the dependent variable (the *response variable*) with  $i = 1, \dots, N$ . Suppose the data shall be fitted with a function  $f(x, \beta)$  that has the parameter vector  $\beta$ . The goal is to determine the parameters  $\beta$  such that the model represents the data as best as possible. This implies minimizing some measure of the distance between the data points and the model. The distance at each data point is the *residual*  $r_i = y_i - f(x_i, \beta)$ . The "goodness" of the model can be specified as the sum of the squared residuals (SSR) with  $SSR = \sum_{i=1}^N r_i^2$ .

In the case of the ordinary least squares method, the model has the following form:

$$y_i = \beta_0 + \beta_1 x_i + \epsilon_i, \quad (\text{A.30})$$

## A Mathematical methods

where  $\epsilon_i$  is the error term that is assumed to be a random variable (independent and identically distributed, i.i.d.). The task is now to find  $\beta_0, \beta_1$  to minimize the SSR:

$$\min_{\beta_0, \beta_1} SSR = \sum_{i=1}^N (y_i - (\beta_0 + \beta_1 x_i))^2. \quad (\text{A.31})$$

Furthermore, one can define the *coefficient of variation*,  $R^2$ , a measure of the "goodness of fit" capturing the percentage of the variation in the dependent variable that is "explained" from the linear model [82, 89]. With the mean value  $\bar{y} = \frac{1}{N} \sum_{i=1}^N y_i$  one can write:

$$R^2 = \frac{\sum_{i=1}^N (f(x_i, \beta) - \bar{y})^2}{\sum_{i=1}^N (y_i - \bar{y})^2}. \quad (\text{A.32})$$

## A.5 Optimization methods

In this section, we introduce the algorithm of the method L-BFGS-B which will be used in the thesis to optimize the fishing pattern. This method belongs to the class of Quasi-Newton methods. To provide the background for understanding the concept of the method, we begin with a brief overview of optimization methods, to the degree to which it is relevant for the idea of the Quasi-Newton method.

### A.5.1 Newton-Raphson methods

Assume that  $f(x)$ ,  $f \in \mathbb{R}$  is a multivariate function of the input vector  $x \in \mathbb{R}^n$ . Now one seeks to find the vector  $x^*$  that minimizes the function value:

$$x^* = \arg \min_x f(x). \quad (\text{A.33})$$

The idea is an iterative approach that aims to generate a sequence of estimates,  $x_n$ ,  $n = 0, 1, 2, \dots$  that approaches the "true" global minimizer  $x^*$ . So, given an estimate, one wants to use the algorithm to find an improved estimate such that  $f(x^{n+1}) < f(x^n)$ . The Newton method is based on the idea to find a quadratic approximation of the problem that is valid in a neighborhood of  $x_n$ . Let us assume that  $f$  is twice-differentiable. Then, in some region "close" to a fixed point, one can build the Taylor approximation:

$$f(x + \Delta x) = f(x) + \Delta x^T \nabla f(x) + \frac{1}{2} \Delta x^T \nabla^2 f(x) \Delta x. \quad (\text{A.34})$$

where  $\nabla f(x)$  denotes the gradient and  $\nabla^2 f(x)$  the Hessian matrix of  $f$  [88].

As an iterative procedure, one starts from an initial guess  $x^0$  and, in each step, finds a step direction and step width,  $t^k \Delta x^{k+1}$ , such that the function after the step, at  $x^{k+1} =$

$x^k + t^k \Delta x^{k+1}$ , is minimized. The quadratic approximation of the function  $f$  is given by the Taylor approximation, therefore the increment  $\Delta x^k$  comes from solving the quadratic problem (QP):

$$\min_{\Delta x} \frac{1}{2} \Delta x^T H^k \Delta x + \nabla f(x^k)^T \Delta x, \quad (\text{A.35})$$

where  $H^k$  denotes the Hessian matrix [18].

## A.5.2 Quasi-Newton methods

Similar to the Newton method, the Quasi-Newton methods use a second-order approximation, however the Hessian  $H$  is not calculated directly, but rather given by some approximation.

Given an estimate  $x_k$ , the second order approximation of the function at the next iterate,  $x_{k+1} = x_k + \Delta x_k$ , is:

$$f(x_k + \Delta x_k) \approx f(x_k) + \nabla f(x_k)^T \Delta x_k + \frac{1}{2} \Delta x_k^T H(x_k) \Delta x_k. \quad (\text{A.36})$$

A necessary condition of the next iterate to be (approximately) optimal, is that the gradient, given by

$$\nabla f(x_k + \Delta x_k) \approx \nabla f(x_k) + H(x_k) \Delta x_k, \quad (\text{A.37})$$

vanishes at the next iterate:

$$\nabla f(x_k + \Delta x_k) = 0. \quad (\text{A.38})$$

This condition provides, if  $H$  is invertible, the Newton step:

$$\Delta x_k = H^{-1}(x_k) \nabla f(x_k) = 0. \quad (\text{A.39})$$

The approximation of the Hessian has to fulfill the "secant equation"

$$\nabla f(x_k + \Delta x_k) = \nabla f(x_k) + H(x_k) \Delta x_k. \quad (\text{A.40})$$

### A.5.3 BFGS method

In the Broyden–Fletcher–Goldfarb–Shanno (BFGS) algorithm [24, 23, 70, 77, 180, 18], which is widely used [1], the next iterative of the approximation of the Hessian is given by

$$H_{k+1} = H_k + \frac{y_k y_k^T}{y_k^T \Delta x_k} - \frac{H_k \Delta x_k \Delta x_k^T H_k^T}{\Delta x_k^T H_k \Delta x_k}, \quad (\text{A.41})$$

where  $\Delta x_k$  is the solution of the secant equation (A.40) (in the literature also referred to as  $s_k$ ) and  $y_k = \nabla f(x_{k+1}) - \nabla f(x_k)$ .

This construction has the property that  $H_{k+1}^{-1}$  is positive definite, if  $H_k^{-1}$  is. By induction it follows that, if  $H_0^{-1}$  is positive definite, each iterate also is. The condition can always be satisfied by choosing the unit matrix as the initial matrix. Additionally, one can formulate a recurrence formula for  $H_{k+1}^{-1}$ , such that the sequence of iterates  $y_j$  and  $\Delta x_j$  ( $j = 1, \dots, k$ ) is sufficient to construct  $H_{k+1}^{-1}$  and one does not require the knowledge of  $H_k^{-1}$ . This allows, in another step, to calculate  $H_{k+1}^{-1} \nabla f(x_{k+1})$  without explicitly calculating  $H_{k+1}^{-1}$  [88]. The method is also well described in [151].

### A.5.4 L-BFGS-B method

The BFGS method has the advantage that the Hessian need not be calculated explicitly, but it still requires to store the complete sequence of  $y_j$  and  $\Delta x_j$ . For a high dimensional problem, this can require a large memory space. For this, the Limited-memory BFGS algorithm (L-BFGS) was constructed that only requires the last  $m$  iterates of  $\Delta x$  and of  $y$ , namely  $\Delta x_k, \Delta x_{k-1}, \dots, \Delta x_{k-m-1}$  and  $y_k, y_{k-1}, \dots, y_{k-m-1}$  to compute the next iterate [88].

In order to handle simple box constraints, one has to extend the L-BFGS algorithm. For each component  $x_i \in \mathbb{R}$  of  $x = (x_1, x_2, \dots, x_i, \dots, x_n)^T$ , the user can prescribe an upper and a lower bound, such that  $l_i \leq x_i \leq u_i$ . For each component, no bound, one bound, or both lower and upper bound can be prescribed [25, 198, 151, 55].

## A.6 Density conversion

### A.6.1 Age and weight

As explained in Chapter 3, many of the relevant biological processes scale as a power-law function of the weight. Therefore, the main part of the model is formulated using the weight density, this means the number density in the weight domain. The density has the unit of numbers per gram. However, much of the mathematical literature is formulated in the age domain, i.e. in terms of the age density in units of numbers per year. The reason

is that, for the mathematical analysis, the age density is more convenient because the partial time derivative of age is simply one. Independent of its size, a fish has become one year older after one year, while the weight increment in one year depends on the weight itself, thus the time derivative of the weight is not simply constant.

As can be seen in the following, there is a direct (and unique) translation between the weight density and the age density. This implies that the mathematical results obtained using the age density carry over to the model formulated in the weight density.

The inverse function theorem states that, if  $f$  is a continuously differentiable function of one variable and its derivative does not vanish in the point  $x$ , then there exists a neighborhood of  $x$  where  $f$  is injective and near  $y = f(x)$ , the inverse is continuously differentiable. The derivative of the inverse function  $f^{-1}$  at the point  $y$  equals the reciprocal of the derivative of  $f$  at  $x$ :

$$(f^{-1})'(y) = \frac{1}{f'(x)} = \frac{1}{f'(f^{-1}(y))}. \quad (\text{A.42})$$

This translates to the case of the fish model as follows: The function  $w(a)$  is the weight of a fish at age  $a$ . If it is continuously differentiable in a domain where  $w'(a) = g(w(a)) \neq 0$ , then for the derivative of the inverse function,  $a = h(w)$  it holds:

$$h'(w) = \frac{1}{w'(a)} = \frac{1}{g(w(a))}, \quad (\text{A.43})$$

or, equivalently,

$$\frac{dw(a)}{da} = \left( \frac{da(w(a))}{dw} \right)^{-1}. \quad (\text{A.44})$$

This leads to the following equation:

$$\int_{w_1}^{w_2} u(w, t) dw = \int_{a(w_1)}^{a(w_2)} u(w(a), t) \frac{dw}{da} da = \int_{a_1}^{a_2} p(a, t) da, \quad (\text{A.45})$$

where  $u(w, t)$  is the density in the weight domain,  $p(a, t)$  the density in the age domain, and  $a_1 = a(w_1)$ ,  $a_2 = a(w_2)$ . In the first step of the equation,  $dw$  is replaced by  $\frac{dw}{da} da$  in accordance with the inverse function theorem, and the boundaries of the integral are replaced accordingly. The second step holds because the integral equals the total number of fish with size between  $w_1$  and  $w_2$ , or, equivalently, with age between  $a_1$  and  $a_2$ , which must be the same number irrespective of the representation of the integral in weight or age. Thus, this equation allows to identify  $p(a, t)$  with  $u(w(a), t) \frac{dw}{da}$ , which provides the formula for the conversion of the density from one domain to the other [54]:

$$p(a, t) = u(w(a), t) \frac{dw(a)}{da} = u(w(a), t) g(w(a)). \quad (\text{A.46})$$

## A Mathematical methods

Without the proper conversion, one risks errors because of the non-linearity of the length-weight conversion (Fig. A.1).

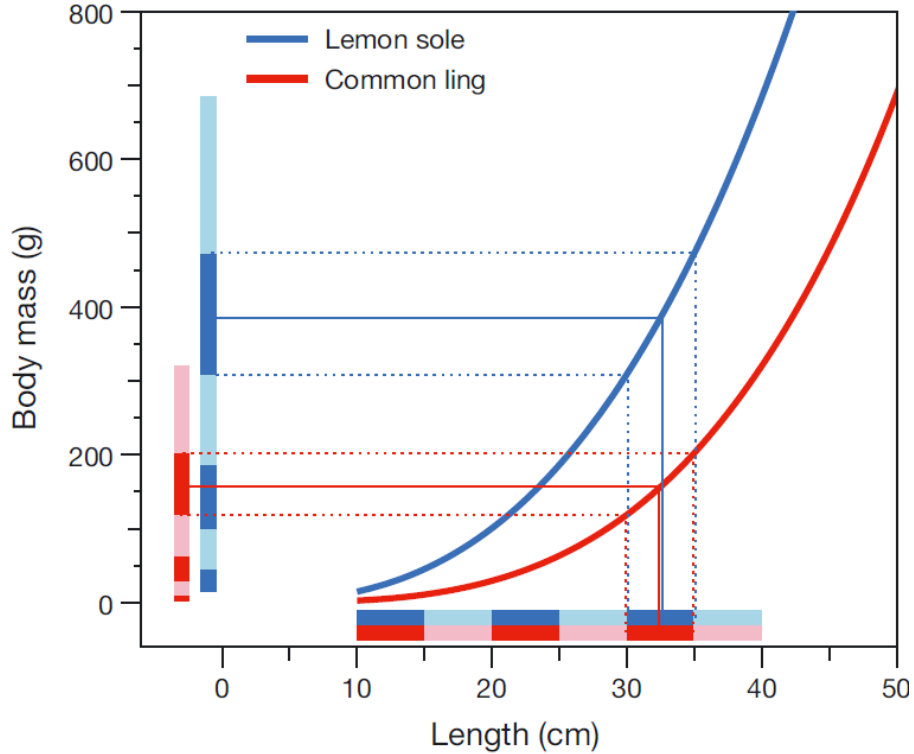


Figure A.1: Length-weight relationship for two example fish species (*lemon sole* in blue and *common ling* in red). Equidistant bins in the length domain correspond to non-equidistant bins in the size domain due to the non-linear length-weight relationship. From [63].

### A.6.2 Length and weight

We can apply the same line of thought of the conversion between age and weight density also to the conversion between length and weight. A fish population can be represented with a length spectrum or a weight spectrum. The number spectrum can be converted between the two representations from the following considerations. Let  $n_L(L)$  denote the number density in the length spectrum, such that the number of fish in the interval  $[L_1, L_2]$  is:

$$N = \int_{L_1}^{L_2} n_L(L) dL. \quad (\text{A.47})$$

This number must not differ from the number in the weight representation:

$$N = \int_{w(L_1)}^{w(L_2)} n_w(w) dw, \quad (\text{A.48})$$

## A.6 Density conversion

where  $w(L)$  denotes the length-weight relationship, and  $n_w(w)$  is the number density of the weight spectrum. As the equations are true for any pair  $L_1, L_2$  and the respective pair  $w(L_1), w(L_2)$ , it holds that

$$N = \int_{L_1}^{L_2} n_L(L) dL = \int_{w(L_1)}^{w(L_2)} n_w(w) dw = \int_{L_1}^{L_2} n_w(w(L)) \frac{dw}{dL} dL, \quad (\text{A.49})$$

and thus

$$n_w(w) \left( \frac{dw}{dL} \right) = n_L(L), \quad (\text{A.50})$$

where

$$\frac{dw}{dL} = \frac{d}{dL} w(L) = cbL^{b-1} \quad (\text{A.51})$$

is the derivative of the length-weight relationship

$$w(L) = cL^b, \quad (\text{A.52})$$

which is commonly applied in fisheries sciences.

Hence the density conversions is:

$$n_w(w) = n_L(L)(cbL^{b-1})^{-1}, \quad (\text{A.53})$$

and, analogously,

$$n_L(L) = n_w(w)bc^{1/b}w^{(b-1)/b}, \quad (\text{A.54})$$

where we used the inverse length-weight relationship  $L(w) = (w/c)^{1/b}$  and its derivative  $\frac{dL(w)}{dw} = bc^{1/b}w^{(b-1)/b}$ . This length-to-weight conversion was validated against the method LBNbiom, which uses the logarithmically binned biomass [64].



# B Ecological parameters

## B.1 Growth parameter

In [2, eq. (3.10)], it is shown how the growth parameter  $A$  can be estimated from the Bertalanffy parameters  $K$  and  $L_\infty$  for  $n = 3/4$  and  $b = 3$ . We extend the derivation for arbitrary values of  $n$  and  $b$ . From the length-weight relationship

$$w = cL^b, \quad (\text{B.1})$$

it follows that

$$\frac{dL}{dt} = \frac{1}{b} c^{-1/b} w^{1/b-1} \frac{dw}{dt}. \quad (\text{B.2})$$

Inserting the van Bertalanffy equation

$$\frac{dL}{dt} = KL_\infty \quad (\text{B.3})$$

and the juvenile growth model

$$\frac{dw}{dt} = Aw^n, \quad (\text{B.4})$$

one gets

$$KL_\infty = \frac{A}{b} c^{-1/b} w^{1/b-1+n}. \quad (\text{B.5})$$

Following [2], let us assume the two are identical at  $w = w_m = \eta_m W_\infty = \eta_m cL_\infty^b$ . Then

$$KL_\infty = \frac{c^{-1/b}}{b} (\eta_m cL_\infty^b)^{1/b-1} A (\eta_m cL_\infty^b)^n. \quad (\text{B.6})$$

Therefore:

$$A = bc^{1-n} \eta_m^{1-1/b-n} KL_\infty^{b(1-n)}. \quad (\text{B.7})$$

For  $n = 3/4$  and  $b = 3$  one gets the special case shown in [2, eq. (3.10)]:

$$A = 3c^{1/4} \eta_m^{-1/12} KL_\infty^{3/4}. \quad (\text{B.8})$$

With the standard parameter values (Table 3.1), one gets here  $A = 13.02$ .

## B.2 Physiological mortality

There are two different ways to calculate the parameter  $a$  which represents the physiological mortality [2, eqs. (4.41) and (4.42)]. The first method builds on the size spectrum theory and the energy budget. Using the parameters from [2], we can write the estimate of the physiological mortality  $a$  from the predator-prey interactions in the marine size spectrum and the metabolism as

$$a = a(\beta, \sigma, n, q, f_0, \epsilon_a, f_c) = \frac{\Phi_p f_0}{\epsilon_a (f_0 - f_c)}, \quad (\text{B.9})$$

where the constant  $\Phi_p$ , describing the predator-prey size preference, is

$$\Phi_p = \beta^{2n-q-1} \exp((2n - q - 1)(q - 1)\sigma^2/2) \quad (\text{B.10})$$

and comes from the feeding kernel for a community spectrum. With the standard parameter values (Table 3.1) one gets here  $a = 0.522$ .

The advantage of this approach is that is derived from very general principles and thus applies broadly, the disadvantage is that there are no direct observations of the parameters  $q, f_0, \epsilon_a, f_c$ . Therefore general species-unspecific and not directly observable values have to be used.

The second method to estimate  $a$  is from empirical observations of the van Bertalanffy parameters  $M$  and  $K$  with the advantage of using species-specific values which are often measured or estimated in the literature. However, as the natural mortality depends on the weight,  $M$  is not actually a constant. Therefore, one has to set, rather arbitrarily, a weight at which the size-based natural mortality equals  $M$ . Following [2] in setting this point at the size of maturation, one gets:

$$a = a(M, K, \eta_m, b) = \frac{M \eta_m^{1/b}}{K b}. \quad (\text{B.11})$$

With the standard parameter values (Table 3.1) one gets here  $a = 0.244$ .